Influence of cell-cycle phase in hematopoietic stem cell lineage production and expansion

Adrianus J. J. van den Berg

Dissertation der Fakultät für Biologie
der Ludwig-Maximilians-Universität
München, Deutschland

Research Unit of Stem Cell Dynamics
Helmholtz Zentrum Munich

Thesis submitted on the 15th April 2014

In partial fulfillment of the requirements to obtain the degree of
Doctor rerum naturalium

1. Gutachter: Herr Prof. Dr. Heinrich Leonhardt
2. Gutachter: Herr Prof. Dr. Charles David
3. Gutachter: Herr PD Dr. Ralf Heermann
4. Gutachter: Herr Prof. Dr. George Boyan
5. Gutachter: Frau Prof. Dr. Elisabeth Weiss
6. Gutachter: Herr Prof. Dr. Wolfang Enard

Tag der mündlichen Prüfung (Rigorosum): 4. November 2014

Abstract

The role of cell-cycle phase in cytokine-induced lineage production has long been a point of debate. The main shortcomings in todays' research are the lack of live cell-cycle observation in primitive primary cells and a fast yet robust read-out that allows detection of all lineages *in vitro*. Furthermore, a clonal *ex vivo*/*in vitro* culture would be favorable to current analyses that are mostly performed on a population scale since by doing so, a direct effect can be detected and potential influences and contaminations from other cells can be excluded.

The data I present in this thesis provides answers to these questions by employing high-throughput methods that overcome all of these hurdles. Through use of a live cell-cycle reporter combined with time-lapse imaging at single-cell resolution, cell-cycle durations and transitions were quantified in hematopoietic stem cells (HSCs) over multiple generations. I demonstrate a strongly heterogeneous behavior of highly purified primitive stem cells, allowing me to assess the influence of cell-cycle on lineage production upon cytokine administration by use of optimized culture conditions and live antibody staining.

Here, evidence is provided that HSCs that produce all myeloid lineages not only are more frequently found in G_1-phase upon cytokine administration but also have a longer G_1-phase, which can be observed over multiple generations. Strikingly, when cytokines were administered to daughter cells the same phenomenon could be observed, showing the reoccurrence and reversibility of this feature. To test whether this is a cell-intrinsic effect rather than an effect of cytokine administration, HSCs were enriched for G_1-phase using cell-cycle inhibitors. Indeed, this resulted in an overall higher yield of G_1-phase cells that produced all myeloid lineages, despite increased toxicity. In contrast, further administration of GM-CSF resulted in a reduced clonal production of all myeloid lineages. Together with preliminary data that shows signaling pathway activity, these data form a stepping-stone to identify the molecular prerequisites for multlineage production and highlight the involvement of cell-cycle phase in multilineage production from hematopoietic stem cells.

Further in-depth analysis of cell lifetimes in HSC subsets was performed in NUP98-HOXA10homeodomain (NA10hd) overexpressing HSCs, known to increase HSC expansion *in vitro*. However, to date little is known about the behavior of these cells and the mechanism(s) underlying this effect remains elusive. The use of time-lapse imaging resulted in the novel identification of HSC subsets with distinct cell lifetimes in NA10hd-overexpressing cells. Both slow- and fast-dividing cells were generated from the same ancestry, gradually leading to exhaustion of slow dividing NA10hd cells. Through co-culture with non-transduced HSCs NA10hd was unexpectedly found to have a paracrine effect, strongly affecting lineage marker expression and increasing the prevalence of a fetal liver phenotype in these cells, which could not be detected when co-cultured with mock-infected control cells. These phenomena require in-depth follow-up and could help understanding the mechanism of HSC expansion, with great impact on the clinical setting.

Co-culture with stromal cells (PA6) that can maintain HSC stemness over multiple generations revealed an increase in motility and cell lifetime for NA10hd-positive HSCs, which was dependent on cell-cell interactions. Indeed, it may well be the case that reduced NA10hd HSC proliferation upon transplantation is a direct effect of cell-cell signaling in the *in vivo* niche, yet this requires future work for further elucidation. Together, these results elicit new NA10hd-induced behavioral features, which could have implications in deciphering the mechanism behind HSC expansion.

In summary, the data I present here sheds new light on the mechanisms of HSC expansion, self-renewal and multilineage production with important clinical applications.

Acknowledgement

I would first like to thank my supervisor, Professor Timm Schroeder, for granting me the opportunity to perform my doctoral studies within his group and giving me the possibility to learn so many things. With this, I would of course also like to thank my supervisor at the university, Professor Heinrich Leonhardt, as well as my other thesis committee members, Dr Sandra Hake and Professor Justus Duyster, for their great feedback and support.

This 4-year journey I embarked on would not have been possible without my former supervisor, Dr Robert Nordon. Robert, thank you so much for your guidance during my Master's thesis and for inspiring me to take this next step in my scientific development. Indeed, through you I got interested in cell biology and time-lapse imaging in the first place and managed to join one of the best labs in the world in these fields.

I'd further like to thank Dr Adam Filipczyk, not only for his great feedback and help, but also for supporting me in more difficult times. Mate, you are a great friend. I'd wish you'd stick around for a long time and I wish you all the best for your future career! If fate requires you to be at a different place, we will surely continue sharing our passion for gourmet food and all other things online. Merci beaucoup Dr Daniel Legault-Coutu for helping me out with many technical challenges and for your great feedback, that simultaneously taught me how to address and better approach scientific problems. Thanks also to Philipp Hoppe, who introduced me to many technical possibilities when I joined the lab and for showing me around in my new city.

After having lived outside of my home country for 6 years now, it's amazing how my closest friends and my brother never made me feel the distance. You know who you are, Ditmer, Pieter, Wouter, Jorn, Meije, Arjen en Sander; jullie zijn stuk voor stuk toppers! Het betekent echt enorm veel voor me dat jullie er echt altijd voor me zijn!

Of course, my parents, who have always been there for me and made me pursue what I really wanted to do. You've been such a huge support. It makes me sad that you can no longer be there during these important moments in my life, but I'm sure you keep an eye out somehow and feel your presence in my heart.

Life in Munich wouldn't have been the same without my family-in-law. Fritz, Renate, Philipp: Ich kann's nicht in Worte fassen, wie viel es für mich bedeutet, dass ihr immer für mich da seid und mir das Gefühl gebt, mittlerweile komplett zu eurer Familie zu gehören. Ich habe euch lieb und vielen Dank für alles!

Finally, I'd like to thank my soul mate, my best friend, my room mate, my mountain guide, my jogging buddy, my yoga partner, my great chef-de-cuisine and my girlfriend. Caroline, ich wüsste nicht wo ich jetzt stehen würde ohne deine bedingungslose Unterstützung. Du warst immer für mich da in den schwierigen Momenten und harten Zeiten und es macht mir zum glücklichsten Menschen, dass du diese Reise mit mir durchgemacht hast. Ich habe dich unheimlich lieb!

Table of contents

List of tables

List of figures

Abbreviations

AGM	Aorta-gonad-mesonephron
AMEM	Alpha minimal essential medium
AML	Acute myeloid leukemia
APC	Allophycocyanin
ATM	Ataxia telangiectasia mutated
BMP4	Bone morphogenetic protein 4
CBP	CREB binding protein
CD	Cluster of determination
Cdc	Cell division cyclin
CDK	Cyclin-dependent kinase
CEBP/a	CCAAT/enhancer-binder protein alpha
CFSE	Carboxyfluorescein succinimidyl ester
CFU	Colony forming unit
CRU	Competitive repopulating unit
CKI	Cyclin-dependent kinase inhibitor
CLP	Common lymphoid progenitor
CMP	Common myeloid progenitor
CMLP	Common myeloid lymphoid progenitor
CXCL12	Chemokine ligand 12
CXCL5	Chemokine ligand 5
CXCR4	Chemokine receptor
Cy	Cyanine
DAPI	4',6-diamidino-2-phenylindole
DMEM	Dulbecco's modified eagle medium
DMSO	Dimethylsulfoxide
DNA	Deoxyribonucleic acid
ECM	Extracellular matrix
EDTA	Ethylenediaminetetraacetic acid
EPCR	Endothelial protein C receptor
EPO	Erythropoietin
ERK	Extracellular signal-regulated kinase
FACS	Fluorescence activated cell sort
FCS	Fetal calf serum
FITC	Fluorescein isothiocynate
G-CSF	Granulocyte-colony stimulating factor
GB	Gigabyte
GemM	Granulocyte erythrocyte macrophage megakaryocyte
GM-CSF	Granulocyte macrophage-colony stimulating factor
GMP	Granulocyte-macrophage progenitor
GVHD	Graft-versus-host-disease
HOX	Homeobox
HSC	Hematopoietic stem cell
HSPC	Hematopoietic stem and progenitor cell
HVGD	Host-versus-graft-disease
IL-3	Interleukin-3
IL-6	Interleukin-6
IMDM	Iscove's modified Dulbecco's medium
LDA	Limiting dilution assay

LISC	Leukemia-initiating stem cell
LSK	Lineage$^-$ Ly6A/E$^+$ CD117$^+$
LTC-IC	Long-term culture-initiating cell
MAPK	Mitogen-activated protein kinase
MEP	Megakaryocyte-erythrocyte progenitor
M-CSF	Macrophage-colony stimulating factor
MPP	Multipotent progenitor
mTOR	Mammalian target of rapamycin
NA10hd	Nucleoporin98 homeoboxA10 homeodomain
NUP98	Nucleoporin98
nucmem	Nuclear membrane
P/S	Penicillin/Streptomycin
PA6	Pre-adipocyte 6
PBS	Phosphate buffered saline
PCNA	Proliferating cell nuclear antigen
PE	Phycoerythrin
PerCP	Peridinin-chlorophyll cyanine 5
PI	Propidium iodide
PI3K	Phosphatidylinositide 3-kinases
PSLD	Phosphorylation-dependent subcellular localization domain
Rb	Retinoblastoma
RCF	Relative centrifuge speed
RNA	Ribonucleic acid
RPM	Rotations per minute
RT-PCR	Reverse transcriptase polymerase chain reaction
SA	Streptavidin
SCA-1	Stem cell antigen-1
SCF	Stem cell factor
SDF-1	Stromal derived factor-1
SFEM	Serum free essential medium
SLAM	Signaling lymphocytic activation molecule
SP	Side-population
STAT5	Signal transducer and activator of transcription 5
TALE	Three amino acid loop extension
TGF-β	Transforming growth factor-beta
TPO	Thrombopoietin
WBM	Whole bone marrow

1 Introduction

1.1 Hematopoietic stem cells

Were it not for the early 17th century Dutch pioneers, we probably would not be at our current state of knowledge of blood cells and their function. With the invention of the first compound microscope in the late 16th century, Jan Swammerdam and Antoni van Leeuwenhoek were the first naturalists who described and drew the structure of red blood cells, "red corpuscles". Until then, blood was only seen from a holistic perspective, following Hippocrates' and Aristotle's antique and classic theorem. However, even today blood is considered one of the most complex tissues in the human body. Comprising growth factors, hormones and important nutrients such as fatty and amino acids, sugars and oxygen, it is simultaneously providing a gateway for metabolic waste products and carbon dioxide to ensure optimal physiologic homeostasis in our body.

The blood cells involved in all these actions are originally derived from hematopoietic stem cells (HSCs). HSCs form a very rare subpopulation (~1 in 20,000 bone marrow cells in young adult mice (Warr, Pietras et al. 2011)), and fulfill two characteristics: they can self-renew life-long and have the potential to differentiate into every blood lineage. The first experimental evidence of the existence of HSCs dates back to 1963, when Becker, Till and McCulloch discovered that a clonogenic, transplantable marrow cell that fulfilled these characteristics could form spleen colonies. (Becker, McCulloch et al. 1963). In homeostasis, HSCs on top of the hematopoietic hierarchy (Figure 1.1-1), are thought to be in a dormant state (quiescent) with a very low *in vivo* cell division rate, ranging from two to four months in mice (Chesier, Morrison et al. 1999; Sudo, Ema et al. 2000). Upon activation, HSCs transit into cell-cycle and can have either self-renewing divisions, e.g. providing progeny with the same HSC characteristics, differentiate into (committed) multipotent progenitors, or are often hypothesized to have asymmetric cell divisions that sustain HSC numbers whilst simultaneously providing fast proliferating multipotent progenitor cells that eventually differentiate and produce all blood lineages (Akashi, He et al. 2003; Takano, Ema et al. 2004; Giebel, Zhang et al. 2006;

Beckmann and Scheitza S 2007; Wu, Kwon et al. 2007; Knoblich 2008).

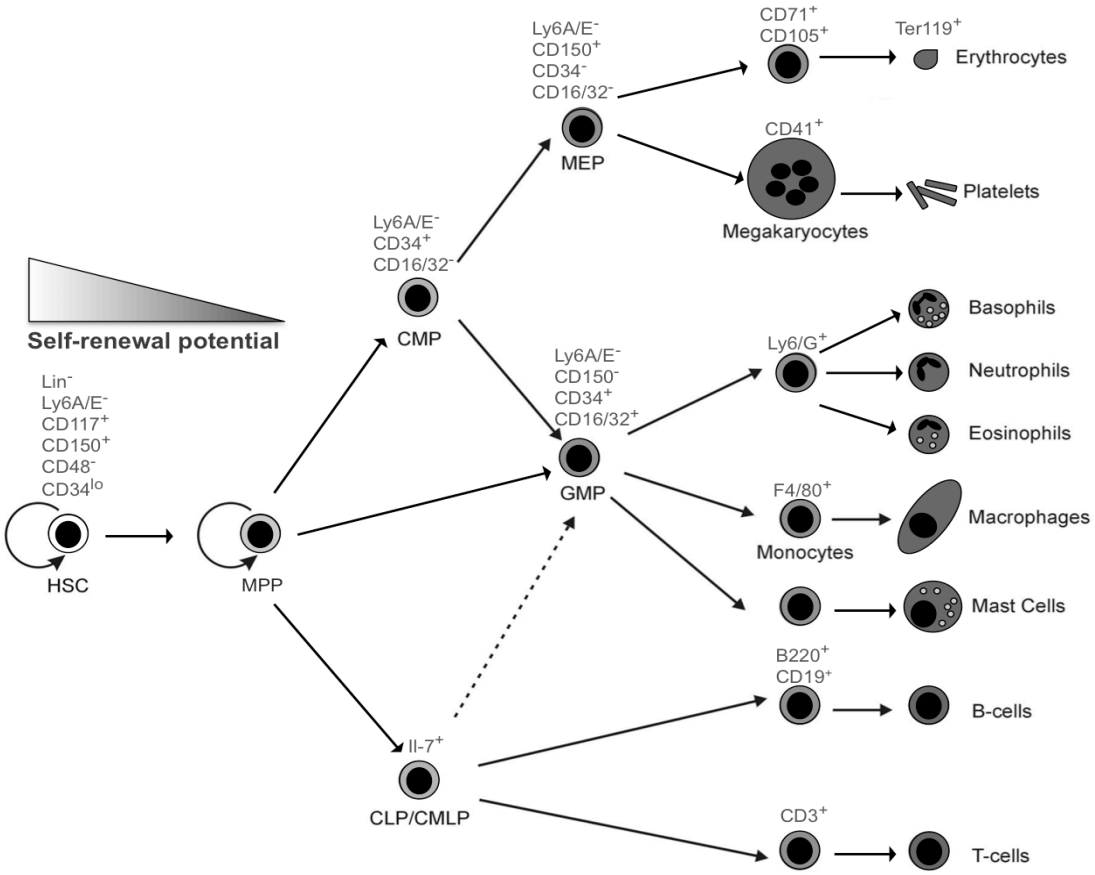

Figure 1.1-1: Hematopoietic hierarchy
Simplified overview of hematopoiesis, containing the key components of the hematopoietic system. HSC (hematopoietic stem cell), MPP (multipotent progenitor), CMP (common myeloid progenitor), CLP (common lymphoid progenitor), CMLP (common myeloid lymphoid progenitor), GMP (granulocyte-macrophage progenitor), MEP (megakaryocyte-erythrocyte progenitor), dendritic cells and osteoclasts are not shown.

In recent years it has become evident that this long-accepted hierarchical system may have bypasses and even the existence of certain progenitor populations has been disputed. HSCs can also be biased towards specific lineages (Müller-Sieburg, Cho et al. 2002; Sieburg, Cho et al. 2006; Dykstra, Kent et al. 2007; Challen, Boles et al. 2010; Benz, Copley et al. 2012), posing the question again: what really defines hematopoietic stem cells?

The factors and mechanisms controlling cell fate have been extensively studied but are still poorly understood. The *in vivo* HSC pool is very small and not readily accessible due to its primary location in the bone marrow, a tissue that is in itself poorly understood in term of anatomical, cellular and molecular architecture.

Studies on HSC function furthermore struggle with classic *in vivo* read-outs that can take up to two years for completion. *Ex vivo* (e.g. *in vitro*) studies require cell culture techniques. Although ultimately only partially mimicking physiological conditions, they allow us to study the behavior of these cells, manipulate them and directly read-out the effect of different conditions. For many progenitor types that are often found at different locations in the body, depending on the state of activity and developmental stage, this is common practice and has led to the discovery and characterization of many genetic and molecular fingerprints.

HSCs cannot be kept in culture long-term. They either undergo apoptosis or lose their multipotency or self-renewal capacity after even short culture. Taking these cells out of their highly structured microenvironment, the so-called niche, signaling pathways are changed and disrupted and the physiologic conditions are altered, eventually leading to a loss of quiescence and activation of HSCs. It is for this reason that many studies are focusing on mimicking the *in vivo* niche by optimizing culture conditions with cytokines and growth factors, co-cultures and media perfusion in order to retain quiescence or induce self-renewal divisions.

On the other hand, a great interest lies in the *in vitro* large-scale production of specific lineages. Many patients with blood disorders cope with a depletion of mature lineage subsets. Platelets that initiate wound healing are derived from megakaryocytes and pathological defects in their maturation cause severe bleeding. Erythrocytes are crucial for oxygen transport within the body and their differentiation and maturation are often impaired by leukemic cells or by genetic defects causing anemia. Both cell types are descendants of megakaryocyte-erythrocyte progenitor cells (MEPs), yet it remains unclear what exactly causes these cells to differentiate in either lineage. When foreign bodies enter our circulation, as is the case during e.g. injury or infection, granulocytes and macrophages act first to clear our system and together form our innate immune system. Although it has recently become clear that cytokines can instruct lineage choice in their common ancestor, granulocyte-macrophage progenitor (GMP) (Rieger, Hoppe et al. 2009), still little is known about the hierarchical level at which this decision can occur and the potential of lineage priming is still a point of debate (Luc, Buza-Vidas et al. 2008; Ng, Yoshida et al. 2009; Heffner, Clutter et al. 2011).

Together, GMPs, MEPs and their mature progeny form the myeloid compartment with the hematopoietic system. The lymphoid compartment, which contains T-cells, B-cells and natural killer cells (NKs) forms the adaptive immune system. These cells are much more effective and efficient in eradicating foreign bodies and cooperate through opsonization by the complement system. Although these cells require more time to develop, they are also long-term retained in the body in order to respond quickly during future relapse.

Developing culture methods to boost the efficiency of this production not only satisfies this high clinical demand, but also provides deeper knowledge and understanding about the critical pathways that are involved. Cytokine function and pathway activation have been established for many progenitor populations (Rieger, Hoppe et al. 2009), but a direct effect or a direct targeting of specific lineage production at the HSC level is still difficult. For many cytokines, little is known about how they affect individual cell fates. Since most studies have been performed in bulk populations, important information about apoptosis, proliferation, differentiation and activation had been lost or could not be directly assessed. Furthermore, now that the existence and potential of different cell populations as common myeloid progenitors (CMP), common lymphoid progenitors (CLP) and even different stages of multipotent progenitors (MPP) are disputed due to recent findings that the hematopoietic system may have bypasses (Wilson, Laurenti et al. 2008; Gekas and Graf 2013; Yamamoto, Morita et al. 2013), more than ever, the effect of cytokines on the cell fate of more primitive HSCs needs to be assessed. In order to distinguish proliferation and apoptosis rates and prevent cross-contamination from cells with distinct potential, these read-outs are best performed continuously, clonally and at single-cell resolution to reveal individual cell fates caused by cytokine addition.

1.2 The concept of the HSC niche

During development, HSCs journey through different locations in the body. From the early yolk sac (Yoder, Hiatt et al. 1997) to the aorta-gonad-mesonephron (AGM) (Bertrand, Chi et al. 2010) and then fetal liver (Rebel, Miller et al. 1996), they eventually migrate towards the bone marrow shortly before birth (Moore and Metcalf 1970). Whereas HSCs have a highly active cell-cycle state in the fetal liver, they are

deeply quiescent in the bone marrow (Bowie, McKnight et al. 2006; Bowie, Kent et al. 2007). There is substantial evidence that the microenvironment forms a highly specialized tissue controlling the state of the HSC (Schofield 1978; Calvi, Adams et al. 2003; Zhang, Niu et al. 2003). Inside the bone marrow, most of the HSCs are found at the endosteal niche, periosteal region or vascular niche, where they are in indirect contact with the blood circulation and are subjected to minimal oxidative stress by keeping them in a required hypoxic state (Kiel, Yilmaz et al. 2005; Jang and Sharkis 2007; Mendez-Ferrer, Michurina et al. 2010; Rehn, Olsson et al. 2011; Arai, Hosokawa et al. 2012; Ding, Saunders et al. 2012; Ding and Morrison 2013). The bone marrow niche comprises many cell types, most of them of osteoblastic and endothelial lineage, which secrete cytokines and extracellular matrix proteins (ECM) important for HSC function.

Although still a matter of debate, many factors have been shown to play crucial roles in HSC function. The bone morphogenetic protein 4 (BMP4) is important for engraftment and stem cell activity and its transforming growth factor-β (TGF-β) related receptor mediates hibernation through lipid raft clustering and SMAD activation (Goldman, Bailey et al. 2009; Yamazaki, Iwama et al. 2009). TGF-β has also been linked to HSC bias. After brief culture with TGF-β, HSCs show an *in vivo* bias towards the myeloid compartment. The concomitant up-regulation of p18 and p19, both repressing cell-cycle progression (Latres, Malumbres et al. 2000; Larson, Singer et al. 2009; Challen, Boles et al. 2010), indicates the potential importance of cell-cycle regulators in cell fate regulation.

Another factor derived from the osteogenic lineage is stromal derived factor-1 (SDF-1 or CXCL12), a chemokine ligand involved in homing and recruitment of HSCs at the endosteal surface (Sugiyama, Kohara et al. 2006). Cells expressing its receptor, CXCR4, are found to be either directly at the endostium or surrounded by sinusoidal endothelial cells, which postulates heterogeneity within the HSC niche, possibly related to their function (Kiel, Yilmaz et al. 2005; Omatsu, Sugiyama et al. 2010; Nagasawa, Omatsu et al. 2011; Ding and Morrison 2013; Greenbaum, Hsu et al. 2013). Furthermore, the adrenergic nerve system has been shown to be capable of reducing CXCL12 expression in target cells that are present in the HSC niche. Upon

ablation of neurotransmitters, HSCs were found to mobilize outside of their niche, implicating a role of the sympathetic nerve system in HSC regulation, to add to the already highly complex microstructure (Katayama, Battista et al. 2005; Mendez-Ferrer, Battista et al. 2010).

Other factors such as angiopoietin-1, Tie-2 and osteopontin have also been suggested to maintain quiescence of HSCs at the endosteal bone surface (Arai, Hirao et al. 2004; Nilsson, Johnston et al. 2005). Moreover, the extensively studied classical Wnt and Notch-1 signaling pathways have been shown to be indispensable at the endosteal niche for maintaining quiescence and self-renewal of HSCs (Stier, Cheng et al. 2002; Reya, Duncan et al. 2003; Fleming, Janzen et al. 2008; Schaniel, Sirabella et al. 2011). Taken together, all these tightly regulated interactions point towards a highly complex signaling network, rather than a sole master pathway regulating *in vivo* HSC fate.

Although much is known about the structure and function of the hematopoietic niche, many findings remain ambiguous. *Ex vivo* imaging has been employed to visualize HSC niche dynamics using real-time detection and has made a great step forward into functional characterization by tracking cell dynamics and kinetics (Xie, Yin et al. 2009). Former models that postulate HSC activity correlates with a dynamic cross-talk between different HSC niches (Wilson and Trumpp 2006) as well as future models can now be tested in a more reliable manner, providing answers to a field still coping with many unsolved questions and lacking a thorough understanding of what determines HSC fate. All these signaling pathways together form a very complex network of HSC extrinsic factors. The majority of this signaling is lost or disrupted upon HSC isolation. However, the great advantage of *in vitro* cultivation lies in the fact that this provides a controllable system. Not only can medium or stromal co-culture conditions exactly be determined, their effect on cell fate can be directly read-out in terms of e.g. survival, proliferation and differentiation and conditions can be adjusted as such. Combining this with further measurement of signaling pathway activation, essential mechanisms for survival or self-renewal as well as cell intrinsic mechanisms may be unraveled. Furthermore, lineage potential and multipotency can be measured and lineage production could be directed more effectively. Together, the signaling pathways that are activated *in vivo* can be selectively re-established or

manipulated. The effect of cell-cell or receptor-ligand signaling can be studied to explore the direct effect of many molecules on cell fate and determine whether these are sufficient or essential to establish or sustain known pathway activity and cell-cycle progression. It is for this reason that simplified models are mostly preferred in *in vitro* cultures, using only one or few co-culture cell types and using minimal essential medium to reduce variables, providing a highly controllable factorial system while minimizing compensatory mechanisms that exist *in vivo*.

1.3 HSC isolation methods

HSCs are one of the best-characterized stem cell-types and can be isolated with high purity. The first achievement in the quest for HSC purification was in 1961 by Becker, Till and McCulloch, where they developed the spleen colony assay to assess the potency of hematopoietic cells (see Table 1.3-1). In this assay different numbers of bone marrow cells were transplanted in lethally irradiated mouse recipients. The nodules that were formed in the spleen after 8 to 12 days were equivalent to the number of bone marrow cells transplanted and were derived from a single cell with self-renewal capacity although the majority were later found to be multipotent progenitors rather than HSCs. Hodgson and Bradley developed an improvement of this method in 1979, when 5-fluoroacil was used to ablate cycling cells and increase the yield of cells with more self-renewal and differentiation capacity through HSC mobilization (Hodgson and Bradley 1979). Although better results were obtained, this crude method still resulted in low purities of HSCs.

Much better results were obtained after the discovery of Sca-1 (stem cell antigen, Ly6A/E) (Spangrude, Heimfeld et al. 1988; Okada, Nakauchi et al. 1992) and c-kit (CD117) (Okada, Nakauchi et al. 1991; Ikuta and Weissman 1992). This population of lineage marker negative, Sca-1/c-kit positive (LSK) cells comprises both HSCs and non-committed progenitor cells and transplantation of 100 LSKs was sufficient to repopulate a sublethally irradiated recipient mouse. Alternatively, similar results were obtained using dye efflux and the purification of a side-population (SP) at the low end of the distribution, following the theory that HSCs show a stronger dye efflux due to active ABC-transporter expression, providing a self-defense mechanism (Goodell, Brose et al. 1996).

It was long assumed from the human counterpart that murine HSCs had to be CD34 positive, until a CD34 monoclonal recombinant antibody showed that the HSC compartment was CD34 negative (Osawa, Hanada et al. 1996; Ogawa, Tajima et al.). The lineage hierarchy between HSC and common myeloid progenitors (CMP) was further characterized by use of Thy-1.1 and CD11b (Morrison, Wandycz et al. 1997), but even more so by the identification of Flk-2 as a MPP marker that provides higher HSC purity and a better classification of the MPP population and downstream progenitors (Adolfsson, Borge et al. 2001; Christensen and Weissman 2001).

Following combined purification methods that led to increasing levels of purity (Matsuzaki, Kinjo et al. 2004), HSC purification in the 21st century has taken a leap further with many more antibodies to isolate both HSC and MPP subsets. Further addition of antibodies against a family of signaling lymphocytic activation molecules (SLAM), CD150 and CD48 increased HSC purity up to almost 60% (Kiel, Yilmaz et al. 2005). Similar results were obtained when substituting lineage depletion and c-kit for endothelial protein C receptor (EPCR, or CD201), drastically reducing effort and antibody requirement whilst maintaining efficiency and purity (Kent, Copley et al. 2009). It is plausible that HSCs from different sorting regimes show similar co-expression of marker subsets and combinations of these could further increase HSC purity and could provide a deeper understanding of functionality. With the current high isolation purities, it is also of interest to study the correlation between different sorting schemes and surface marker expression with a potential related functional difference. Such a direct comparison between different isolation methods and combinations has not yet been performed *in vivo* using single cell transplantations.

Given that HSCs are in direct contact with their niche, the hypothesis that they would therefore express cell adhesion molecules such as integrins has been proposed. However, CD49b was shown not only to be exclusively expressed in short-term HSCs and progenitors, its expression also correlated with faster cell-cycle division rates *in vitro* (Benveniste, Frelin et al. 2010). Aside from providing new surface markers to further characterize and distinguish the HSC compartment, this also supported previous studies that found that a slow cell-cycle or late cell-cycle entry correlated with HSC purity when compared with MPPs (Nygren, D et al. 2006) and leads the way to assess the influence of other surface molecules and integrins in the future.

Although MPPs possess self-renewal potential and are multipotent, they do not have HSC potential. For this reason, optimizing HSCs purification methods have played a central role in studies aiming for higher HSC yield and expansion for clinical therapies. The potential to induce an HSC phenotype in multipotent progenitor cells has been poorly studied. Combining purification schemes with a time-lapse microscopy read-out therefore posed the question whether slow cell-cycle could not only be used as a method to assess overall HSC purity, but also whether this correlated with *in vitro* multipotency or lineage production. The slow cell-cycle or late cell-cycle entry could furthermore point to extended cell-cycle phase durations or heterogeneity thereof. Furthermore, it is unknown whether these phenomena exist during *in vitro* culture in subsequent generations, i.e. progeny after division, and whether lineage production can be directed or limited prior to reaching a multipotent progenitor stage. To date, these questions have not yet been answered due to the lack of tools that allow both continuous non-invasive assessment of cell-cycle phase and detection of lineage commitment without losing starting cell identity.
Table 1.3.1. provides a chronological overview of improvements in HSC purification.

Table 1.3.1: History of HSC purification

Purification method	Read-out	HSC Purity	Author	Year
Nucleated WBM	CFU-S	0.01%	Becker	1963
5-fluoroacil	CFU-S / CRU	0.02%	Hodgson	1979
Ly6A/E	CFU-S / LDA	2.5%	Spangrude	1988
Ly6A/E, CD117 (LSK)	CFU-S / CRU	2.5-12%	Okada	1991
Hoechst Rhodamine (SP)	LDA	3%	Goodell	1996
LSK CD34	LDA	21%	Osawa	1996
LSK Thy-1.1 CD11b CD4	LDA / 2°	10-20%	Morrison	1997
LSK Flk-2	CRU	8-20%	Christensen	2001
LSK CD34 SP	Single-cell	> 90%	Matsuzaki	2004
LSK CD150 CD48 (SLAM)	Single-cell	47%	Kiel	2005
EPCR SLAM (E-SLAM)	Single-cell	56%	Kent	2009
LSK SLAM CD49b	Sinlge-cell	29%	Benveniste	2010

The development and improvement of different purification techniques. WBM (whole bone marrow), CFU-S (spleen colony forming unit), CRU (competitive repopulating unit), LDA (limiting dilution assay), LSK (lineage$^-$ Ly6A/E$^+$ CD117$^+$). Peripheral blood counts were used to determine donor contribution.

1.4 HSC assays

Following half a century of HSCs characterization and defining their phenotype, the conclusion must be drawn that despite large improvements, a uniform HSC marker or combination thereof has not yet been discovered. With purities ranging from 50 to potentially 90 percent (Matsuzaki, Kinjo et al. 2004), heterogeneity has been much reduced. However, stem cell potential, i.e. having both life-long self-renewal capacity and the potential to differentiate into every blood lineage, vary.

The gold standard to measure potency is transplantation. While in early days the *in vivo* lineage contribution was assessed after 8 to 12 days, now 16 weeks to 32 weeks or longer is required to prove HSC potency, including secondary and even tertiary transplants. Moreover, initially bulk bone marrow transplants were performed, in contrast to today where single-cell transplants are the norm. To date, an *in vitro* assay to read-out HSC potential unfortunately does not exist. However, many important questions regarding cell fate such as self-renewal, survival, apoptosis and even multipotency can be read-out *in vitro*. With recent studies proving the existence of HSCs that are biased towards specific lineages, which can also vary with age (Dykstra, Kent et al. 2007; Gekas and Graf 2013), more than ever assays are required to not only assess lineage potential but also to address the question of how these cells behave and how cell fate decision is orchestrated. This is difficult to attain *in vivo*. To define their behavior in terms of migration, division rate and survival, continuous observation and monitoring is required, which is limited in living and moving animals. Furthermore, *in vivo* imaging of HSCs requires deep-tissue penetration, which limits both temporal and spatial resolution for single-cell quantification. Other methods such as genetic manipulation and use of tissue sections, often leads to unwanted effects on both the microenvironment and hematopoietic hierarchy and leaves uncertainties about exact localization of other cell types in many cases, respectively. Thus, an *in vitro* assay to read-out both cell fate and cellular behavior

would form a desirably faster, more robust and more controllable alternative for the laborious and time-consuming and complicated *in vivo* read-out.

Colony assays have been performed in semi-solid media, with a mixture of cytokines and growth factors, for almost fifty years (Bradley and Metcalf 1966). They directly reveal the clonal potential of cells, but despite the detection of blast (non-differentiated) cells and self-renewal through serial re-plating it cannot assess HSC potential. However, this assay does serve the purpose of assessing multipotency by allowing detection of clonal lineage production. Since behavior cannot be defined due to the lack of single-cell resolution, early cell fate decisions cannot be measured and correlated.

Methods not directly driving differentiation, such as co-culture techniques for long-term culture initiating cells (LTC-IC) (Sutherland, Lansdorp et al. 1990), cobble-stone formation (Ploemacher, Sluijs et al. 1989; Song, Bahnson et al. 2010) or retention of HSC numbers using premature feeder layers (Moore, Ema et al. 1997; Nolta, Thiemann et al. 2002) also allow classification of multipotency while preserving clonal identity. Single-cells can still be distinguished and cell behavior such as motility or division rate can be measured. The remaining bottleneck of HSC visualization under stromal co-culture conditions, which impairs detection due to loss of optical clarity, focus and contrast, requires further improvements and can be overcome when further optimizing culture conditions by developing a stroma free liquid culture assay.

Attributing cell behavior to lineage potential would not only provide a functional correlation to molecular and gene expression, but would ultimately allow to predict cell fate, lowering the need for long-term assays. Benveniste et al. showed that CD49b- and CD49b+ HSCs showed a significant difference in initial cell-cycle division rates. While both cell types developed chimerism in recipient mice, the former would sustain multilineage contribution much longer and this correlated with a profoundly longer cell-cycle *in vitro* (Benveniste, Frelin et al. 2010). CD49b is an integrin and as such is involved in cell adhesion. It is therefore quite possible that other features such as cell adherence, motility, cell size or morphology could further characterize this HSC subset. However, the difference in initial cell-cycle division

rates not only points to heterogeneity with respect to cell-cycle entry, but also to potential differences in cell-cycle phase durations. Since the *in vivo* long-term repopulation assays revealed marked distinctions in chimerism, it would be of key interest to assess whether *in vitro* lineage potential correlates with cell-cycle transit in early divisions. The lack of continuous cell-cycle data and the ability to continuously read-out cell fate on a single-cell resolution are the main problems that have made it yet impossible to prove this correlation. With the development of advanced technology such as continuous time-lapse imaging, many of these hurdles have been overcome, yet need to be adjusted to specific needs and cell types and is not yet readily available.

1.5 Cell-cycle

Cells have different fates they can adopt. They can e.g. differentiate, migrate, proliferate, be quiescent, senescent, necrotic or apoptotic. These states can occur during different active cell-cycle phases. Quiescence is the only state reserved for non-cycling cells, such as HSCs and post-mitotic differentiated cells. This phase is depicted as the G_0-phase. From this resting phase, HSCs can be activated and transit into cell-cycle.

During replication, two major checkpoints exist that secure DNA integrity and under normal conditions prevent tumorigenesis by controlling division rate. Hence, the first checkpoint is encountered before DNA is replicated, the so-called G_1-phase (gap1) (Figure 1.5-1). The key factors that drive G_1-phase progression are cyclin D and retinoblastoma (Rb). The cyclin family had been first identified in yeast by Hartwell in the 1970`s, after which Nurse and Hunt discovered analogs and further characterized their function in *xenopus* and human, for which they were awarded the NobelPrize in 2001 (Hartwell, J et al. 1970; Lee and P 1988; Hunt 1989). Cyclin D levels (1 from over 15 family proteins from cyclin A to Y) regulate the phosphorylation state of Rb. Upon binding its complementary cyclin-dependent kinases 4-6 (CDK4-6), it forms an active complex that phosphorylates Rb. p16 (INK4a) and p18 (INK4c), G_1-phase-specific cell-cycle inhibitors, can block this activity and since in HSCs levels of p18 in G_0-phase are often found to be high and cyclin D levels are minimal, Rb resides in an unphosphorylated state. However,

during quiescence p130, part of the Rb family, and p18 have a more prominent role in retaining the quiescent state since p16 and p19 are actively repressed through *bmi1* (Lessard and Sauvageau 2003; Park, Qian et al. 2003; Passegue, Wagers et al. 2005). When homeostasis is disrupted, cyclin D levels can be triggered, overcoming this threshold and putting retinoblastoma in a hypophosphorylated state.

In late G_1-phase stage, cyclin E has a more prominent role and together with its complementary CDK2 it can further phosphorylate retinoblastoma. The cell-cycle inhibitors repressing CDK2 activation are p21 and p27, part of the Cip/Kip family. These inhibitors are also found in low levels on the active CDK4-6 complex, but are displaced and bind CDK2 upon increasing concentrations of cyclin D. Similarly, higher concentrations of p21 and p27 result in CDK2 inhibition. If levels of cyclin E are sufficiently high, CDK2 activation completes the phosphorylation state of retinoblastoma, which releases and activates the E2F transcription factors that orchestrate the DNA replication machinery.

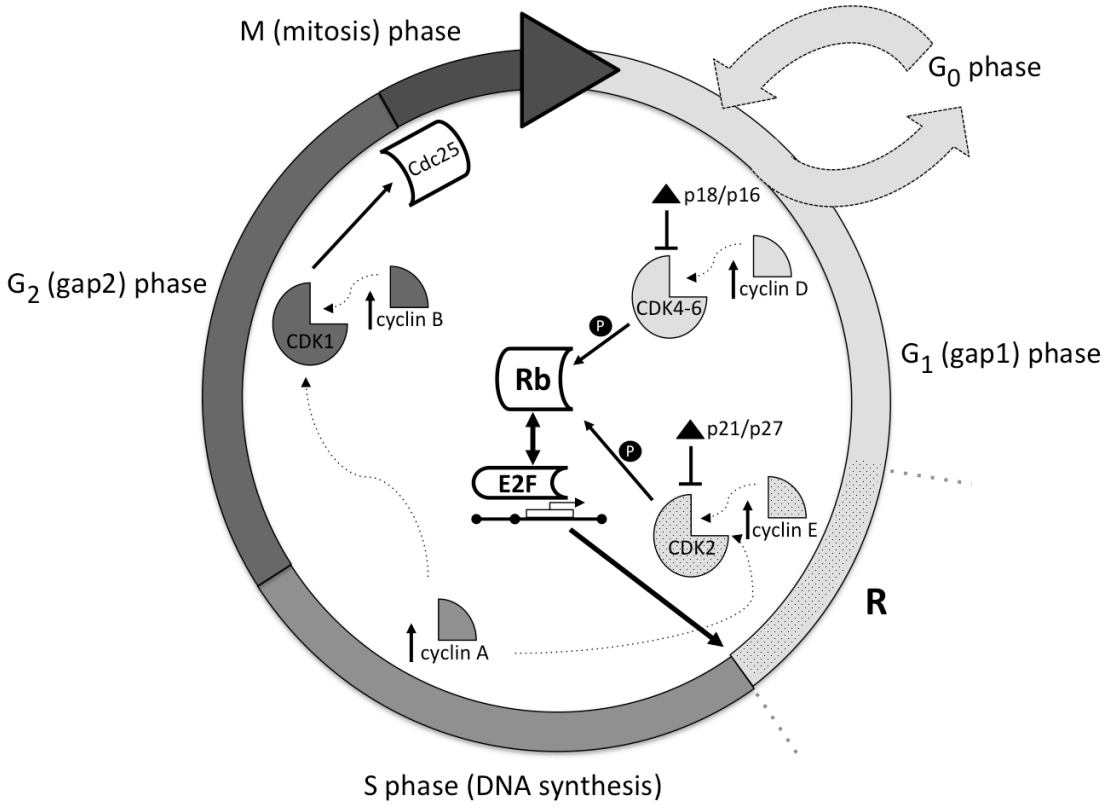

Figure 1.5-1: Cell-cycle
Simplified cell-cycle progression. CDK (cyclin-dependent kinase), Rb (retinoblastoma), R (restriction point, Cdc (cell division cycle).

At this stage, synthesis (S-phase) has started and is further driven by cyclin A in early S-phase. Between synthesis and mitosis (M-phase), the G_1-phase equivalent checkpoint is found in G_2-phase (gap2). Up-regulation of Cdc25 by G_2-phase specific cyclin B, activates mitosis promoting factor. However, when DNA damage occurs, Ataxia telangiectasia mutated (ATM) kinase degrades Cdc25 and therefor prevents transition into M-phase, leading to cell-cycle arrest or induced apoptosis and forming the second major checkpoint. The cell then continues mitosis by condensing the chromatin structure, building of the spindle and separation of the centrosomes (prophase), degradation of the nuclear membrane, chromosome alignment and polarization (metaphase), chromatin separation (anaphase) and eventually lengthening of the cell and nuclear membranes are established (telophase), after which the cell separates into two daughter cells (cytokinesis). This process is highly complex and occurs within a very short time frame, relative to the other phases of the cell-cycle.

The name and function of retinoblastoma are derived from a type of cancer in children that arises when gene mutations in both alleles occur, causing defects in the retinoblastoma protein (Herwig and Strauss 1997). Furthermore, its importance in both embryo development and hematopoiesis has been supported by studies in which a Rb double knockout caused embryonic lethality through the absence of mature erythrocytes and impaired neuronal growth (Clarke, Maandag et al. 1992). Together this shows that Rb not only forms an important tumor suppressor in controlling cell proliferation, but also is essential for differentiation. This was further underlined in studies that showed modified Rb in tumor cells causes a differentiation block and fails to provide mature blood lineages (Santamarina, Hernandez et al. 2008). The differential Rb expression at distinct stages in hematopoietic lineage production (Szekely, Jiang et al. 1992) together with the fact that Rb mainly drives G_1- to S-phase progression, led to the hypothesis that cell-cycle phase may play an important role in lineage production i.e. posed the question whether different cell-cycle phases have opposing cell fates or lineage potential upon cytokine addition.

Although not yet proven to date, this hypothesis does not seem farfetched since previous studies have shown a reversible differential gene expression pattern throughout different cell-cycle phases (Lambert, Liu et al. 2003). During replication, chromatin is modulated and access for different transcription factors is enabled.

However, despite evidence that shows diverging cell fates of daughter cells after one cell-cycle division (Suda, T et al. 1984), it is still unknown whether this yields a cell intrinsic or extrinsic mechanism.

The binding of Rb to myeloid transcription factors as CEBP/a, is mostly found in a hypophosphorylated state, which supports a role of early G_1-phase in providing a time-frame for differentiation. Furthermore, this indicates that the involved signaling pathways may be cell-cycle phase dependent (Herwig 1997; Lipinski 1999; Zhang 1999). p16, known to repress phosphorylation of Rb by blocking cyclin D function, is expressed in undifferentiated cells but is rapidly downregulated during lineage maturation (Furukawa, Kikuchi et al. 2000). Overexpression of p16 reduces both proliferation and differentiation in hematopoietic stem and progenitor cells (Bergh 2001) and indeed, a double knock-out of p16 leads to tumorigenesis (Sharpless, Bardeesy et al. 2001). However, a clear role of Rb could not be detected, probably due to *in vivo* compensatory mechanisms by the family pocket proteins p130 and p107 (Santamarina, Hernandez et al. 2008). Low-level expression of late G_1-phase regulators of p21 and p27 have been shown to facilitate the production of erythroid lineages. Even lineage-specific expression of cell-cycle regulators could be revealed, however only in mature cell types (Furukawa, Kikuchi et al. 2000; Hsieh 2000; Tamir 2000; Bergh 2001). This further supports the hypothesis that the key regulators of G_1-phase progression also form a crucial role in determining cell fate.

To date, real evidence to prove a role of cell-cycle phase in determining cell fate in hematopoiesis is still missing. While most studies have been performed on cell lines or cultures of tumor cells, studies that have used primary cells are primarily based on bulk population assays that read-out total lineage production but not single cell fates. Furthermore, the existence of differential gene expression patterns and even cell-cycle regulators in distinct differentiated populations, does not prove the point that these cell-cycle phases and regulators play a role in lineage decision and cell fate in upstream cells, i.e. ancestor cells that did not yet express lineage specific differentiation markers. To add to the complexity, overexpression and genetic modification are tools that mostly possess an invasive character that could alter or influence the observed effect on cell fate. Together, a read-out is required that could prove the influence of cell-cycle phases in multipotent cells rather than lineage

restricted and differentiated cells. An *in vitro* read-out would provide a controllable system and allows clonal assessment of cell fate. By doing so, different cytokine combinations that are known to direct lineage production can be added during different cell-cycle phases in order to reveal a cell-cycle dependency in cell fate.

The difficulty in studying the influence of cell-cycle in cytokine induced differentiation lies in (1) providing a clean read-out that allows quantification and determination of lineage commitment on a single-cell level and (2) providing a method that allows measuring cell-cycle phase whilst keeping the cells viable and without perturbing intracellular signaling pathways. The former has been achieved by both classic colony assays and LTC-IC assays and cell fate can be easily determined using a snapshot-based read-out at different time-points. Using lineage tracing or specific viral integration patterns (barcoding), culture and *in vivo* read-outs can be initiated with different starting cell numbers since lineage contribution can be assessed without loss of ontogeny (Lu, Neff et al. 2011; Kretzschmar and Watt 2012). The latter however is much more difficult to obtain since current methods to measure cell-cycle mostly require fixation and (immuno-) staining.

In a 2007 study by Quesenberry et al. cell-cycle of quiescent hematopoietic stem and progenitor cells (HSPCs) was indirectly measured based on bulk population propidium iodide quantification using flow cytometry. Although cell-cycle phase prevalences at various time-points were reproducible, cell-cycle phases between cells were never fully synchronous. In addition, since genealogy was lost, uncertainties existed whether cells after 32 and 48 hours had yet divided *in vitro*. Nevertheless, building on this assumption, the influence of different cytokines was assessed, leading to the interesting hypothesis that certain cytokines may increase the yield of megakaryocytic lineages, when added in the right cell-cycle phase or at the right time (Colvin, Dooner et al. 2007). Indeed, despite generating data based on bulk culture and cell-cycle phase probabilities, they found that cytokine change during early S-phase increased the total production of megakaryocytes, whereas cytokine addition during G_1-phase increased the yield of granulocytes. However, when performing clonal analysis, their data showed inconsistencies. It might well be that in bulk culture cell-cell contact occurs with a higher frequency and secreted molecules are more

abundant, raising the question what formed the major component in orchestrating different lineage production?

1.6 Cytokines in lineage production

Since the emergence of *in vitro* culture of hematopoietic cells, medium optimization to promote maintenance, proliferation or differentiation has become of key interest. The following cytokines have been used to study the influence of cell-cycle in cytokine induced lineage production and maintenance of multipotency.

Stem cell factor

Culture and maintenance of HSCs *ex vivo* is a complex and difficult procedure. After isolation they eventually undergo apoptosis without the proper growth factors. Found as one of the first crucial cytokines for *ex vivo* HSC maintenance stem cell factor (SCF), also known as steel factor or c-kit ligand, is indispensable for prolonging survival of HSCs *in vitro*. SCF binds its CD117 (c-kit) receptor and represses apoptosis through PI3K and Erk signaling and Wnt inhibition. However, culture of HSC in SCF alone does not yield self-renewal divisions but only transient survival and maintenance of multipotency can be achieved, as shown by studies on proliferation kinetics and colony assays (Li and Johnson 1994; Keller, Ortiz et al. 1995). Although this points to SCF involvement in G_1-phase progression, other studies have shown that its target receptor CD117 is expressed through all cell-cycle phases (Lambert, Liu et al. 2003; Passegue, Wagers et al. 2005; Dooner, Colvin et al. 2008). Since SCF is indispensible for *in vitro* HSC survival through all cell-cycle phases (Zhang and Lodish 2008), its effect on lineage production with cell-cycle phase correlation has not yet been revealed.

Thrombopoietin

Known for its function in megakaryocyte production, thrombopoietin (TPO) not only helps maturation and development of proplatelets (Kaushansky 1995) but also and synergistically with SCF stimulates both survival and proliferation of *in vitro* cultivated HSCs (Matsunaga, Kato et al. 1998). Binding its receptor Mpl, TPO activates amongst other pathways PI3K signaling, which stimulates and directs the cell to transit into cell-cycle. In concert with SCF, addition of TPO in *ex vivo* cultures

can (to a limited extent) even induce self-renewal as well as multilineage differentiation of HSCs (Ku, Yonemura et al. 1996; Ramsfjell, Borge et al. 1996; Yagi, Ritchie et al. 1999; Ema, Takano et al. 2000). Its importance for HSC maintenance is further illustrated by the fact that *in vivo* TPO knock-out and Mpl receptor blocking through neutralizing antibodies show hematopoietic deficiencies (Kimura, Roberts et al. 1998; Fox, Priestley et al. 2002; Qian, Buza-Vidas et al. 2007; Yoshihara, Arai et al. 2007). In addition, $CD34^-$ HSCs show an increased expression of Mpl when compared with $CD34^+$progenitors, which may point to the necessity of TPO signaling in both *in vivo* and *in vitro* of HCS function (Morita, Ema et al. 2010). A potential cell-cycle phase dependency of TPO with respect to lineage production was hypothesized after the discovery that TPO induces PI3K signaling which can stabilize cyclin D while simultaneously repressing transcriptional activity of p21 and p27 (Massague 2004). Indeed, in accordance, TPO signaling during G_1-phase has been shown to increase the potency to produce megakaryocytes (Colvin, Dooner et al. 2007). Taken together, the role of TPO in HSC fate remains ambiguous, being involved in survival, cell-cycle, self-renewal and differentiation.

Interleukin-3

Produced by activated T-cells and mast cells, interleukin-3 (IL-3) can not only suppress induced apoptosis but, upon binding its receptor, also orchestrate myeloid lineage development and stimulate proliferation (Miyajima, Mui et al. 1993; Kinoshita, T et al. 1995). In progenitors, increased levels of IL-3 can direct megakaryocyte differentiation and functions synergistically with the receptor homologue of granulocyte-macrophage colony-stimulating factor (GM-CSF) (Hoffman, R et al. 1990; Briddell and JE Brandt 1992). However, upon addition of interleukin-6, this co-stimulation leads to a loss of megakaryocytes and an increase in granulocyte macrophage progenitors (GMPs). For both, the exact mechanism including potential cell-cycle phase relevancy still needs to be elucidated.

Granulocyte macrophage colony-stimulating factor

Originally defined as a growth factor specific for neutrophils and macrophages, granulocyte macrophage colony-stimulating factor (GM-CSF) has been shown to be important for maturation and survival of committed progenitor cells in the myeloid lineage (Burgess and D 1980; Kinoshita, T et al. 1995). It is also known

that GM-CSF can trigger immune responses, either directly or through up-regulation of interleukin-1, thereby activating the adaptive immune system (Khameneh, Isa et al. 2011). In contrast to what its name originally suggested however, GM-CSF also has the potential to increase megakaryopoiesis, either directly (Briddell and JE Brandt 1992) or in synergy with interleukin-3 (Robinson, McGrath et al. 1987; Hoffman, R et al. 1990). Furthermore, data based on bulk culture has shown a cell-cycle relevancy for GM-CSF, specifically increasing megakaryocyte production when added during early S-phase and increasing granulocyte production when added during G_1-phase (Colvin, Dooner et al. 2007). In addition, leukemic cancer cell lines have been established that respond to this factor by differentiation into the megakaryocytic lineage. This makes it of particular interest in a clinical setting and for studies on the potential of directing lineage production from HSPCs by cytokines (Komatsu, H et al. 1991).

Erythropoietin

The difficulties in obtaining erythroblasts *in vitro* have mainly been overcome by the addition of erythropoietin (EPO). With previous studies requiring adherent stromal layers for the production of mature erythrocytes, a stroma free culture technique was established using erythropoietin, allowing erythropoiesis without disturbing production of other blood lineages (Eliason, Testa et al. 1979; Estment and Ruscetti 1982). In 1996 it was shown with an EPO receptor double knock-out mouse that the EPO receptor, being expressed on different myeloid cell types, is essential for the development of full grown erythrocytes. Erythroid progenitors however could be produced but could not differentiate past the erythroblast state (Kotkow and Orkin 1996). Through up-regulation of c-jun, EPO was found to be controlling cyclin D levels, necessary for hypophosphorylation of Rb and which points to a potential influence of G_1-phase in erythroid lineage production (Lopez-Bergami, Huang et al. 2007). EPO also affects cell-cycle progression through c-kit down-regulation, Erk1/2 and STAT5 signaling (Fang, Menon et al. 2007; Wang, Akbarian et al. 2013). Together this indicates EPO can alter both cell-cycle phase progression and cell surface marker expression, but a direct influence on HSC level with respect to cell-cycle phase and lineage production has not yet been elaborated.

Medium conditions that allow production of all myeloid lineages from multipotent progenitors ("permissive conditions")

To date it remains difficult to attain production of all myeloid lineage subsets from a single starting cell *in vitro*. Whilst purification may disrupt viability of primitive hematopoietic cells, the main problem is thought to be cytokine conditions that, when not mixed in optimal concentrations, do not allow production of all lineages. This major hurdle has been overcome with the establishment of optimized culture conditions by Takano et al., which revealed the highest yield of granulocytes (neutrophils), erythrocytes, macrophages and megakaryocytes (GemM) producing cells on a clonal basis (Takano, Ema et al. 2004). In addition to SCF and TPO, required for survival and proliferation of HSCs, these conditions comprise IL-3, EPO and fetal calf serum (FCS). Further media additions are 2-mercaptoethanol and L-glutamine to ensure low oxidative stress (Das, Kar Mahapatra et al. 2007).

Although the effect of many of these cytokines on lineage production does not necessarily require clonal culture, read-out of individual cell fates cannot be performed in bulk culture. If the effect on early cell fates is lost or unknown, clonal proliferation and apoptosis rates may mask the overall production of mature lineages and individual cell-cycle dependency cannot be assessed (Figure 1.6-1). Most of current published data regarding cell-cycle progression has been acquired with loss of single-cell clonal identity and therefore pose ambiguous outcome. To be able to conclusively identify the role of cell-cycle phase in cytokine induced lineage production, current data requires continuous observation rather than snapshot or endpoint analysis.

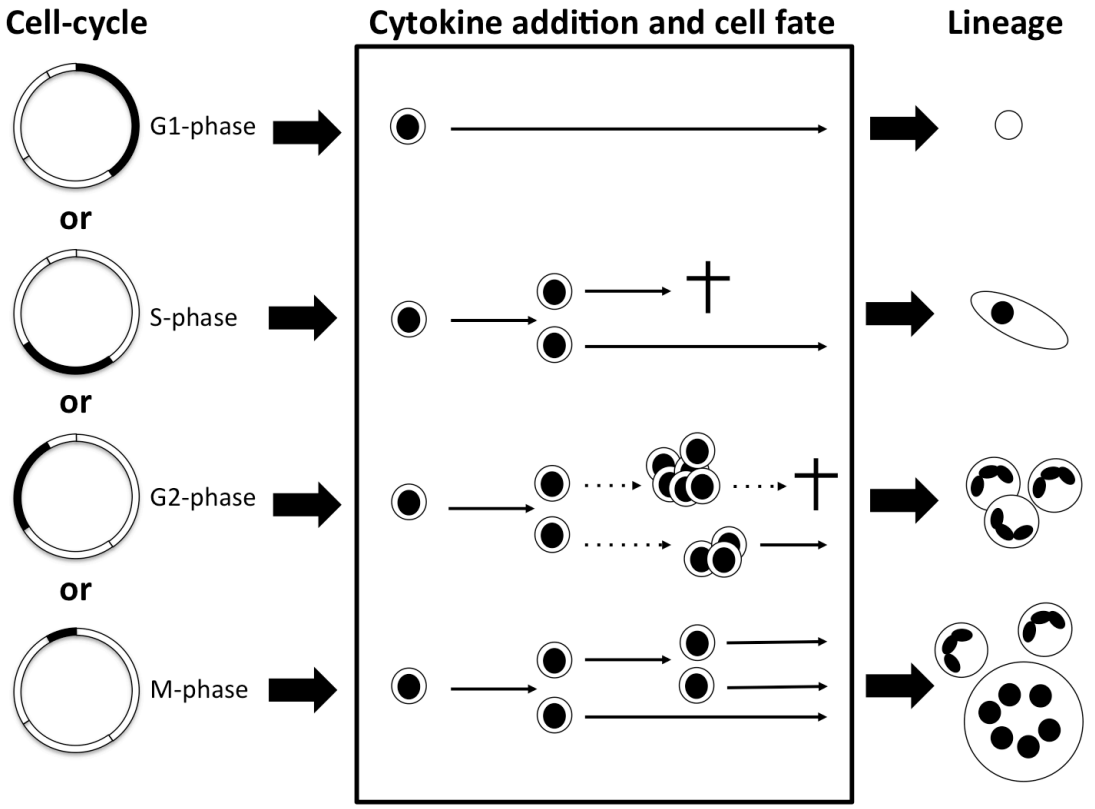

Figure 1.6-1: Cell fate detection requires continuous observation
Cartoon representing cellular behavior including few of many possible cell fates. Depending on cell-cycle different cell fates may occur leading to different lineage outcome and production. Black circles indicate nucleus, not on scale.

1.7 Cell-cycle reporters

In order to assess the influence of cell-cycle phase in lineage production upon cytokine addition, a non-invasive method needs to be applied to read-out both cell-cycle state on a clonal level and allowing detection of lineage production without cell state interference. Furthermore, measurement of cell-cycle phase durations and cell cycle transit in order to read-out a potential effect of cytokines on cell fate and cellular behavior, requires continuous data on a singular level that is exclusively obtained in live time-lapse imaging. To date, live antibody staining does not provide such tools and other mechanisms to e.g. read-out DNA content through fluorescent labeling with Hoechst33342 could potentially interfere with intracellular signaling. For this reason, different knock-in mice have been generated that are based on a fluorescent reporter that is either directly bound or linked to cell-cycle specific expression of cell-cycle regulators. Unfortunately, only few cell-cycle reporter mice are available. Based on Cdt-1 (G_1-phase accumulation) and Geminin (S/G_2-phase accumulation), a double knock-in containing two different fluorescent proteins was

made allowing visualization of the G_1 to S-phase transition by flow cytometry and microscopy using fluorescence (Sakaue-Sawano, Kurokawa et al. 2007). The limitations however lie in the fact that for optimal quantification, two fluorescent wavelengths are required and time-consuming quantification needs to be done post-acquisition. Furthermore, the transition does not reveal differences within G_1-phase and since the reporter is not-ubiquitously expressed in blood (detectable in ~1% of HSCs), usage of this reporter mouse may not prove beneficial for HSC studies.

Another reporter mouse allows distinction between interphase and metaphase, which is based on a fluorescent biosensor with a nuclear localization sequence during interphase and a plasma membrane targeting sequence that shows membrane localization upon nuclear envelope breakdown during metaphase. Hence, this cell-cycle biosensor unfortunately provides no distinction between G_1, S and G_2-phase. Combined with its non-ubiquitous expression, it is not a good candidate to follow-up the influence of cell-cycle phase in differentiation (Burney, Lee et al. 2007; Hesse, Raulf et al. 2012).

A very powerful tool, yet not available as a reporter mouse, is a proliferating cell nuclear antigen-based (PCNA) biosensor. PCNA tethers DNA polymerase delta to the DNA upon DNA synthesis in S-phase specific replication and the replication foci that are formed consist of trimers. This biosensor links each monomer to a fluorescent protein, thereby visualizing S-phase progression (Bravo, R et al. 1987; Leonhardt 2000). Its nuclear localization throughout all cell-cycle phases requires continuous high magnification fluorescent microscopy in HSCs to read-out both cell-cycle state and cell-cycle phase durations and the absence of these foci during G_1 and G_2-phase furthermore requires a high temporal resolution to distinguish these phases due to the gradual, yet fast transition of replication foci and provides cell-cycle data retrospectively. For expression in primitive primary blood cells, this requires viral transduction with relatively high multiplicity of infection (MOI) to allow visualization at early time-points. For specific questions that can be answered with short-term imaging, rather than high-throughput imaging, testing and optimization, this may prove a very powerful tool.

To date, one of the best candidates to continuously detect cell-cycle state is based on the C-terminus of human DNA helicase-B, active and with nuclear localization during G_1-phase to allow DNA repair. This phosphorylation-dependent subcellular localization domain (PSLD) consists of a nuclear localization signal and seven cyclin-dependent phosphorylation sites. Upon expression of cyclin E and cyclin A in the late G_1-phase, PSLD is phosphorylated and pumped out of the nucleus by activation of a nuclear export signal. From early S-phase its localization is then purely cytoplasmic. This transition allows the observation of G_1 to S-phase transition as well as metaphase when the nuclear membrane is degraded (Gu, Xia et al. 2004; Stubbs 2005; Hahn, JT et al. 2009) (Figure 1.7-1).

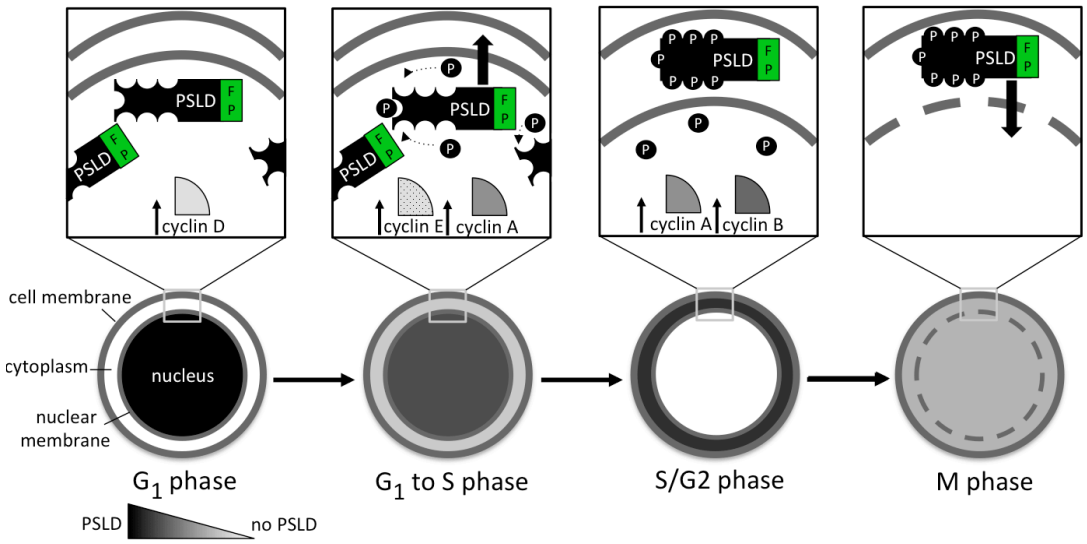

Figure 1.7-1: a PSLD-based cell-cycle fluorescent reporter
PSLD subcellular localization during cell-cycle transition. Simplified cartoon does not indicate true scaling. PSLD (phosphorylation-dependent subcellular localization domain), FP (fluorescent protein).

Using PSLD allows continuous quantification of cell-cycle phase transitions and furthermore fulfills the requirements to non-invasively study the effect of cytokines on cell fate in different cell-cycle phases. In addition, this would also allow further quantification of cytokine directed signaling pathway activation through e.g. immunofluorescence or by use of biosensors in a cell-cycle dependent manner to elicit underlying molecular mechanisms that orchestrate cell fate.

1.8 Signaling pathways involved in lineage production

With so many factors influencing the cell fate, it is ultimately the signaling

pathways that mediate the effects of cytokines. Activated receptors, either by ligand binding or stimuli such as shear stress, cause intracellular and sometimes also extracellular modifications and attract adaptor molecules to activate kinases. They phosphorylate other proteins that can either dimerize and translocate or are directly transported to the nucleus, where they act on regulatory proteins to induce or repress transcription factor activation.

Several cytokine-induced signaling pathways that are known to play a role in survival also have been shown to be important for HSC regulation. SCF mediated signaling through the c-kit receptor activates different signaling pathways, perhaps the best established being p42/44 (extracellular signal-regulated kinase, ERK1/2) and phosphatidylinositide-3 kinase (PI3K). Kit signaling has been shown to be crucial to maintain quiescence of HSCs (Thorén, Liuba et al. 2008) and defects in its downstream signal transducer and activator of transcription 5 (STAT5) have revealed major hematopoietic deficiencies (Bradley and Hawley 2002; Wang, Li et al. 2009). In addition to their importance in Kit signaling during quiescence, ERK1/2 and PI3K can directly affect survival and proliferation through up regulation of cyclin D1/2 levels, facilitating transit into cell-cycle (Blomen and Boonstra 2007).

PI3K, also activated through TPO/Mpl signaling (Kirito, Watanabe et al. 2002), can also activate beta catenin and mediate different signaling cascades, including *p300/CBP*, *Myc*, *Notch1* and cell-cycle regulators. Hence, it is not surprising that PI3K is not only important for HSC survival and proliferation but is also involved in the maturation of different committed progenitors towards the megakaryocytic lineage, possibly through the downstream target mTOR (mammalian target of rapamycin) (Raslova, Baccini et al. 2006).

Mitogen activated protein kinases, including p38 and ERK1/2, can be activated by Mpl-signaling and are important for both proliferation and maturation of megakaryocytic progenitors (Melemed, JW et al. 1997; Whalen, SC et al. 1997; Fichelson and Freyssinier JM 1999). Furthermore, there is strong evidence that their activation is crucial for endomitosis in the megakaryocytic lineage, whereas Src kinases form negative factors for megakaryopoiesis (Rouyez, C et al. 1997; Rojnuckarin, JG et al. 1999; Kaminska, Klimczak-Jajor et al. 2008; Severin, Ghevaert et al. 2010). Although often found present throughout different phases of the cell-

cycle, it has been hypothesized that their nuclear translocation is transient and cell-cycle specific, creating a time window for MAPK to act and facilitate maturation of megakaryocytic progenitors (Blomen and Boonstra 2007; Kaushansky 2008). With the prospect of defining cytokine-induced differentiation, it should therefore be of extra interest to further investigate the role of cell-cycle phase and its dependency in signaling pathway activation.

1.9 Clinical relevance for *ex vivo* HSC expansion

Despite all the medical advances in the blood field, there is no fully reliable cure for leukemia. Patients that are confronted with severe blood disorders often have poor chances of survival and high chances of relapse. Furthermore, the burden they are facing every day when treated for blood malignancies strongly reduces quality of life. The underlying reason for blood disorders such as acute myeloid leukemia (AML) can often be traced to the existence of a single gene mutation or chromosomal aberration in a single cell, often termed leukemia initiating stem cell (LISC). The existence of such a cell, or pool of cells, is the main target in therapies targeting leukemia. Independent of their position in the hematopoietic hierarchy, these cells have three things in common, they: (1) proliferate fast due to an increased rate of self-renewal divisions, (2) are stuck in differentiation and do not fully mature, and (3) often have a mechanism that protects them from standard drugs that target proliferating cells. In addition, these fast proliferating cells are often found to inhibit production of certain lineage subsets and drastically change the architecture of the bone marrow.

Current therapies are mostly comprised of a combination of chemotherapy, radiation therapy, hormone treatment and daily medication. Ultimately, ablation of autologous bone marrow is performed. With the microenvironment staying relatively intact but drastically changed after bone marrow irradiation, depletion of all blood cells including HSCs requires the patient to undergo HSC transplantation. The problem that arises is that previously taken biopsies may again contain LISC and relapse may occur. Furthermore, these cells contain both HSCs and mature cells to sustain hemopoiesis at long-term and short-term, respectively, often in too low numbers to be effective. Consequently, non-autologous, or allogeneic HSC

transplants are often performed with the risk of inducing host-versus-graft-disease (HVGD), but mostly increasing the risk of graft-versus-host-disease (GVHD), in which the donor immune system induces an immune response and attacks recipient tissues (Ferrara, Levine et al. 2009; Blazar, Murphy et al. 2012).

Some studies focus on the relief of the burden associated with GVHD and facilitating the efficacy of HSC transplants, by for example co-injection of mesenchymal stromal cells (Tolar, Le Blanc et al. 2010). Other studies focus on improving ways to induce stem cell expansion. Considering the fact that HSCs are hard to maintain *ex vivo* in short-term culture, it is obviously a challenge to induce self-renewal divisions without losing the potential to differentiate into all blood lineages life-long. With the discovery that umbilical cord blood cells are not only enriched for HSCs but simultaneously have a much lower immune response upon stimulation with mismatched human leukocyte antigen (HLA) cells (and therefore are less susceptible to the recipients foreign body reaction to trigger GVHD) these cells have become a topic of interest (Harris, Schumacher et al. 1992; Rocha, Cornish et al. 2001). Their better reconstitution potential and the fact that they do not require biopsies would further make this procedure highly effective and lower the patient's burden in clinical setting. However, their low abundance and the high number of HSCs necessary per effective treatment still require *ex vivo* expansion.

1.10 Expansion methods and limitations

A net *ex vivo* expansion of murine HSCs has first been achieved in 1997, where freshly isolated HSCs were kept under different culture conditions for different periods of time, after which they were transplanted. Using limiting dilution assays, they found a ~4 fold increase after 10 day when cultured with interleukin-11, SCF and Flt-3. Similarly and by using the same conditions, a ~4 fold increase in HSC number was found by transplanting cells that had already divided, as determined by reduced levels of CFSE in flow cytometry (Miller and Eaves 1997; Oostendorp, Audet et al. 2000). Using SCF and thrombopoietin, Ema et al. pointed to the existence of potential self-renewal divisions *in vitro*, although overall absolute numbers resulted in a net loss (Ema, Takano et al. 2000). These studies showed that without stroma co-culture it was possible to not only maintain HSCs but potentially even increase their *ex vivo*

numbers. Since then media additions have become popular to induce *ex vivo* HSC expansion.

Addition of retinoic acid receptor agonists retains to some extent the repopulation activity of hematopoietic stem and progenitor cells after two weeks of culture (Purton, Bernstein et al. 2000). However, LSK cells were cultured in bulk and transplanted as such and HSC numbers were not determined through limiting dilution assay. This forms a problem since this could potentially point to an effect caused by repressed differentiation of MPPs rather than HSC maintenance. Moreover, repopulation activity, which was measured by peripheral blood contribution over several weeks, showed a strong decline which is characteristic for MPPs and did not reach the same contribution levels compared to freshly isolated, e.g. non-cultured and transplanted LSK cells. A more recent study found that the G0S2 protein, that is solely up-regulated through retinoic acid in the hematopoietic system, enhanced the quiescence of LSK SLAM HSCs (Yamada, Park et al. 2012). The exact mechanism is however still not known.

Well known for their capacity to maintain stemness of HSCs are the AFT and PA6 stromal cell lines. AFT cells are a clonally expanded cell line that has been shown to maintain HSC numbers up to 4 weeks of *ex vivo* culture by a mechanism still unresolved (Nolta, Thiemann et al. 2002). Originating from fetal liver, these cells were thought to have the potential to induce self-renewal divisions since primary fetal liver HSCs rapidly expand in this environment during development. Although not observed *in vitro*, it might well be that AFT cells could still possess this capability but their immortalization, media conditions and potential changes in karyotype or a combination thereof are the cause of the loss of their potency to expand HSCs. Alternatively, PA6 cells (pre-adipocytes from mouse calvaria) have been shown to be able to maintain HSC numbers and potentially increase their numbers in short-term culture (Kodama, Sudo et al. 1984; Shimizu, Noda et al. 2008). However, stromal co-cultures seem only capable to a limited extent to maintain HSC potency rather than inducing HSC expansion.

Through genetic manipulation, further efforts in HSC expansion have been successful. Deletion of a G_1-phase inhibitor, p18, in an *in vivo* mouse model has been

shown to increase self-renewal divisions in HSCs and facilitate engraftment upon transplantation (Yuan, Shen et al. 2004). Despite the increased cell-cycle entry, no long-term exhaustion of the HSC pool has been observed after deletion of p18 even to an extent of quaternary transplants, in contrast with previous studies that showed increased HSC cell-cycle activity (Yu, Yuan et al. 2006).

From *in vivo* expression levels, it is known that Notch signaling plays an important role in maintaining quiescence of HSCs. Its overexpression in LSK cells results in the immortalization of cells with an undifferentiated, blast-like phenotype. By culturing them with specific cytokines, these cells were capable of long-term donor contribution upon transplantation, but showed lineage-bias *in vitro* and *in vivo* (Varnum-Finney, Xu et al. 2000). Immortalization of LSK Thy-1.1^{low} cells by overexpression of the *bcl*-2 gene, an anti-apoptotic gene, resulted in a minimal increase *in vivo*. *In vitro* plating efficiencies were higher and chimerism was stronger even in competitive repopulating units with wild-type HSCs (Domen, Cheshier et al. 2000). Although not present in younger mice, adult and aging mice showed an increased prevalence of myeloid and lymphoid leukemia. Its *in vitro* potential has not been reported to date.

The limited expansion that was achieved through various HSC manipulations did not lead to improvements in a clinical setting and requires genetic engineering and modification. This not only should provide a more robust method but also shows a direct effect from gene up-regulation rather than a heterogeneous effect of extrinsic factors. Simultaneously, genetic engineering could not only be directed to expansion of existing HSCs but also to induction of an HSC phenotype in multipotent progenitors that have a much higher *in vivo* prevalence. Furthermore, in order to understand the underlying mechanism of HSC function and expansion as well as how they relate to leukemic cells, HSC behavior will need to be studied and compared to correlate with gene function. From gene expression profiling many hematopoietic regulators have been identified and through overexpression of various genes that are highly and/or exclusively expressed in HSCs, the potential for HSC expansion has been further explored. The exclusive expression of several of the homeobox genes at the HSC level made them of key interest in genetic engineering to induce HSC expansion. However, differences in their behavior towards non-expanding or

differentiating HSCs still need to be elucidated in order to understand the underlying mechanism.

1.11 Homeobox genes

During development, proliferation and differentiation as well as induced apoptosis are tightly controlled in order to form highly specialized tissues. Master regulators of these processes are a set of genes called homeobox genes (HOX), from *homeosis,* a process in which one body part transforms into another, which occurred in *drosophila melanogaster* upon mutations in these genes. Highly preserved during evolution and amongst species, they are found clustered on 4 chromosomes and are abbreviated HOXA-D, having a total of 39 genes in both mouse and human. Each cluster contains between 9 and 11 genes that are not only linked within each cluster but also have synergistic functions between parallel HOX clusters forming a total of 13 functional groups that show large homology (Lappin, DG et al. 2006). Not only do their temporal expression correlate with their chromosomal location (3` to 5`), their expression is also spatially defined, occuring from the anterior to posterior region, respectively (Figure 1.11-1, (Lappin, DG et al. 2006).

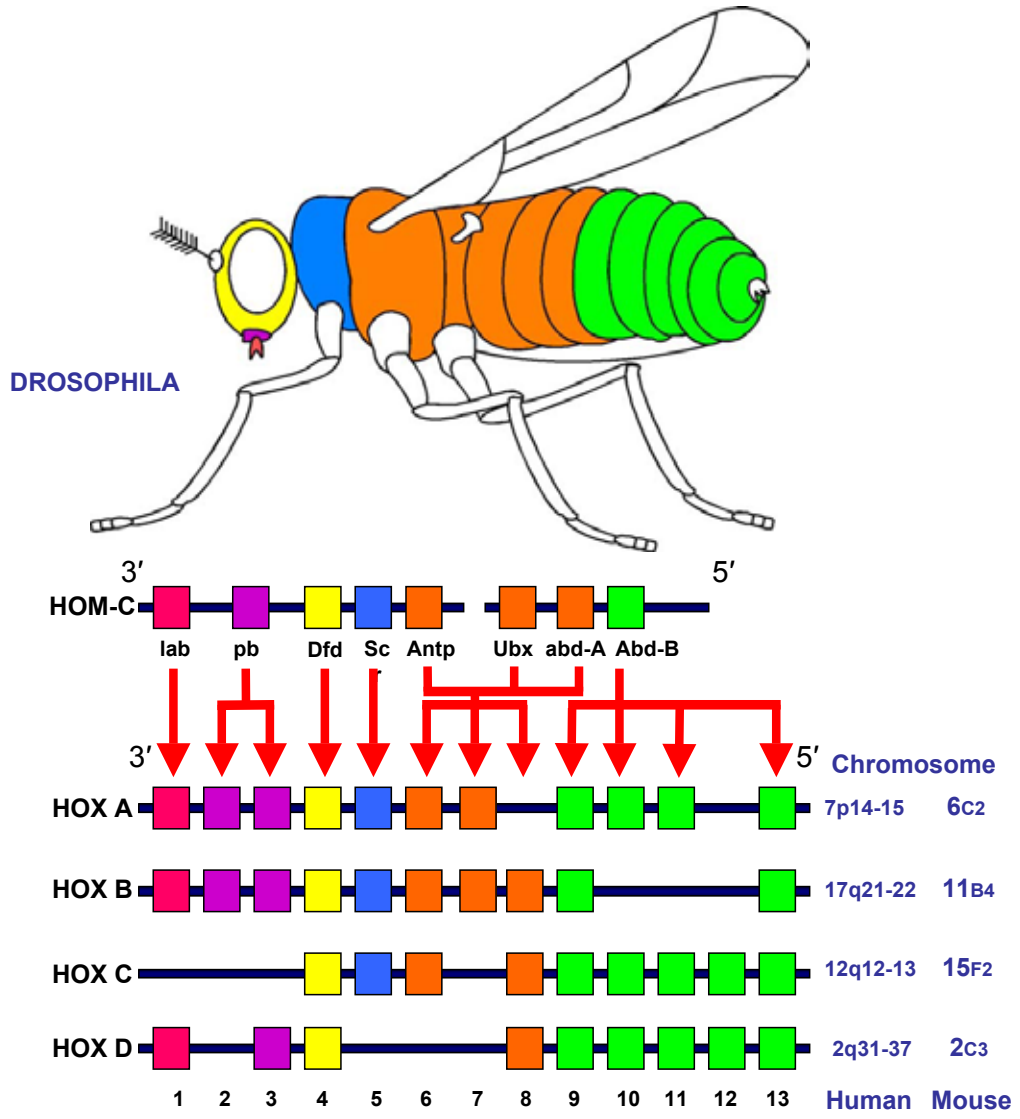

Figure 1.11-1: Conservation between the *HOM-C* and *HOX* gene clusters
Classification and organization of 39 *HOX* genes in 13 parallel functional clusters. The 3`genes are expressed more anteriorly and in earlier developmental stages than the 5`genes. With copyright permission from author (TRJ Lappin).

The main functional parts of HOX proteins are the homeodomain (HD) at the C-terminus, the nuclear localization sequence and the TALE (three amino acid loop extension) region, both found at the N-terminus. The homeodomain consists of 60 amino acids that define its DNA binding specificity. The N-terminus facilitates the DNA binding through binding of co-factors at the TALE region, such as Meis-1 and Pbx (Lappin, DG et al. 2006; Ohta, Sekulovic et al. 2007) (Figure 1.11-2).

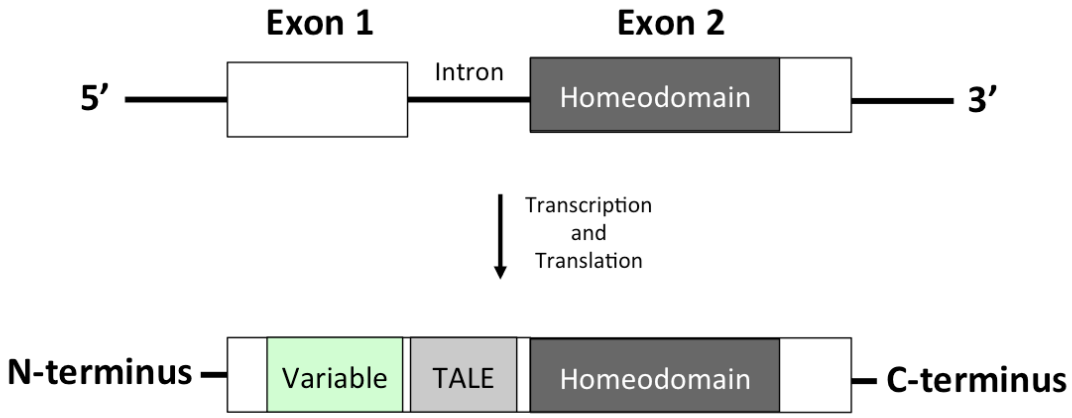

Figure 1.11-2: Conserved homeobox gene and protein structure
Schematic overview of *HOX* gene and HOX protein structure with different domains (not on scale). TALE (three amino acid loop extension) binding domain and variable domain are located at the N-terminus whereas the homeodomain (DNA binding) is found at the C-terminus.

In HSCs, HOX genes A, B and C are highly expressed. Upon differentiation, their expression is down-regulated, as during development, from 3`to 5`, suggesting that 3` HOX genes play a role in retaining multipotency or self-renewal capacity. The high expression level of HOXB3 and HOXB4 in HSCs (Sauvageau, Thorsteinsdottir et al. 1995; Lawrence, Sauvageau et al. 1996) has proven the plausibility of this hypothesis, since overexpression studies revealed a significant increase in HSC numbers in *ex vivo* culture (~80 fold), more comparable to the normal *in vivo* proliferation capacity upon transplantation (~100 fold) (Pawliuk, Eaves et al. 1996; Antonchuck, Sauvageau et al. 2002; Buske, Feuring-Buske et al. 2002; Sauvageau, Iscove et al. 2004). Moreover, HOXB4 overexpression leads to a much better engraftment potential compared with freshly isolated HSCs (Antonchuk, Sauvageau et al. 2001). This striking effect not only lies in the potency of HOXB4 to expand HSCs under culture conditions normally pushing myeloid differentiation, but similarly in the fact that this is reversible upon transplantation and homing into the *in vivo* HSC niche.

On the other hand, overexpression or deregulation of other HOX genes leads to many blood disorders and malignancies, ranging from a perturbed lymphoid differentiation potential to the onset of latent leukemia (Thorsteinsdottir, Sauvageau et al. 1997; Buske, M et al. 2001; Thorsteinsdottir, Kroon et al. 2001; Owens and Hawley 2002; Thorsteinsdottir, Mamo et al. 2002; Sitwala, Dandekar et al. 2008). HOXA9 overexpression was found to further increase HSC expansion but resulted in

a latent leukemia onset. The fast proliferation of these cells and their blast-like phenotype, residing in an undifferentiated state *in vitro*, made it of key interest to further investigate the potential of different HOX gene-based engineered constructs that could further enhance HSC expansion but with leukemia exclusion.

1.12 NA10HD

About 5% of all AML cases are related to chromosomal rearrangements or translocations affecting HOX genes. The translocation t[(7;11)(p15;p15)]- HOXA9, with nucleoporin 98 (NUP98)- results in rapid onset of AML and rapid proliferation (Borrow, Shearman et al. 1996). This was confirmed by overexpression of a construct containing this fusion gene in healthy primary HSCs, which indeed led to rapid leukemia onset upon transplantation (Kroon, Thorsteinsdottir et al. 2001; Calvo, Sykes et al. 2002). Other HOX fusions with NUP98 were found to increase HSC expansion with sometimes a very latent leukemia onset. The underlying mechanism is most likely the binding of CREB binding protein (CBP) and p300, both having a high affinity for the FG repeats at the N-terminus of NUP98 and acting as adapter molecules and co-activators (Kasper, PK et al. 1999; Ghannam, Takeda et al. 2004) (Figure 1.12-1). The question then was whether upon overexpression, different HOX genes are intrinsically oncogenic or became oncogenic upon fusion with NUP98 (Abramovich, N et al. 2005). To test this, constructs were engineered containing fusions of NUP98-HOXB4 and NUP98-HOXA10, which were then transduced into HSCs and transplanted after *ex vivo* cultivation. While overexpression of NUP98-HOXB4 further increased the HSC expansion potential without developing leukemia, NUP98-HOXA10 overexpression also resulted in a strong fold expansion of HSCs, albeit with a latent leukemia onset (Pineault, Abramovich et al. 2004).

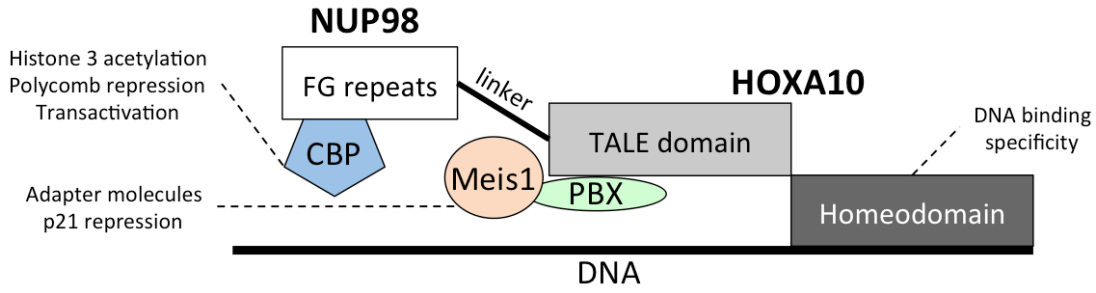

Figure 1.12-1: NUP98-HOXA10 fusion protein with protein complex partners

The TALE domain can bind adapter molecules PBX and Meis1, which can coactivate other down-stream targets, whereas the NUP98 is often co-localized with CBP/p300. In NA10hd the TALE domain is missing.

Interestingly, the leukemic potential of NUP98-HOXA10 seemed to be dependent on binding of Meis-1and independent of its DNA binding capacity. Thus, upon binding of CBP through NUP98 interaction, the flanking domains of the HOX gene containing the TALE domain seemed sufficient to induce leukemia (Pineault, Abramovich et al. 2005). By deletion of this TALE domain (NA10hd), Ohta et al. postulated the potential of HSC expansion could be maximized while the risk of latent leukemia was lost. Using limiting dilution assays in competitive repopulating assay, they showed a 1000 fold net increase in HSCs after 10 days of *in vitro* cultivation (Ohta, Sekulovic et al. 2007), in the range of the maximum *in vivo* HSC proliferation (~8400 fold, (Sauvageau, Iscove et al. 2004). Moreover, no leukemia was detectable and no *in vivo* lineage bias was observed, contrary to lymphoid bias upon HOXB4 overexpression (Haddad, Pflumio et al. 2008).

Due to their promising clinical potential, most studies now focus on further improving HSC expansion, using NA10hd or HOXB4 overexpression as a standard base line. Initially providing good results and potential genes of interest (Deneault, Cellot et al. 2009), these studies have recently been interpreted with care since the observed effect may come from an altered phenotype in overexpressing feeder lines, inducing different secreted molecules (Deneault, Wilhelm et al. 2013). Until now, NA10hd overexpression is therefore the most effective HSC expansion method. With recent advances in primate models, clinical applications may be the next step to proceed (Watts, Zhang et al. 2011).

Despite the strong contrast from control HSCs that rapidly lost their self-renewal potential due to myeloid differentiation, a NA10hd specific mechanism has yet to be defined. At first sight, no direct differences in proliferation rates were found. Although initially tested in bulk cultures with poor HSC purities by 5-fluoroacil treatment, a drug that ablates cycling cells and mobilizes quiescent cells such as HSCs, a recent paper could show similar results using clonal culture and higher HSC purity (Sekulovic, Gasparetto et al. 2011). In addition they showed that further addition of thrombopoietin fully diminishes HSC expansion. With data suggesting the

acquisition of a fetal liver HSC phenotype due to its high proliferation capacity, until now nothing is known about the mechanism of NA10hd induced HSC expansion, although preliminary comparisons have revealed multiple down-stream targets such as *FLT3*, *HLF* and *JAG2* (Palmqvist, Pineault et al. 2007).

Together this shows that recent gene profiling studies and further categorization and modification of NA10hd-induced expansion were still insufficient to elicit an underlying mechanism. Both the influence of extrinsic factors as well as behavioral differences are poorly understood. Furthermore, little is known about the *in vivo* reversibility and control of both self-renewal and differentiation. Since the majority of these studies were performed in bulk culture, large heterogeneity would mask the existence of distinct classes and behavioral subsets would not be detected. In addition, inheritance of daughter cells with respect to both marker expression and proliferation rate cannot be assessed since genealogy is lost, which furthermore leaves the question unanswered whether true HSCs are expanded or HSC potential is induced. For these reasons, a clonal *in vitro* read-out using continuous time-lapse imaging would prove an outcome in defining NA10hd behavior. Long-term imaging for more than 7 days has been difficult to implement due to either accumulation of high numbers of cells or following low density seeding. While the former results in loss of clonal identity, the latter has the consequence that larger surface areas need to be covered with the consequence of impairing temporal resolution. Further optimization of both culture conditions as well as software and imaging techniques should allow such read-outs with preservation of genealogy. Not only would this provide deeper insight in NA10hd behavior, combined with quantification of surface marker expression through live fluorescent antibody labeling, co-culture with stroma cells or control cells this would furthermore elicit cellular subsets and the influence of extrinsic factors such as cell-cell contact, respectively.

1.13 Stroma co-culture

PA6 cells are known to have the capacity to maintain HCSs stemness over multiple days under co-culture conditions. Their expression of SCF, Sca-1 and CD34 as well as interleukin-6 indicates their importance for survival and HSC maintenance and differentiation, respectively (Satoh, Mioh et al. 1997; Satoh, Mioh et al. 1997).

The expression of chemokine ligand 5 (CXCL5) further functions as a chemoattractant (Shimizu, Noda et al. 2008), similar to the production of the related CXCL12 in the *in vivo* niche. For HSC maintenance it has been shown that cell-cell interaction of the HSCs with the stromal cell layer is indispensable (Kodama, Amagai et al. 1982). Although PA6 cells do not permit B lymphoid development, addition of interleukin-7 can fully reestablish this potential (Sudo, Ito et al. 1989).

Due to their high optical clarity and their contact inhibition of growth upon confluence, these stromal cells form an excellent substrate to study HSC behavior. Mimicking *in vivo* cell-cell interactions with their niche or mimicking physiological conditions, HSCs can be observed long-time. With use of time-lapse imaging, HSCs can be tracked and factors as adherence, motility, apoptosis, and cell lifetime can be quantified in progeny of late generations and inheritance can be assessed, which to date has not been shown due to technical difficulties in both imaging and cultivation and cannot be detected in bulk culture or by snapshot analysis. Moreover, with use of fluorescent imaging and live antibody staining, marker expression can be accurately attributed on a clonal basis (Eilken, Nishikawa et al. 2009). Taken together, this method provides new insight and allows defining a signatorial behavior of HSCs during *in vitro* expansion.

1.14 Conclusion

There is evidence that cell-cycle phase may play a direct role in cytokine induced lineage production but HSC heterogeneity and technical challenges so far didn't allow to make the point. The lack of live cell-cycle quantification and the fact that most studies are performed on a population level furthermore hampered the assessment of cell-cycle dynamics and the existence of behavioral subsets. In addition, cytokines are known to direct blood lineage production but to date the question remains whether the effect on cell fate can be dependent on the cell-cycle phase at the time-point of administration. Such an effect on HSCs has not yet been shown. Finding such a correlation and unraveling the underlying molecular mechanism would potentially improve lineage specific production in a clinical setting *in vitro* and *in vivo*. For this reason, a clonal read-out that allows live cell-cycle

quantification while assessing lineage commitment would be of key interest to answer these long-standing questions.

Instead of directing lineage production to derive specific mature subsets, another focus lies in *ex vivo* expansion of HSCs to treat patients that require transplantation. The engineered fusion protein NA10hd has been shown to induce over a 1000-fold expansion *in vitro* within 1 week of culture. However, its mechanism is still unknown. To further understand what drives this expansion and how these cells differ from non-manipulated HSCs that differentiate *in vitro*, the behavior of these NA10hd cells, in terms of cell division rate, apoptosis, marker expression, adherence and migration needs to be followed up. The *in vivo* reversion of the differentiation block found *in vitro* as well as the reduced proliferation kinetics furthermore require in-depth assessment how niche or cell-cell interactions are involved in altering NA10hd behavior.

2 Aims of the thesis

It has long been an outstanding question whether cells receiving the same cytokine in different cell-cycle phases will have diverging cell fates. Moreover, it still remains unclear whether at the level of the most primitive HSCs, cytokines can already direct lineage decision. The aim of this thesis is to verify whether both phenomena exist using time-lapse imaging at single-cell resolution. For this purpose, live cell-cycle quantification first needs to be established in primary HSCs. This not only allows assessing and scoring of cell-cycle phase upon cytokine addition but also allows observing how HSCs transit through cell-cycle over multiple generations.

End-point lineage production and thus multipotency can be correlated with both the initial cell-cycle phase and cell-cycle durations and transitions in subsequent generations, identifying a lineage-specific behavior so far not possible due to either loss of ontogeny or initial cell-cycle state. Using time-lapse imaging, cytokines can be also added after the first *in vitro* cell-cycle division to test whether cell-cycle specific cell fates are equally applicable to daughter cells and test for HSC specificity. With such a technique, the effect of specific additional cytokines can be directly measured.

Focusing specifically on cells with multilineage potency, in-depth analysis of *in vitro* NA10hd HSC behavior will be completed by comparison of cell lifetimes of progeny and ancestry, which to date remained elusive. Finally, the effect of stromal co-culture will shed light on the effect of cell-cell contacts on NA10hd HSC behavior, mimicking the reduced proliferation found in the *in vivo* niche.

3 Materials, methods and experimental procedures

3.1 Purification

3.1.1 HSC isolation

Femurs, tibiae and pelvic bones were dissected from male 12 weeks old C57Bl/6 mice and excessive tissue was removed. Bones were crushed using a mortar and pestle, re-suspended in 2% fetal calf serum (FCS) (cat. no. A15-101, PAA) in Dulbecco's phosphate buffered saline (PBS) (cat. no. 14190-094, Gibco, Life Technologies, Paisley, UK) and passed through a 100 µM cell strainer (cat. no. 352360, BD Falcon, Schubert & Weiss Ombilab GmbH, Munich, Germany) into a 50 mL polypropylene (PP) tube (cat. no. 352070, BD Falcon, Schubert & Weiss Ombilab GmbH, Munich, Germany). After centrifugation (all centrifugation steps performed at 240 RCF, 5 min 4°C, (cat. no. 5805, Rotanta 460R, Hettich Zentrifugen, Tuttlingen, Germany)), erythrocyte lysis was performed using ACK lysing buffer (cat. no. 10-548E, Lonza, Walkersville, USA) for 2 min on ice at 2.5 µL/10^6 cells. Cells were washed and resuspended in FACS buffer containing 5% FCS in PBS with 1 mM EDTA (cat. no. ED4SS-100G, Sigma-Aldrich, Steinheim, Germany) at 10^8 cells/mL and lineage depletion was performed using the following antibodies:

Table 3.1-1: Lineage depletion for HSC purification

Antibody	Clone	Cat. No.
B220-biotin	RA3-6B2	13-0452-86
CD3-biotin	145-2C11	13-0033
CD19-biotin	1D3	13-0193-85
CD11b-biotin	M1/70	13-0112-85
Gr-1-biotin	RB6-8C5	13-5931-85
Ter119-biotin	TER-119	13-5921-85

Cells were stained at 50 ng/10^6 cells. All antibodies were obtained from eBioscience, San Diego, USA.

After 20 min incubation on ice, cells were re-suspended in buffer and Roti-MagBeads Streptavidin (cat. no. HP57.1, Carl Roth, Karlsruhe, Germany) was added at 0.4 µL/10^6 cells. After 10 min at room temperature (RT), cells were transferred into 14 mL polypropylene tubes (cat. no. 352059, BD Falcon, Schubert & Weiss Ombilab

GmbH, Munich, Germany) and lineage depletion was performed for 7 min at RT using an Easy Sep magnetic assisted cell sorter (cat. no. 18001, Stem Cell Technologies, UK).

Lineage negative (Lin^-) cells were stained with fluorescent protein conjugated antibodies for further purification in 100 µL buffer:

Table 3.1-2: HSC and MPP purification using fluorescence in flow cytometry

Antibody	Concentration	Clone	Company	Cat. No.
CD48 FITC	40 ng/10^6 cells	HM48-1	Biolegend	103404
CD150 PE	40 ng/10^6 cells	TC15-12F12.2	Biolegend	115904
CD135 PE Cy5	40 ng/10^6 cells	A2-F10	eBioscience	15-1351-81
CD117 PE Cy7	60 ng/10^6 cells	2B8	eBioscience	25-1171
CD34 E660	100 ng/10^6 cells	RAM34	eBioscience	50-0341-82
SA APC E780	40 ng/10^6 cells		eBioscience	47-4317-82
Ly6A/E PB	40 ng/10^6 cells	D7	Biolegend	108120

Fluorescence-conjugated antibodies were used for HSC enrichment. Used abbreviations: Fluorescein isothiocynate (FITC), phycoerythrin (PE), phycoerythrin cyanine 5 (PE Cy5), phycoerythrin cyanine 7 (PE Cy7), eFluor660 (E660), streptavidin allophycocyanin eFluor 780 (SA APC E780), Pacific Blue (PB).

Compensation tubes were prepared with Lin^+ cells at 0.2 µg/50µL cell suspension with the above antibodies. Cells were incubated for 60-90 min at 4°C. Before cell sort, cells were strained through a 35 µM filter (cat. no. FALC352235, BD Falcon, Schubert & Weiss Ombilab GmbH, Munich, Germany) into a 5 mL PP tube.

3.1.2 Flow cytometry

All cell purifications and analyses were performed on a FACSAria III machine (Becton Dickinson, San Jose, USA) with FACSDiva software. Equipped with 4 lasers, following filters were used for different fluorochromes and fluorescent proteins:

Table 3.1-3: Fluorescence activated cell sort

Laser	Filter	Fluorochrome / fluorescent protein
405 nm	450/40	PB
488 nm	530/30	FITC, VENUS
	695/40	PerCP E710
561 nm	586/12	PE
	610/20	PI, mCHERRY
	670	PE Cy5
	780/60 I	PE Cy7
633 nm	660/20	E660
	730/45	Alexa700
	780/60 II	APC E780

Multicolor flow cytometry allows usage and detection of up to 10 antibodies simultaneously and facilitates high purification of HSCs. Laser, excitation and emission settings for flow cytometry.

Compensation was performed using biexponatial settings and single stain compensations. Gates were set using unstained control and contour plots. Before sorting, drop delay was performed using auto settings and accudrop fluorescent beads (cat. no. 345249, BD) and a test sort was performed. Purification was then performed using a 70 μM nozzle and a frequency of 87 kHz at an average of ~10^4 events/second into 5 mL PP tubes containing 2 mL of serum free essential medium (StemSpan SFEM, StemCell Technologies Inc.). Stream instabilities were prevented by cleaning the nozzle using a ultrasonic cleaner (cat. no. USC100T, VWR, Leuven, Belgium).

3.2 Vector cloning

3.2.1 Plasmids

Plasmids were cloned according to standard digestion and ligation protocols (Fermentas). DNA was generated by reverse transcriptase polymerase chain reaction (RT-PCR, cat. no. 28104, Qiagen) when necessary and purified using gel electroporation and extraction kits (cat. no. 20021, Qiagen). Following vectors were used in the course of both projects:

Table 3.2-1: Plasmids

In-house #	Domains
442	pRRL.RRE.PPT.SFFV.**IRES-VENUSnucmem**.PRE.SIN
638	pRRL.RRE.PPT.SFFV.**FNA10HD.IRES-VENUSnucmem**.PRE.SIN
663	pRRL.RRE.PPT.SFFV.**IRES-VENUSPSLD**.PRE.SIN
679	pRRL.RRE.PPT.SFFV.**mCHERRYPSLD**.PRE.SIN
860	pRRL.RRE.PPT.SFFV.**FNA10HD.IRES-mCHERRYPSLD**.PRE.SIN

The pRRL vector contains the promoter of the Rouse sarcoma virus (RSV), the 5´unique region (RU5), the primer binding site (PBS) for viral reverse transcriptase and the *gag* domain that provides core structural proteins. The *rev* (nuclear localization signal and for synthesis) responsive element (RRE) allows translation. The polypurine tract (PPT) facilitates initiation of the DNA plus strand, the post-transcriptional regulatory element (PRE) enhances levels of transcripts and the self-inactivating (SIN) domain provides further safety by leaving a defective promoter. All vectors contain ampicillin resistance.

Expression of all proteins of interest (bold) is driven by the spleen focus-forming virus (SFFV). Fluorescent proteins (VENUS or mCHERRY) were chosen for their strong emission, their low phototoxicity and their ease of combination with many live fluorescent antibodies. In co-expressing vectors, expression of fluorescent reporters was driven by an internal ribosome entry site (IRES). The nucmem domain stands for nuclear membrane localization and contains the human importin alpha 1 domain. The PSLD domain is described in 1.7. The Nup98-HOXA10homeodomain (NA10hd) contains a Flag-tag (F) at the N-terminal end combined with a linker protein, thereby not hampering its functional domains.

3.2.2 DNA preparation

DNA was extracted using a QIAGEN Plasmid Kit (cat. no. 12125, Qiagen Sciences, Hilden, Germany). Briefly, DNA from ligation products was transformed into DH5 competent bacteria using heat-shock and incubated overnight on agar plates containing ampicillin.

Single colonies were picked and inoculated overnight on a 37°C shaker in 4 mL of ampicillin containing LB medium. DNA extraction was then performed according to protocol using a microcentrifuge (Mikro 200, cat. no. 2400, Hettich Zentrifugen, Tuttlingen, Germany) and DNA was eluted in 30 µL milli-Q water. Test digests were performed and DNA quantity was measured. DNA was stored at -20°C.

3.2.3 Transfection

Polyethylenimine (PEI) solution was prepared by dissolving 100 mg PEI (cat. no. 23966, Polysciences Inc., Warrington, USA) in 900 mL 150 mM NaCl (cat. no. 32038-1EA, Sigma-Aldrich, Steinheim, Germany) at 80°C overnight. Solution was cooled and pH was adjusted to 7.8 using HCl. Volume was adjusted to 1 L using 150

mM NaCl and solution was filtered and stored at 4°C. 500 ng of plasmid DNA was then added to 66 µL polyetylenimine solution, vortexed for 10 s and incubated for 10 min at RT. Solution was then carefully added to each well containing 500 µL medium on HEK 293 cells and gently mixed by shaking. Expression and localisation were assed after 24 to 48 hours by epifluorescent microscopy.

3.3 Lentiviral production and transduction

3.3.1 DNA preparation

High quantities and concentrations of DNA were obtained using a QIAGEN Plasmid Kit (cat. no. 12165, Qiagen Sciences, Hilden, Germany). Briefly, 500 µL of 4 mL DNA containing bacterial culture was pipetted or DNA containing bacteria from glycerol stocks was inoculated into 100 mL ampicillin containing LB and incubated overnight on a 37°C shaker. DNA was then extracted and purified according to protocol and eluted in 100 µL milli-Q water. DNA was stored at -20°C.

3.3.2 HEK 293 culture

Immortalised human embryonic kidney cells from the 293rd experiment (Lenti-X HEK 293 T, (cat. no. 632180, Clontech)) were kept in 24-well plates (cat. no. 353047, BD Falcon, Schubert & Weiss Omnilab, Munich, Germany) for maintenance and were seeded at ~10^5 cells per well in Dulbecco's modified eagle medium (DMEM, cat. no. 31053-028, Invitrogen) containing 10% FCS. Cells were passaged every second day at a 1:8 to 1:10 ratio, using 0.05% trypsin (cat. no. 25300-054, Gibco) and re-suspended in media without centrifugation. For up scaling for lentiviral production, 9-cm dishes were used (cat. no. 150350, Thermo Scientific, Roskilde, Denmark). HEK 293 cells were kept until passage number 40.

3.3.3 Lentiviral production

4 plates of HEK 293 cells were plated at 5x10^6 cells/60cm^2 in DMEM containing 10% FCS. After 24 hours, media was aspirated and 10 mL of transfection media was added per plate (DMEM containing 2mM L-glutamine (cat. no. 25030-081, Gibco) and 0.1 mM sodium pyruvate (cat. no. 41966-029, Invitrogen), 10% FCS 1% penicillin/streptomycin, 100 U/mL and 0.1 mg/mL respectively (P/S, cat. no. 15070063, Gibco, Life Technologies, Paisley, UK) 20 mM HEPES (cat. no. 15630-056, Invitrogen). Then viral envelope vectors were added, diluted in 500 µL 0.25 M $CaCl_2$ in H_2O and mixed with 500 µL 2x HEPES buffered saline (50 mM HEPES,

280 mM NaCl, 1,5 mM Na_2HPO_4 (cat. no. P030.3, Carl Roth, Karlsruhe, Germany) in H_2O (pH 7.1)) with added $CaPO_4$ (cat. no. CAPHOS-1KT, Sigma-Aldrich, Steinheim, Germany) to 1M:

Table 3.3-1: Viral envelope DNA used for transduction

Plasmid	Function	Quantity
pUC19.RSV.REV (392)	Packaging	2 µg
CMV.betaglobin.gag.pol.RRE.PolyA.pUC19 (393)	Packaging	5 µg
pMD2-VSVG.IRES-Puromycin (495)	Envelope	5 µg
pAdVAntage (cat. no. E1711, Promega)	Translation	6 µg
Gene containing plasmid	Expression	5-8 µg

Abbreviations: Cytomegalo virus promotor (CMV), vesicular stromatitis Indiana virus (VSVG). For others see 3.2.1.

Cells were incubated overnight. At 48 hours, media was aspirated, 4.5 mL of transfection media was added containing 50 mM sodium butyrate (cat. no. B5887, Sigma-Aldrich, Steinheim, Germany).

At 72 hours, supernatant was collected and stored at 4°C. 4.5 mL of transfection media was added to all plates. At 96 hours, supernatant was again collected and pooled before centrifugation (200 RCF, 5 min at 4°C) in ultracentrifuge tubes (cat. no. 326823, Beckmann). Supernatant was filtered through a 0.22 µM filter into a new ultracentrifuge tube and centrifuged at 50000G for 1 hour at 4°C after calibration. Supernatant was removed and pellet was vortexed with 200 µL SFEM after 15 min incubation on ice. Virus was then aliquotted and stored at -80°C.

Titer was calculated using dilution series and calculating the percentage of positive cells per cell number by FACS analysis on NIH 3T3 cells at day 2 after virus addition in DMEM 10% FCS.

3.3.4 Lentiviral transduction

Cells were washed and counted by spinning down (240 RCF, 1 min at 4°C) 5 µL cell suspension into a well of a Nunc minitray (cat. no. 163118, Thermo Fisher Scientific, Roskilde, Denmark). The volume and amount of viral particles was calculated by dividing the cell number with the titer multiplied with the desired multiplicity of infection (MOI). For cell lines, a MOI between 1 and 10 was found sufficient, higher numbers were toxic in some cases. For primary cells, an optimum

was found at MOI 600, providing highest transduction efficiency (~80%) and no detectable increase in toxicity. Cells were transduced in 100 µL media in a 96-well Nunclon microwell plate (cat. no. 167008, Thermo Fisher Scientific, Roskilde, Denmark) and incubated for 24 to 48 hours before use.

3.4 Cell-cycle reporter validation

3.4.1 Propidium Iodide staining

Cells were washed and resuspended in 1 mL PBS. 2.5 mL of absolute ethanol (cat. no. 1009831000, Merck) was added drop wise and cells were fixed on ice for 5 min with repeated vortexing. Cells were centrifuged at 300 RCF for 5 min at 4°C and resuspended in 300 µL of 50 µg/mL propidium iodide (PI) (cat. no. P4170-25MG, Sigma-Aldrich, Steinheim, Germany) with 100ng/mL RNase A (Qiagen Sciences, Hilden, Germany) in PBS. After 1 hour of incubation at 37°C 5% CO_2, cells were centrifuged and 200 µL of supernatant was pipetted off before analysis.

Analysis was performed with FACSAria III using a 488 nm laser and 610 nm BP filter (see 3.1.2). Data was then processed with Flowjo software (Flowjo version X, Tree Star, Inc., OR, USA), using a Watson-Pragmatic or Dean-Jett-Fox model for distribution to set gates for different cell-cycle phases.

Alternatively, PI signals were quantified in a 384-well plate (cat. no. 88401, IBIDI, Martinsried, Germany) using Lumencor 590 nm (Laser2000) and suiting mCHERRY filter (cat. no. F36-508, AHF, Germany). Images were quantified using AMTsingle software (unpublished).

3.4.2 PSLD quantification

To verify the validity of PSLD in determining cell-cycle phase, cells stained with PI were directly compared with cells that had been transduced with a mCHERRYPSLD expressing lentiviral vector (see 3.2 and 3.3). Cells were categorized using published descriptions and cell numbers were assessed using FIJI software (ImageJ 1.47k, NIH, USA). Comparison was then performed using MS Excel plotting and Graphpad Prism 5 (GraphPad Software, Inc., CA, USA).

3.5 Erythrocyte detection using fluorescent antibodies

Granulocyte-macrophage progenitors (GMPs) and megakaryocyte-erythrocyte progenitors (MEP) were sorted by flow cytometry (Lin^- $Ly6A/E^-$ $CD117^+$ $CD34^+$ $CD16/CD32^+$ and Lin^- $Ly6A/E^-$ $CD117^+$ $CD34^-$ $CD16/CD32^-$, respectively). GMPs were cultured for 5 days in SFEM with 10 ng/mL M-CSF, with live antibody staining using anti-F4/80-conjugated APC and CD71-conjugated FITC (See 5.7). MEPs were cultured in SFEM 100 ng/mL SCF 100 ng/mL TPO 10 ng/mL IL-3 2 U/mL erythropoietin (cat. no. C-60022, Promokine) 10% FCS 50 µM 2-mercaptoethanol (cat. no. M3148-25ML, Sigma-Aldrich, Steinheim, Germany) and 1% L-glutamine with anti-CD105-conjugated Alexa 555 and anti-CD71-conjugated FITC (see 3.7). Cultures were analyzed after 5 and 7 days and CD71 signals were quantified.
As a comparison, freshly stained lineage subsets from whole bone marrow were compared for CD71 expression using flow cytometry.

3.6 Cell culture

Cells were incubated at 37°C, 5% CO_2 and 99% humidity in a controlled incubator (CD210, Binder, Tuttlingen-Möhringen, Germany). Tips were obtained from Greiner Bio-one (cat. no. 710190 (2 mL), 606180 (5 mL), 607180 (10 mL) and 760180 (25 mL), Frickenhausen, Germany) and Omnitip (cat. no. 81710 (10 µL), 83710 (200 µL) and 85710 (1200 µL), Warsaw, Poland).

3.6.1 Cell line maintenance

Alpha minimal essential medium (aMEM, cat. no. 11900-016, Invitrogen, Germany) containing 10% FCS and 1% P/S was prepared and pre-heated at 37°C. Cells were taken out of liquid nitrogen tank and cryotube was put on ice to avoid thawing to complete. Cells were then transferred into a 37°C water bath (cat. no. 1002, GFL, Burgwedel, Germany) to thaw. Upon dissolving of last crystals, cell suspension was gently transferred into a 15 mL PP tube (cat. no. 352095, BD Falcon, Schubert & Weiss Omnilab GmbH, Munich, Germany) and 10 mL of pre-heated media was added drop wise while rolling the tube on an inclined angle to mix gently. Cells were centrifuged at 200 RCF for 5 min at 4°C. Supernatant was removed and cells were gently re-suspended in 3 mL media and transferred into a 6-well plate (cat. no. 140685, Thermo Fisher Scientific, Roskilde, Denmark). Media was refreshed after

24 hours. Cells were grown as desired and re-frozen to maintain cell lines and to avoid batch depletion. Confluent cells were trypsinised with 1 mL 0.05% trypsin for 2 min at 37°C 5% CO_2. Trypsin was inactivated by adding 9 mL of media and cells were centrifuged at 200 RCF for 5 min at 4°C. Cells were re-suspended in 3 mL FCS 10% dimethylsulfoxide (DMSO, cat. no. D2650, Sigma-Aldrich, Steinheim, Germany) and 1 mL of cell suspension was gently pipetted into each cryovial (cat. no. 290174707, Neolab). Cryovials were stored at -80°C for 24 hours and then transferred to liquid nitrogen tanks.

3.6.2 PA6 culture

MC3T3-G2/PA6 cells were cultured in alpha minimal essential medium (aMEM, cat. no. 11900-016, Invitrogen, Germany) with 10% FCS and 1% penicillin/streptomycin, 100 U/mL and 0.1 mg/mL respectively (P/S, cat. no. 15070063, Gibco, Life Technologies, Paisley, UK) in a 37°C incubator. Cells were passaged every 3 to 4 days, when reaching approximately 95% confluence, by trypsinisation for 2 min at 37°C and re-suspension in medium at a 1:4 ratio. For experiments, passage numbers from 3 to 15 were used.

3.6.3 NA10HD culture

NA10HD cells for time-lapse experiments and cells that were kept for long-term culture, were incubated in a 37°C incubator. Media consisted of 100 ng/mL SCF (cat. no. 250-03), 3 ng/mL IL-3 (cat. no. 213-13), 10 ng/mL IL-6 (cat. no. 216-16), all obtained from Peprotech, 10% FCS and 1% PS in DMEM. Media was refreshed every third day and cells were serially diluted when reaching confluence (~10^6 cells/mL).

3.6.4 Co-culture

MC3T3-G2/PA6 cells were inoculated in 100 µL cell suspension at 5000 cells/cm^2 into a silicone culture insert (cat. no. 80209, IBIDI, Martinsried, Germany) and cultured for 2 days in aMEM 10% FCS 1% P/S. After reaching confluency at day 2 of culture, media was aspirated and HSCs were inoculated in Iscove's modified Dulbecco's medium (IMDM, cat. no. P04-20451, PAN) containing 100 ng/mL SCF, 10% FCS, 20% horse serum (cat. no. 16050-122, Invitrogen), 10^{-7} M hydrocortisone (cat. no. H0888-1G, Sigma Aldrich, Steinheim, Germany) and 1% P/S. Experiments were performed in either 25 mL tissue culture flasks (cat. no. 353018, BD Falcon,

Schubert & Weiss Ombilab GmbH, Munich, Germany) or 24-well Nunclon plates (cat. no. 167008, Thermo Fisher Scientific, Roskilde, Denmark). In both cases, pre-incubated media was added (15 mL and 1.5 mL, respectively) after cells had set at the bottom (approximately 1 hour)). After additional 2 hours of CO_2 saturation, flasks were screwed tight and multi-well plates were sealed using 15 mm Tesa film tape (cat. no. 57370-00002, Tesa SE, Hamburg, Germany) before conducting the experiment.

3.6.5 Clonal analysis and media optimization

Freshly isolated HSCs were virally transduced with a lentiviral vector expressing mCHERRYPSLD (see 3.1-2 and 3.3.4) in SFEM 100 ng/mL SCF and 100 ng/mL TPO (MOI 600) for 24-44 hours.

For media testing, limiting dilution was applied to obtain an average of 1 cell per 3 wells. Cells in media suspension were then pipetted into a 1536-well plate (cat. no. 783892, Greiner Bio-One, Frickenhausen, Germany) using a multi-pipette (Rainin Pipet-Lite (cat. no. L12-20, Mettler Toledo, Oakland, USA)) set at 10 µL and special Rainin tips (cat. no. RT-L10, Mettler Toledo, USA) and a 50 mL reagent reservoir (cat. no. 4870, Corning Incorporated, NY, USA).

In experiments for media optimization, phenol red free SFEM was used with SCF and a combination of TPO, IL-3, erythropoietin (cat. no. C-60022, Promokine), GM-CSF (cat. no. 167315-03-B), G-CSF (cat. no. 167250-05-B, both Peprotech), FCS, 2-mercaptoethanol (cat. no. M3148-25ML, Sigma-Aldrich, Steinheim, Germany) and L-glutamine. Media was filtered using a 0.2 µM Minisart filter (cat. no. 16532, Sartorius, Goettingen, Germany) and a 20 mL injekt syringe (cat. no. 4606205V, B.Braun, Carl Roth, Karlsruhe, Germany).

For clonal analysis at 24 or 44 hours, cells were washed in 15 mL PP tubes and re-suspended in FACS buffer and single mCHERRYPSLD expressing cells were sorted into a 384-well plate (cat. no. 88401, IBIDI, Martinsried, Germany) using a single-cell sorting mode and gates set according to a non-transduced control. Wells were filled with 100 µL media, pipetted with a multi-pipette (Transferpipette-12 (cat. no. 0533267, Eppendorf)) and using a reagent reservoir. Wells were sealed using a

gas permeable membrane to prevent evaporation (Breathe Easy, cat. no. BEM-1, Diversified Biotech, USA).

Small holes were drilled with needles in 2 opposite corners of each lid and bent needles (26G x 1", cat. no. 4657863 and 23G x 1.25", cat. 4657640, B.Braun, Carl Roth, Karlsruhe, Germany) were fixed with silicone for fixation (Aquasil, cat. no. 6139100V00, JBL GmbH, Neuhofen, Germany) to allow gas perfusion. After cell seeding, plates were sealed using Tesa film to ensure optimal gas flow.

3.7 Protein detection on living cells

Cells were characterized according to marker expression, detected by fluorochrome conjugated antibody addition to culture medium. For both quantification using epifluorescent microscope imaging and for FACS analysis, different combinations of the following antibodies were used, depending on experiment:

Table 3.7-1: Live in culture antibody quantification

Antibody	Clone	Fluorochrome	Company	Cat. No.
CD11b	M1/70	FITC	3.8 eBioscience	11-0112-82
		A488	e	53-0112-82
		PE	eBioscience	12-0112-83
CD16/CD32	2.4G2	A647	e	553142
	93	A700	eBioscience	56-0161-82
	93	PerCP Cy5	e BD	45-0161-82
CD41	MWReg30	PE	Pharminge	558040
CD43	S7	FITC	n	561856
			eBioscience	
			e	
			Biolegend	
			BD Pharmingen	
			BD Pharmingen	
CD48	HM48-1	A647	Biolegend	103404
CD71	R17217	FITC	eBioscience	111-0711-82
CD105	MJ7/18	A647	eBioscience	14-1052-82
CD117	2B8	PE Cy7	eBioscience	25-1171
CD150	TC15-12F12.2	PE	Biolegend	115904
CD135	A2-F10	PE	eBioscience	12-1351-83
CD34	RAM34	E660	eBioscience	50-0341-82
F4/80	BM8	A647	eBioscience	16-4801-85
Gr-1	RB6-8C5	PE	eBioscience	12-5931-82
Ly6A/E	D7	A647	Biolegend	108120
Ly6G	1A8	A555	eBioscience	14-5981-82
Ter119	TER-119	FITC	eBioscience	11-5921-81

Fluorescent antibodies used for live detection of surface marker expression. Abbreviations: Fluorescein isothiocynate (FITC), phycoerythrin (PE), peridinin-chlorophyll cyanine 5 (PerCP Cy5), phycoerythrin cyanine 7 (PE Cy7), eFluor660 (E660), Alexa dye (A). Used at final concentration of 25 ng/mL.

3.8.1 Antibody labeling

Antibodies were conjugated according to manufacturer's protocol. Briefly, 1 mg of primary antibody was mixed with a succinimidyl ester conjugated fluorescent protein, which created a covalent bond at the primary amine group without interfering with the functional domains. Antibodies were filtered and aliquoted and stored at 4°C at a concentration of 0.2 µg/µL. Labeling kits were obtained from Invitrogen (Alexa 488, cat. no. A10468, Alexa 555, cat. no. A20187, Alexa 647, cat. no. A20186).

3.9 Differentiation and proliferation assay

HSCs were virally transduced at 600 MOI (see 3.3.4) for 48 hours with a lentiviral vector containing NA10HD with an IRES-driven nuclear membrane-bound VENUS reporter, or a mock-infect control without NA10HD in DMEM containing 10% FCS, 100 ng/mL SCF, 10 ng/mL IL-6, 6 ng/mL IL-3 and 1% P/S. Cells were washed and re-suspended in media and triplicate wells were seeded with each well containing 100 cells. Cell numbers were assessed by imaging and cell counts using Fiji software for day 1 to 3, and 5 µL aliquots were used for counting in minitrays at later days. Cells were maintained as described (see 3.6.3). Expression of CD48 was quantified using live antibody staining (see 3.7) and both cell numbers and CD48 expression were quantified for NA10HD cells, non-transduced cells (~40 percent) in NA10HD wells and mock-infected cells. Proliferation and differentiation curves were created using MS Excel.

3.10 Immunohistochemistry

3.10.1 NA10HD expression

HSCs were virally transduced in DMEM containing 10% FCS, 100 ng/mL SCF, 10 ng/mL IL-6, 6 ng/mL IL-3 and 1% P/S with a lentiviral vector containing NA10HD with an IRES-driven nuclear membrane-bound VENUS reporter or a mock-infect control without NA10HD at MOI 600 (see 3.1-2 and 3.3.4). Cells were washed and re-suspended in media. 30 µL of cell suspension was pipetted on a 18-well poly-l-lysine coated IBIDI microslide (cat. no. 81806, IBIDI, Martinsried, Germany). Cells were allowed to set for 30 min in incubator after which media was gently aspirated.

Cells were fixed with fresh 4% paraformaldehyde for 10 min at RT. Cells were carefully washed once with PBS and permeabilised with 0.1% Triton X 100 in PBS (cat. no. 3051.3, Carl Roth, Karlsruhe, Germany) for 5 min at RT. After washing

3 times with PBS, cells were blocked with 1% bovine serum albumin (BSA, cat. no. B4287-5G, Sigma-Aldrich, Steinheim, Germany) in PBS for 1 hour at 37°C. Rabbit@FLAG primary antibody (polyclonal, cat. no. F7425, Sigma-Aldrich, Steinheim, Germany) was then added at 2 µg/mL, 1% BSA in PBS and incubated 1 hour at RT. After washing 3 times with PBS, A647@rabbit at 1 µg/mL in 1% BSA in PBS was added for 30 min at RT. 2 mg/mL Hoechst33342 in PBS was added for 20 min at RT and specimen was washed 3 times with PBS before adding mounting solution (Aqua-Poly/Mount mounting solution, cat. no. 18606-20, Polysciences, USA) and mounting microscope slides (cat. no. J1800AMNZ, Thermo Fisher Scientific, Gerhard Menzel, Braunschweig, Germany). Images were obtained using confocal microscopy (see 3.9.3) and a 63x objective.

3.10.2 Pathway activity

Freshly isolated HSCs were virally transduced overnight with an mCHERRYPSLD overexpressing lentiviral vector (see 3.1 and 3.3.4) in media, SFEM containing 100 ng/mL SCF, 100 ng/mL TPO and 1% P/S at MOI 600. Cells were washed, re-suspended in media and 15 µL cell suspension was inoculated onto a cover slip containing silicone micro-wells (cat. no. 9850003, Interchim, France). Cells were allowed to set for 2 hours in incubator, after which media was carefully pipetted off and cells were fixed using 20 µL 10% formalin solution (cat. no. HT5014-120ML, Sigma-Aldrich, Steinheim, Germany) for 10 min at RT. After washing twice with PBS, 10 µL PBS was pipetted on each micro-well and cells were imaged using a 10x Fluar objective and 1.0x Tv adapter for brightfield and fluorescence using a mcherry filter.

Cells were then permeabilised in 20 µL blocking buffer containing PBS, 1% BSA, 0.1% Triton X 100 and 10% donkey serum (cat. no. 017-000-121, Jackson ImmunoResearch Laboratories, Inc., USA) for 60 min at RT. Buffer was then carefully aspirated and 20 µL of primary antibodies (either rabbit@p-p38(Tyr182) (clone D3F9, cat. no. cat. no. 4511S, Cell Signaling) and mouse@p-Src(Tyr416) (clone 9A6, cat. no. 05-677, Upstate (Millipore)), or rabbit@p-p44/42 (clone D13.14.4E, cat. no. 4370, Cell Signaling) and mouse@p-Akt(Ser473) (clone D9E, cat. no. 4060, Cell Signaling) (4 µg/mL in blocking buffer) were added and incubated overnight at 4°C. Cells were washed 3 times for 5 min in PBS 0.1% Triton X 100 after which 20 µL 1 µg/mL biotin@mouse (cat. no. 200-002-211, Jackson

ImmunoResearch, USA) in blocking buffer was added for 1 hour at RT. Cells were washed again 3 times for 5 min in PBS 0.1% Triton X 100 and 20 µL 1 µg/mL Streptavidin-Alexa700 (cat. no. S-21383, Invitrogen) in blocking buffer was added and incubated for 1 hour at RT. After washing 3 times for 5 min, 1 drop (~20 µL) of Vectashield hard set mounting medium with DAPI was added and microscope slides were added.

Cells were imaged with a 10x Fluar objective and 1.0x Tv adapter using epifluorescent microscopy. Lumencor excitation was used to obtain fluorescent images (450nm with DAPI filter for DAPI, 485nm with eGFP filter for p-p38 and p-p44/42-Alexa488, 585nm with mCHERRYfilter for mCHERRYPSLD, 688nm with iRFP filter for p-AKT and p-Src-biotin-Alexa700). Images were processed and analysed using Fiji software.

3.10.3 Confocal imaging

Confocal microscopy was performed on a Leica SP5 spectral scanning confocal microscope with a five photomultiplier tube (PMT) detector array configuration and equipped with the following laser lines: 405 blue diode (405nm), Argon (458nm, 476nm, 488nm, 496nm and 514nm), DPSS 561 (561nm) Helium Neon 1 (HeNe1, 594nm) and HeNe2 (633nm). Images were acquired at 400Hz in the bidirectional mode with phase correction, 512x512 resolution, a pinhole size of 1 Airy unit, using a 63x glycerol immersion lens giving a 0.863mm optical section thickness) in the xyz mode.

3.11 G_1 phase enrichment

3.11.1 Cell-cycle prevalence optima

Using pre-incubated HSCs that were virally transduced for 24 hours with a mCHERRYPSLD expressing lentiviral vector in SFEM with 100 ng/mL SCF 100 ng/mL TPO 1% P/S, cell-cycle phases were quantified for multiple generations (see 3.6.5 and 3.11) and distributions were plotted. The maximum percentage of G_1-phase cells for generation 1 cells was calculated and used for experiments studying the influence of cytokine addition in G_1-phase in subsequent generations.

3.11.2 Cell-cycle inhibitors

For cell-cycle phase synchronization, different chemical inhibitors were used for testing. Multipotent progenitors (LSK $CD150^-$ $CD34^+$ $CD48^+$) were sorted and

transduced as described in 3.1-2, 3.3.4 and 3.10.1. During transduction, chemicals were added at different concentrations and for different incubation times. For G_1-phase enrichment, hydroxyurea (cat. no. H8627-1G) and L-Mimosine (cat. no. M0253-100MG) were used. Nocodazole (cat. no. M1404-2MG), a G_2/M-phase inhibitor was used as a control together with a control without inhibitors. All inhibitors were obtained from Sigma-Aldrich, Steinheim, Germany. Cells were washed and plated in fresh medium and imaged (see 3.6.5 and 3.11) to assess cell-cycle phase, cell-cycle transition and toxicity. As a control, PI staining was used and cell-cycle distribution was assessed as described in 3.4.1.

3.11.3 Hypothermic culture

Multipotent progenitor cells were sorted and transduced as described in 3.10.2. Cells were washed and plated in CO_2 saturated fresh medium and plated into a 384-well plate. Cells were imaged (see 3.6.5 and 3.11) whilst being kept in incubators at 33°C or 37°C and cell-cycle distribution and transition were compared.

3.12 Time-lapse imaging

Imaging was performed on a Zeiss Axio Observer Z1 microscope (Zeiss, Munich, Germany) using a 10x FLUAR objective (440135-0000, Zeiss, Germany), 0.5, 0.63 or 1.0x adapter and an AxioCamHRm camera (1388 x 1040 pixels, Zeiss, Germany). X-Y positioning was enabled using a motorized stage (cat. no. 0431478, Märzhäuser, Wetzlar-Steindorf, Germany) and a PECON heating system combined with a XL incubator (Erbach, Germany) were used to maintain 37°C incubation. CO_2 levels were maintained by either sealing of multi-well plates or culture flasks, both containing cells in pre-CO_2-saturated medium, or by gas perfusion with 5% CO_2 5% O_2 using self-made incubation lids. Image acquisition was done with Axiovision 4.5 using acquisition macros developed by the lab. All pictures were stored as PNG files with 50% compression. Brightfield images were taken with a focus shift to enhance contrast whilst retaining cellular morphology. Fluorescent images were taken using a HXP 120 (Zeiss, Germany) light source and a combination of following filter sets:

Table 3.12-1: Detection of fluorescence in time-lapse microscopy

Protein / fluorochrome	Excitation	Band pass	Emission	Company	Cat. no.
DAPI	387/11	409	447/60	AHF	F36-513
Hoechst33342	436/25	455	480/40	Zeiss	489047-9901-000

FITC	470/40	495	525/50	AHF	F46-002
VENUS	500/25	515	535/30	Zeiss	489046-9901-000
Alexa 555 / PE	550/25	570	605/70	Zeiss	489043-9901-000
mCHERRY	562/40	593	641/75	AHF	F36-508
APC	620/60	660	700/75	AHF	F46-006
Alexa 647	670/30	700	794/160	AHF	F47-670

Data was analyzed using TTT software (Eilken, Nishikawa et al. 2009; Rieger, Hoppe et al. 2009) developed by the lab on Fujitsu Celsius workstations with 48 GB of RAM, dual-core CPU and Windows 64-bit operating systems. Behavior, cell fate and fluorescence of single-cells was manually tracked using contrast enhancement and displayed and stored in pedigree format. The first picture taken in the time-lapse sequence indicated the time of movie start. Each starting cell at this point was considered generation 0 or mother cell and subsequent progeny were considered generation 1 (daughter cells), generation 2 (granddaughter cells) and so on. Cell lifetime was calculated from the first time point at movie start for generation 0 or from the first time point after division until occurrence of cell fate, either apoptosis or cell division.

3.13 Quantification of fluorescent signal

Fluorescence signals were measured using background correction using software developed by the lab, AMTsingle for static snapshots and QTFy for time-lapse quantification.

3.14 Statistics

3.14.1 Data analysis

Data and features obtained by creation of pedigrees or obtained from quantified images was processed with statistics software developed in the lab. Data was exported using CSV format and further processed in either Microsoft Excel for Mac 2011 (version 14.1.0, Microsoft Corporation) or Graphpad Prism 5.

3.14.2 Graphical output

Graphical representation and plots were created using either Graphpad prism or Microsoft Excel for Mac 2011. Mathlab was used to display cell-cycle transition for multiple trees and data sets. Flowjo was used to display FCS files and data obtained by flow cytometry.

3.14.3 Statistical tests

Statistics were performed using Graphpad Prism 5. For data with normal distribution student's t-test or Welsh' test were applied, depending on sample size and using one-tailed hypotheses. For not normally distributed data non-parametric one-tailed Mann-Whitney-U tests were applied, assuming unequal sample size.

4 Results

4.1 PSLD as a live cell-cycle reporter to quantify G_1 to S-phase transition.

It has long been hypothesized how cells transit through cell-cycle and whether cytokines can affect both cell fate and the cell-cycle state or cell-cycle phase durations in dividing cells. The current limitations mainly lie within the inability to obtain live cell-cycle quantification without losing clonal identity. To this extent, PSLD was validated as a live cell-cycle reporter (Figure 4.1-1 and (Hahn, JT et al. 2009). To verify whether PSLD allows detection of different cell-cycle phases, the construct was virally transduced in NIH-3T3 cells and imaged using continuous time-lapse microscopy. In Figure 4.1-1A, the G_1-phase specific nuclear localization can be clearly visualized (i, vii-viii, xii) and the cyclin-dependent nuclear export into the cytoplasm can also be observed (ii-v, iv-x). During M-phase, upon nuclear membrane degradation, the PSLD signal also diffuses into this previous enclosure where it can be detected until cytokinesis (vi, xi). From these pictures, it can be said that the PSLD signal can be detected in distinct subcellular compartments over multiple generations in a cell-cycle dependent manner.

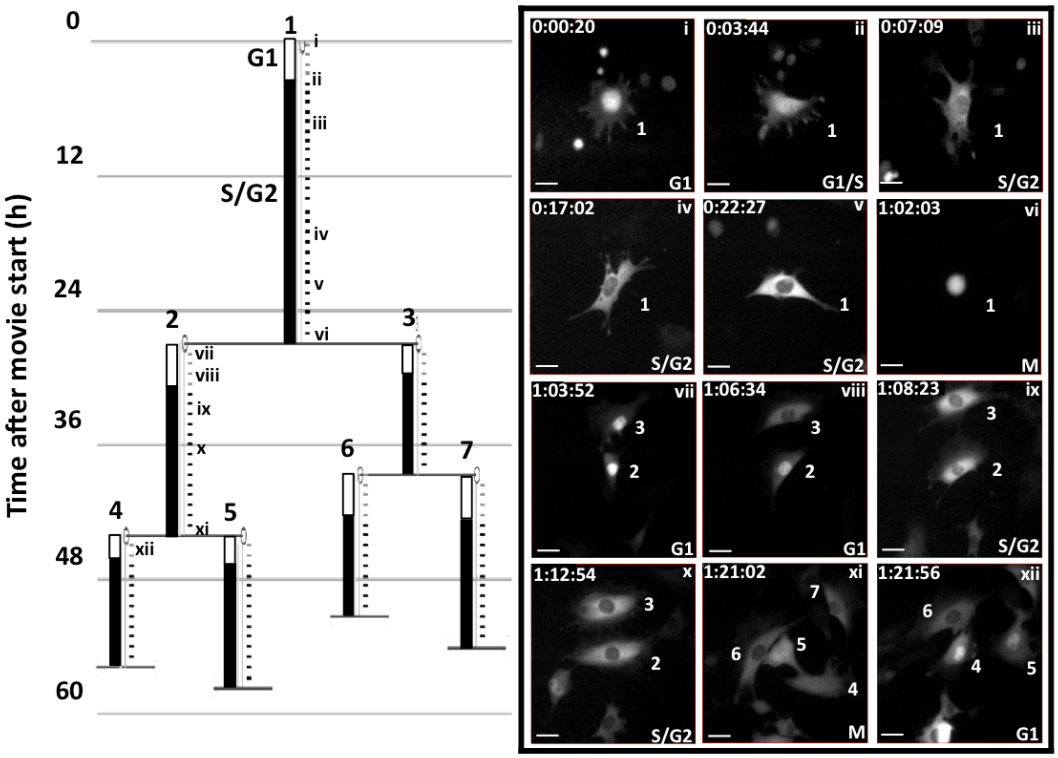

Figure 4.1-1: PSLD can be used to detect cell-cycle phase transitions
PSLD allows quantification of cell-cycle phase durations. Example pedigree of a NIH-3T3 cell transduced with mCHERRYPSLD. Arabic numbers indicate cell hierarchy, Roman numbers indicate stages within cell-cycle. Time-scale in d:hh:mm. Scale bar 20 µm.

Furthermore, it can be observed that cell lifetime of daughter cells can differ due to distinct cell-cycle phase durations (Figure 4.1-1 vii cell 2 and 3). Time-lapse example movies are provided in Supplemental Movie 1 and 2.

Next, characterization was performed to test whether the observed PSLD localization correlates with the postulated cell-cycle phase in order to define the cell-cycle resolution (Figure 4.1-2A).

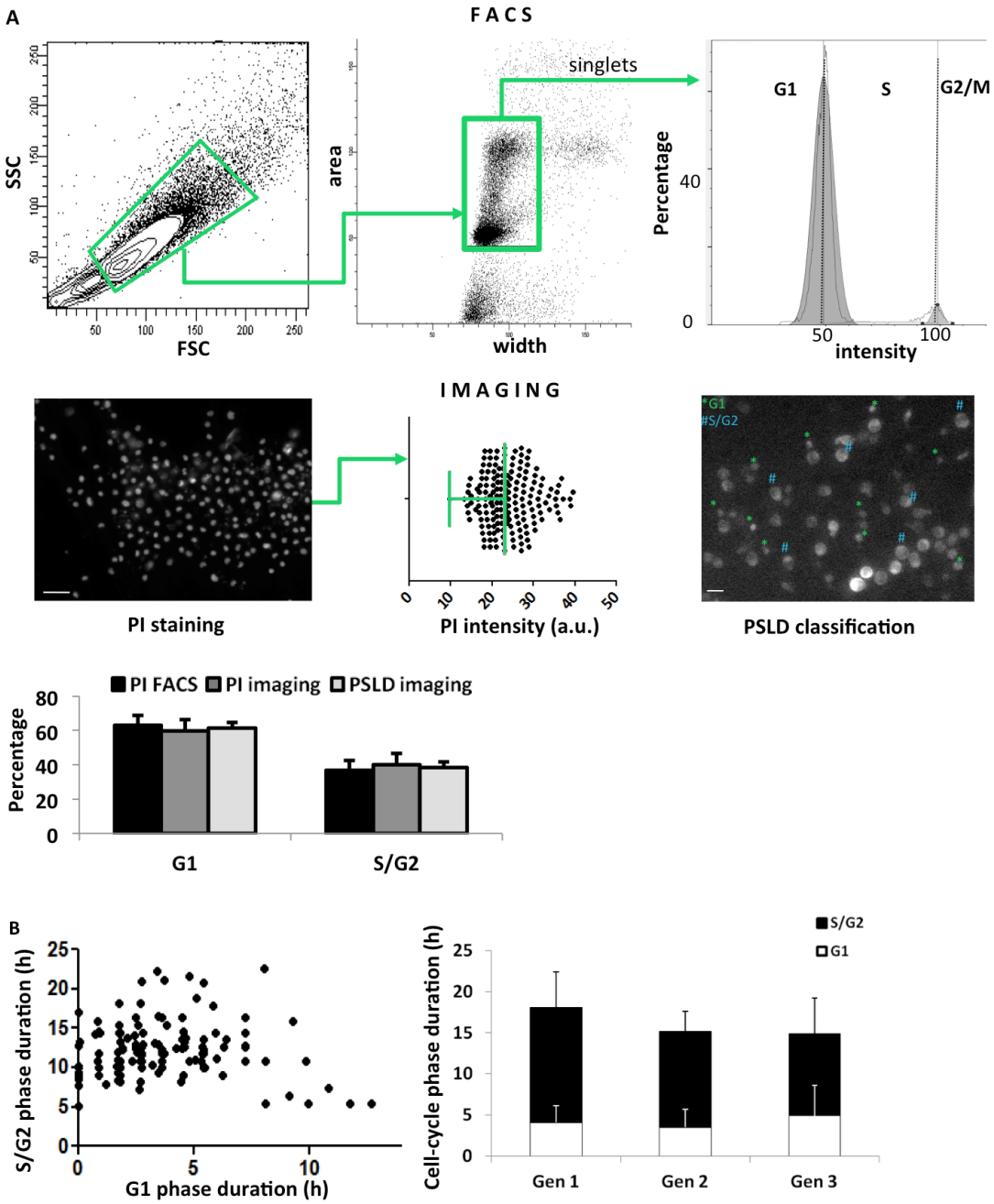

Figure 4.1-2: PSLD quantification provides a valid tool to detect G1- to S-phase transition

A. Live PSLD scoring correlates with established invasive methods to quantify cell-cycle state. PI stained MPPs were gated for single-cells and analyzed for cell-cycle using Watson distribution (10.000 events). A comparison was drawn with imaging (PI stained or PSLD transduced, 300 cells each) (from 3 independent experiments). Green lines show G1-phase gate according to histogram distribution. B. Cell-cycle phase heterogeneity exists in common used cell lines. Cell-cycle distributions for NIH-3T3 cells (generation 1,2 and 3) (n=120 cells). Scale bar 15 µm.

For this, a classic method using propidium iodide (PI) labeling and detection by flow cytometry was compared with manually scored PSLD signal in multipotent blood progenitors (LSK CD150^{-} CD34^{+} CD48^{+}). To support the strength and resolution of microscopy PI labeled cells were also imaged, and quantified signals

were compared with signals obtained by flow cytometry. The lack of significant differences between all methods demonstrates the correlation between PSLD localization and the respective cell-cycle state. Using time-lapse imaging, cell-cycle phase durations were quantified over multiple generations (Figure 4.1-2B). Overall, NIH-3T3 cell-cycle transitions and durations in *in vitro* culture are homogeneous, although it becomes apparent that some heterogeneity exists, especially for G_1-phase duration, showing even heterogeneity in common used cell lines.

4.2 Hematopoietic stem and progenitor cells are sorted with high purities using established sorting schemes

HSCs were enriched as shown in Figure 4.2-1. Since CD34 has been proposed to also be expressed on cycling HSCs, we use $CD34^{lo}$ to increase the prevalence of quiescent cells (Becker, Nilsson et al. 1999; Glimm, Oh et al. 2000; Orschell-Traycoff, Hiatt et al. 2000; Nygren, D et al. 2006; Dooner, Colvin et al. 2008).

Cells were cultured for 48 hours in SFEM 100 ng/mL SCF 100 ng/mL TPO after which they were re-stained to quantify marker expression (Figure 4.2-1B). Following FACS analysis, >95% of the cells did not down-regulate Ly6A/E or CD117 expression and did not up-regulate progenitor markers CD34 and CD16/CD32. According to this data, most cells still reside within a primitive state which confirms previous data that show HSCs can be retained after multiple days of culture using these culture conditions (Ema, Takano et al. 2000). Following these data, this likely allows a pre-incubation necessary for viral transduction without the loss of full multi-lineage potential.

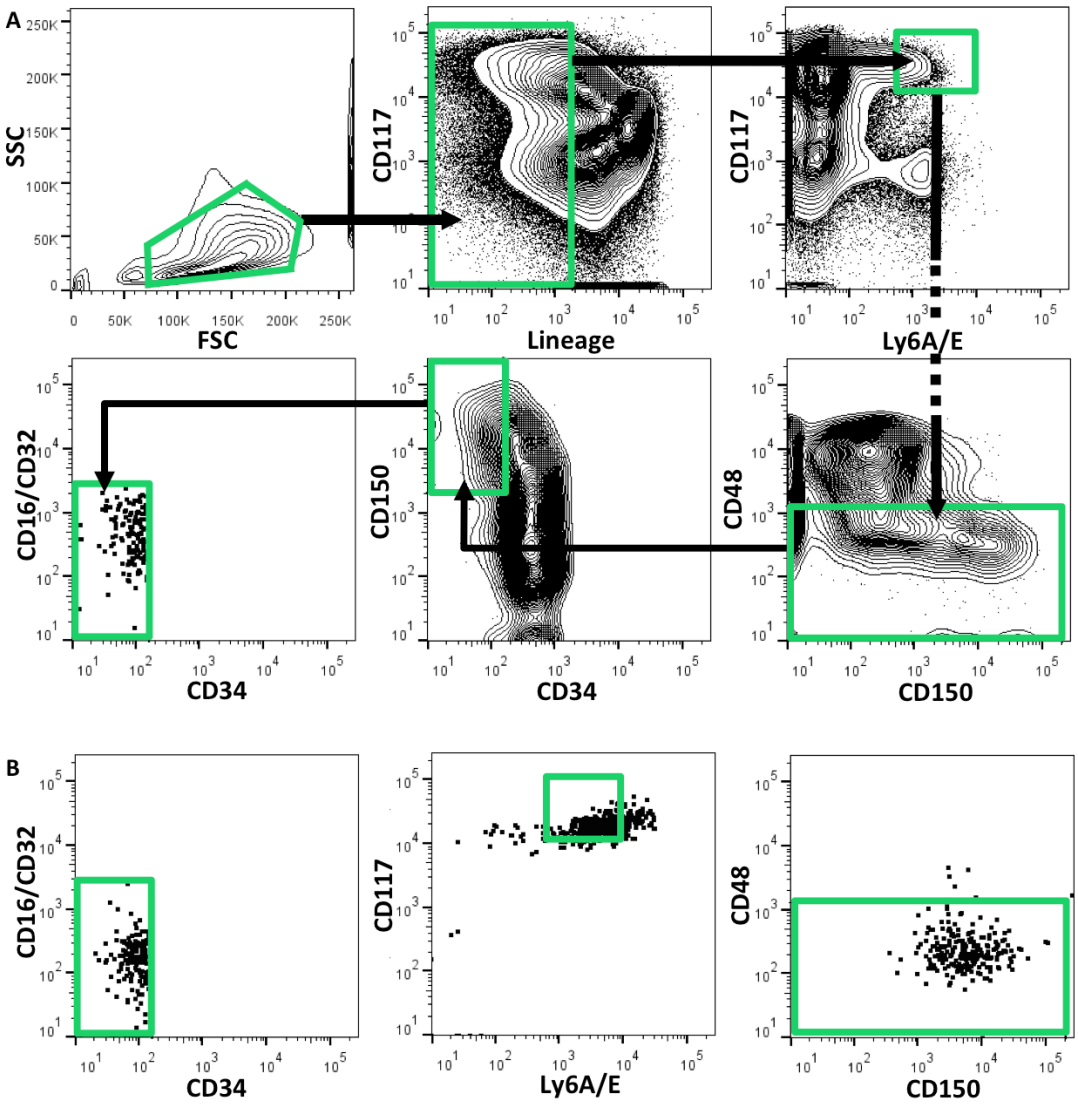

Figure 4.2-1: Pre-incubation does not affect surface marker expression.
A. HSPCs are sorted using 8 fluorescent antibodies. Example of sorting regime used to isolate HSCs (10^6 events from forward-/side scatter gate (top left) shown). Gates were drawn according to unstained controls (not shown). B. Short-term (48h) pre-incubation does not alter surface marker expression. Re-analysis of re-stained sorted HSCs cultured in SFEM 100 ng/mL SCF and TPO for 48h (1000 events shown).

4.3 HSCs go through cell-cycle in a non-synchronous fashion.

To date, most data concerning cell-cycle transitions in primary cells is population-based or is obtained with methods that do not allow quantification in living cells and hence do not provide continuous data and cannot provide information about cell-cycle phase durations. Especially in the blood field, little is known about how HSCs go through cell-cycle over time since these cells are rare and with current methods clonal identity is lost. The PSLD reporter used in this work allows following

HSC cell-cycle over multiple generations, continuously and with single-cell resolution (Figure 4.3-1).

First, HSCs (LSK $CD34^-$ $CD150^+$ $CD48^-$) and MPPs (LSK $CD34^+$ $CD150^-$ $CD48^-$) were isolated and time-lapse imaging was initiated directly after plating, approximately 2 hours after sorting. Previous studies have shown that these cells had not yet entered cell-cycle and can be considered quiescent (Nygren, D et al. 2006; Colvin, Dooner et al. 2007). The *in vitro* division rates were obtained after tracking the first two cell divisions (Figure 4.3-1A) (n=3, 100-120 cells). This data shows that HSCs have a late cell-cycle entry and have a longer initial cell-cycle compared with multipotent progenitors as described previously (Dykstra, Ramunas et al. 2006; Nygren, D et al. 2006; Benveniste, Frelin et al. 2010). At 24 hours, the majority of HSCs are still within their first *in vitro* cell-cycle, since only <5% of HSCs have divided. For the next generation, the same effect can be observed. This not only shows that HSCs can be distinguished from MPPs by cell division time, but furthermore underlines the purity of freshly isolated HSCs, since previous work has shown a strong correlation between HSC *in vitro* cell-cycle and long-term repopulation potential *in vivo* (Benveniste, Frelin et al. 2010).

To further investigate HSC cell-cycle dynamics, HSCs were isolated and virally transduced with a mCHERRYPSLD-expressing vector (Figure 4.3-1B). While lentiviral transduction can occur instantly, in order to detect the signal in the majority of transduced cells in epifluorescent imaging, a minimum pre-incubation time of 24 hours was required (not shown) in which >95% of the HSCs still reside within their first *in vitro* cell-cycle. Quantification of cell-cycle phase durations showed that indeed the majority of the cells were in S/G_2 phase at the start of time-lapse imaging (Figure 4.3-1C) and cell-cycle transit did not occur in a synchronous fashion (n=3, 75 cells). The peaks of G_1 phase prevalence were found at 24 hours and 44-48 hours, in which the latter provided >95% cells that were no longer within their first *in vitro* cell-cycle.

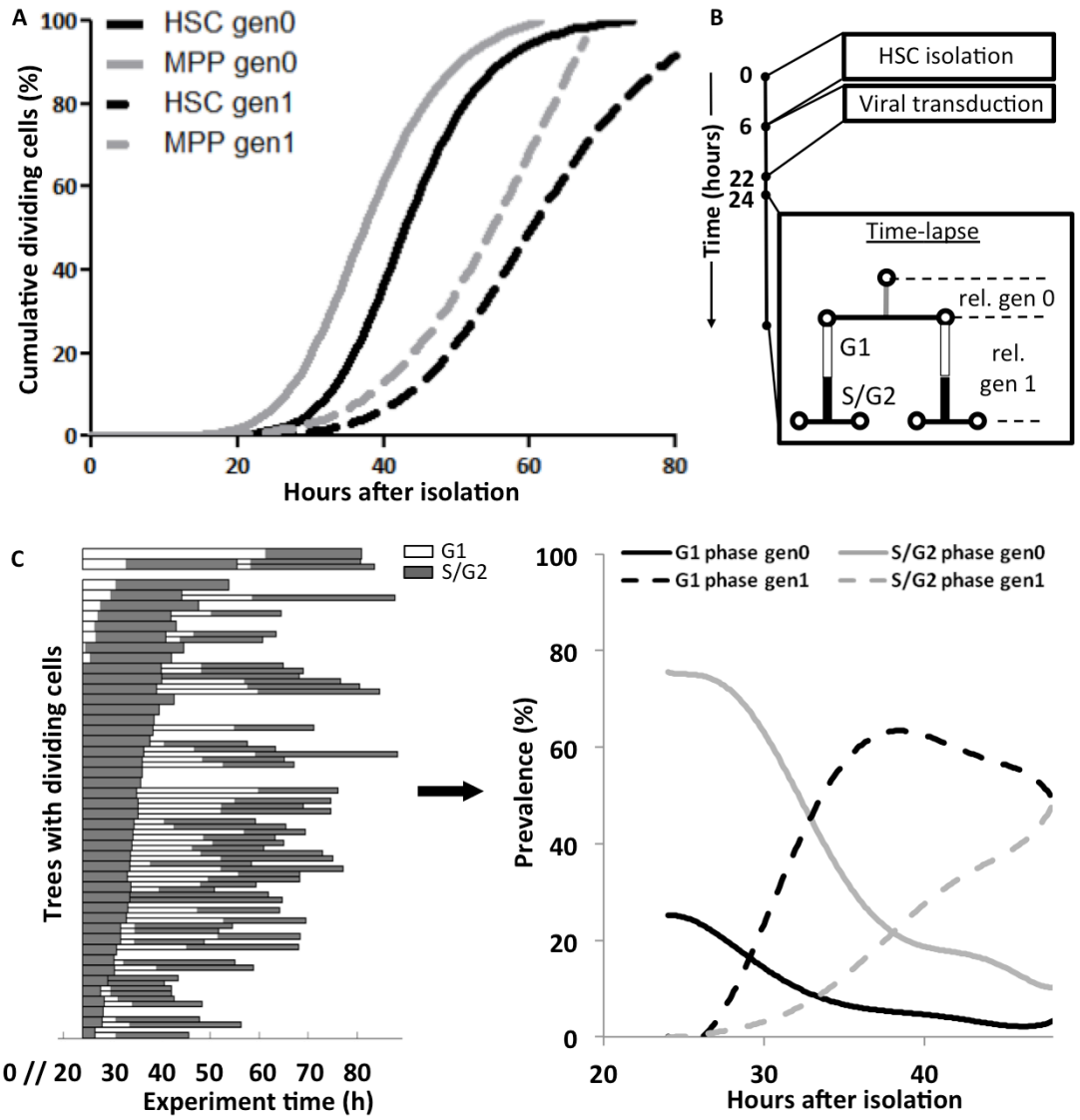

Figure 4.3-1: HSCs transit through cell-cycle in a heterogeneous fashion
A. HSCs show distinct *in vitro* division rates when compared with multipotent progenitors. Cell-cycle division rates (n=3, 100-120 cells). B. Experimental set-up for cell-cycle phase quantification in HSCs. C. HSPCs transit through cell-cycle asynchronously. Majority of HSPCs are in S/G2-phase at time of movie start, but progeny shows distinct cell-cycle phase durations. Continuous quantification and genealogy allows calculation of cell-cycle phase prevalence for different generations (n=3, 75 cells). Cells with lost identity were excluded.

4.4 Optimized media conditions allow live detection of all myeloid lineages.

To test which cytokine conditions allow lineage production without increasing apoptotic events, HSCs were freshly isolated, transduced with mCHERRYPSLD for 24 hours and kept in culture under different cytokine conditions for a total of 14 days (Figure 4.4-1). Live antibody staining with anti-FcyR (CD16/CD32) enabled the detection of granulocytes and macrophages (Akashi, Traver et al. 2000) and

megakaryocytes were detected by morphology, multiple nuclei and the lack of FcyR expression (Figure 4.4-1 top and bottom, respectively).

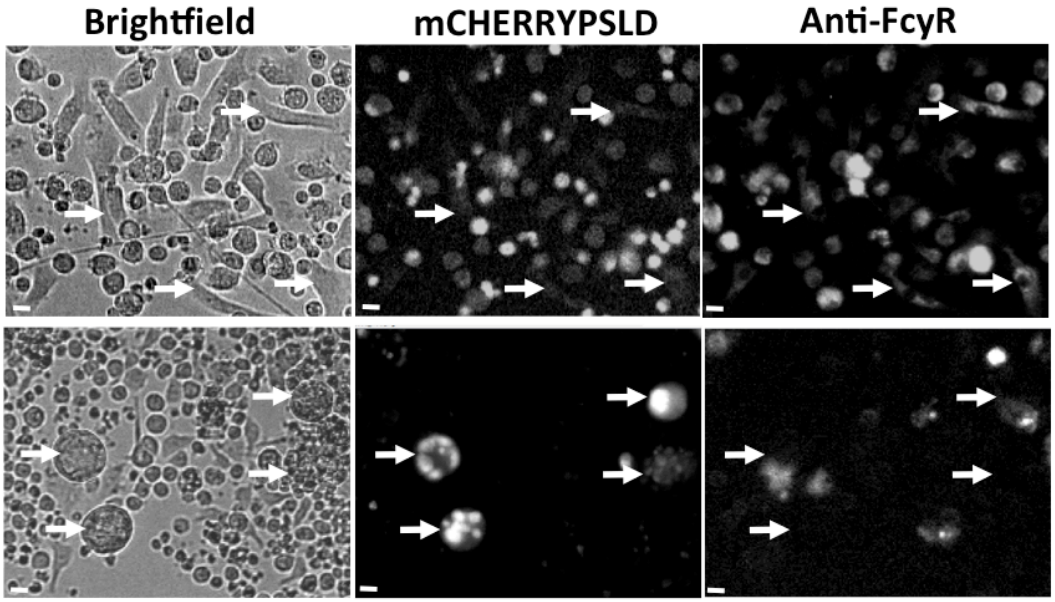

Figure 4.4-1: Lineage commitment can be live detected in culture
A combination of antibody staining and morphological features detects myeloid progenitors. White arrowheads indicate macrophages (top, FcyR positive) and megakaryocytes (bottom, FcyR negative and polynucleated) after 14 days of *in vitro* culture. Scale bar 10 µm.

In order to quantify clonal lineage production, HSCs were isolated and plated using limiting dilution with a Poisson statistic of 1:3 wells containing a single cell. This was confirmed by time-lapse microscopy during the first 24 hours (Figure 4.4-2A). Lineage production was then assessed after 14 days by time-lapse imaging and quantification of PSLD signals and expression of CD16/CD32. Colonies without megakaryocytes and CD16/CD32 expression and wells with no or only apoptotic cells present, were counted as “none” and “apoptotic”, respectively. From 6 different media conditions, “permissive” conditions (Takano, Ema et al. 2004) (Figure 4.4-2B, far right) were least selective since multilineage production was observed and apoptotic events were low, the latter probably due to the addition of serum (n=4, 1340 cells). Furthermore, the prevalence of colonies with no mature lineages was equally low, indicating a faster cytokine-induced lineage production.

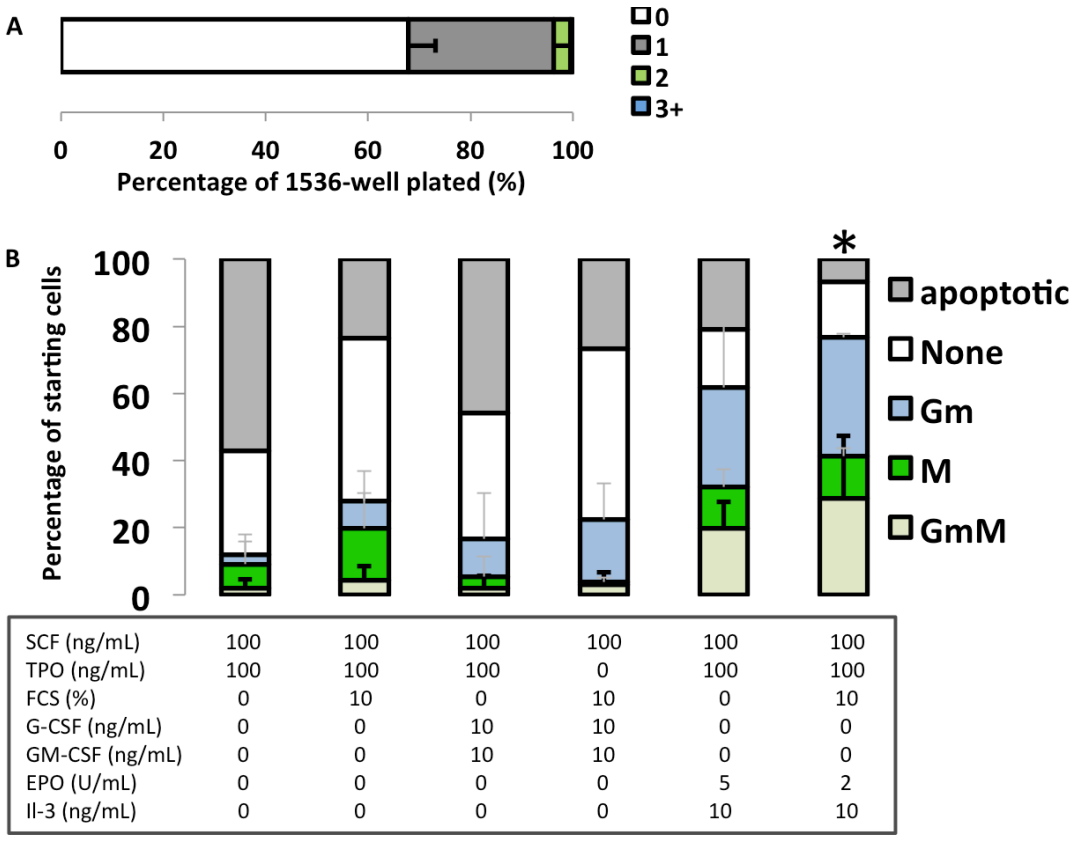

SCF (ng/mL)	100	100	100	100	100	100
TPO (ng/mL)	100	100	100	0	100	100
FCS (%)	0	10	0	10	0	10
G-CSF (ng/mL)	0	0	10	10	0	0
GM-CSF (ng/mL)	0	0	10	10	0	0
EPO (U/mL)	0	0	0	0	5	2
Il-3 (ng/mL)	0	0	0	0	10	10

Figure 4.4-2: Optimized media conditions allow live detection of all myeloid lineages
A. Single-cell plating reliability using limiting dilutions (n=4, 1340 cells). B. Permissive conditions provide highest non-restricted lineage production and survival. HSC lineage production after 14 days culture (n=4, 1340 cells). Permissive conditions are marked with an asterisk.

4.5 Live CD71 antibody staining can be used to detect erythroid production.

Detection of myeloid lineages *in situ* in liquid cultures through automated high-throughput imaging greatly facilitates end-point analysis and eliminates the necessity of cumbersome techniques as semi-solid media-based colony assays or analysis using flow cytometry. The challenge however lies in finding appropriate markers that can simultaneously be detected using fluorescence imaging. For the purpose of this work, different fluorescent antibodies were combined with morphological characteristics and polynucleated structures. As described in Figure 4.4-1, megakaryocytes and macrophages can be identified using an antibody against CD16/CD32 and features such as multiple nuclei and adherence. To further detect the existence of erythrocytes and erythroid progenitors, anti-CD71, a transferrin receptor highly expressed on erythroid cells, as previously reported (Fang, Menon et al. 2007;

Pronk, Rossi et al. 2007; Eilken, Nishikawa et al. 2009), was tested (Figure 4.5-1A).

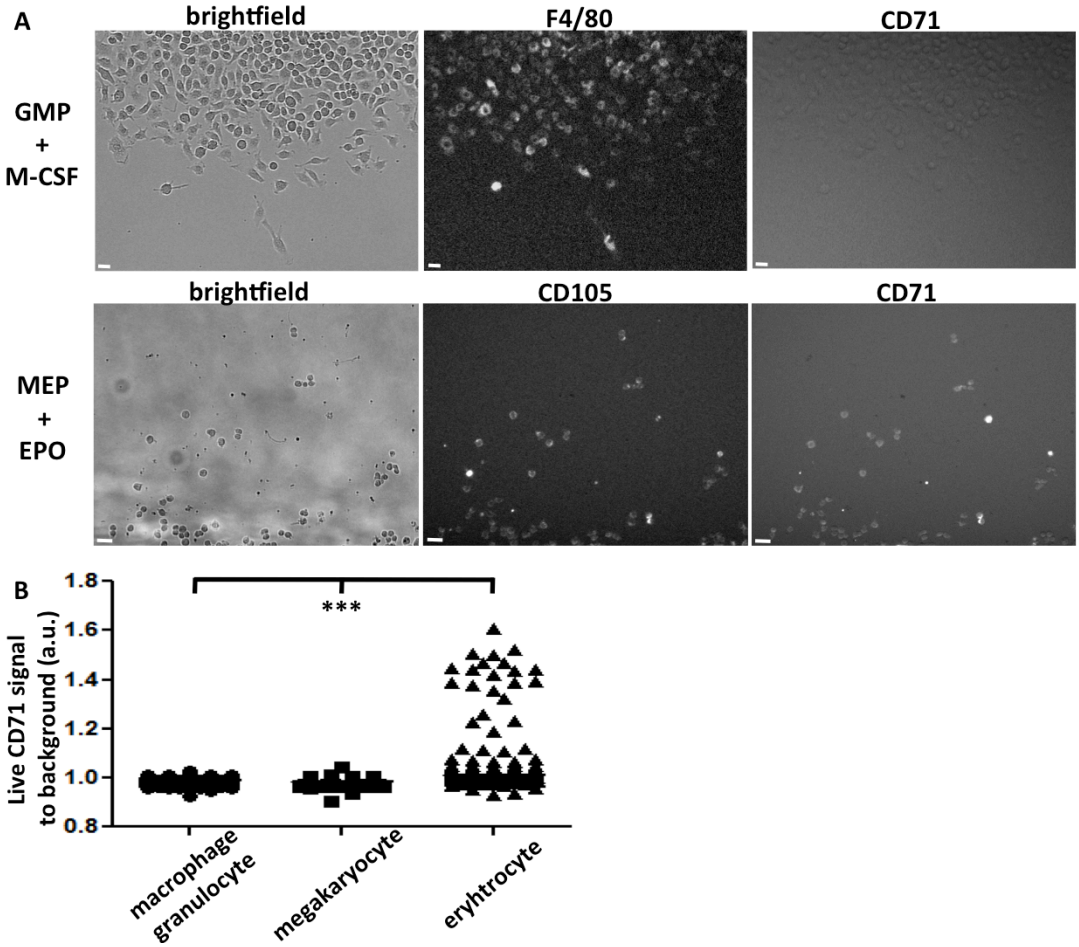

Figure 4.5-1: Live CD71 antibody staining specifically detects erythroid lineages
A. CD71 expression only detects erythroid lineages and co-stain with CD105. Lin$^-$ CD117$^+$ Ly6A/E$^-$ CD16/CD32$^+$ CD34$^+$ (GMP, top) and Lin$^-$ CD117$^+$ Ly6A/E$^-$ CD16/CD32$^-$ CD34$^-$ (MEP, bottom) were freshly isolated and cultured for 7 days in SFEM containing 10 ng/mL M-CSF (top) or SFEM permissive medium including 2 U/mL EPO (bottom). B. CD71 quantification shows exclusive expression on erythroid cells. Data from day 7 imaging (n=3, 150 cells). *** p-value<0.001. Scale bar 15 µm.

To validate CD71 staining, granulocyte-macrophage progenitors (GMP) and megakaryocyte-erythrocyte progenitors (MEP) were sorted and cultured under instructive conditions for macrophages (SFEM + 10 ng/mL M-CSF) and permissive conditions (+ 2 U/mL EPO), respectively. As live antibodies, F4/80 (Alexa-555 conjugated) was used to confirm a macrophage phenotype and CD105 (endoglin, PE conjugated) was used to detect early erythroid progenitors, as previously described (Buhring, Muller et al. 1991). In both cultures CD71 (FITC) was added for validation. All macrophages were adherent and expressed F4/80, whereas erythroid progenitors were non-adherent and expressed CD105 (Figure 4.5-1A). Furthermore, only erythroid progenitors expressed detectable levels of CD71 (Figure 4.5-1A and B),

thereby validating the use of CD71 antibody to detect erythroid lineages, as previously described (Zhang, Socolovsky et al. 2003; Pronk, Rossi et al. 2007). Combining these antibodies with morphological and polynuclear features, all myeloid lineages can be detected to further measure clonal full myeloid lineage production.

4.6 Cytokines induce cell-cycle specific lineage production.

Much of previous work concerning the influence of cell-cycle in cytokine-induced lineage production has been done either on a population level or based on cell-cycle distributions, losing clonal identity. To identify whether some of these hypotheses and correlations also exist on a single-cell level, single-cells expressing a cell-cycle reporter were imaged and followed using continuous time-lapse imaging (Figure 4.6.1). Single HSCs were re-sorted after 24 hour -lentiviral transduction to allow cell-cycle reporter expression in cytokine supplemented medium and time-lapse imaging was initiated immediately (Figure 4.6-1A, left). End-point analysis after 14 days using live antibody staining revealed the clonal lineage production and was then correlated with the initial cell-cycle phase at the time of cytokine addition and movie start (Figure 4.6-1A, right).

Control cells not receiving cytokine supplements (SCF, TPO only) did not survive over the course of the experiment (not shown). However, since these cells retained viability until at least 7 days of culture, cytokine addition to these cells was performed at day 7 in order to identify lineage potential and production. At this time-point, it was assumed that the majority of these cells were no longer primitive HSCs and lineage priming or maturation had already occurred. From this data, it can be observed that none of the control cells produced all myeloid lineages, i.e. granulocytes (G), erythrocytes (e), macrophages (m) and megakaryocytes (M) (GemM) (Figure 4.6-1A, right, n=3). In contrast, HSCs that were cultured under permissive conditions (Permissive) did produce GemM lineage. Although the production of specific lineages was not exclusive for either initial cell-cycle phase, G_1-phase cells produced significantly more GemM lineage than S/G_2-phase cells (n=6).

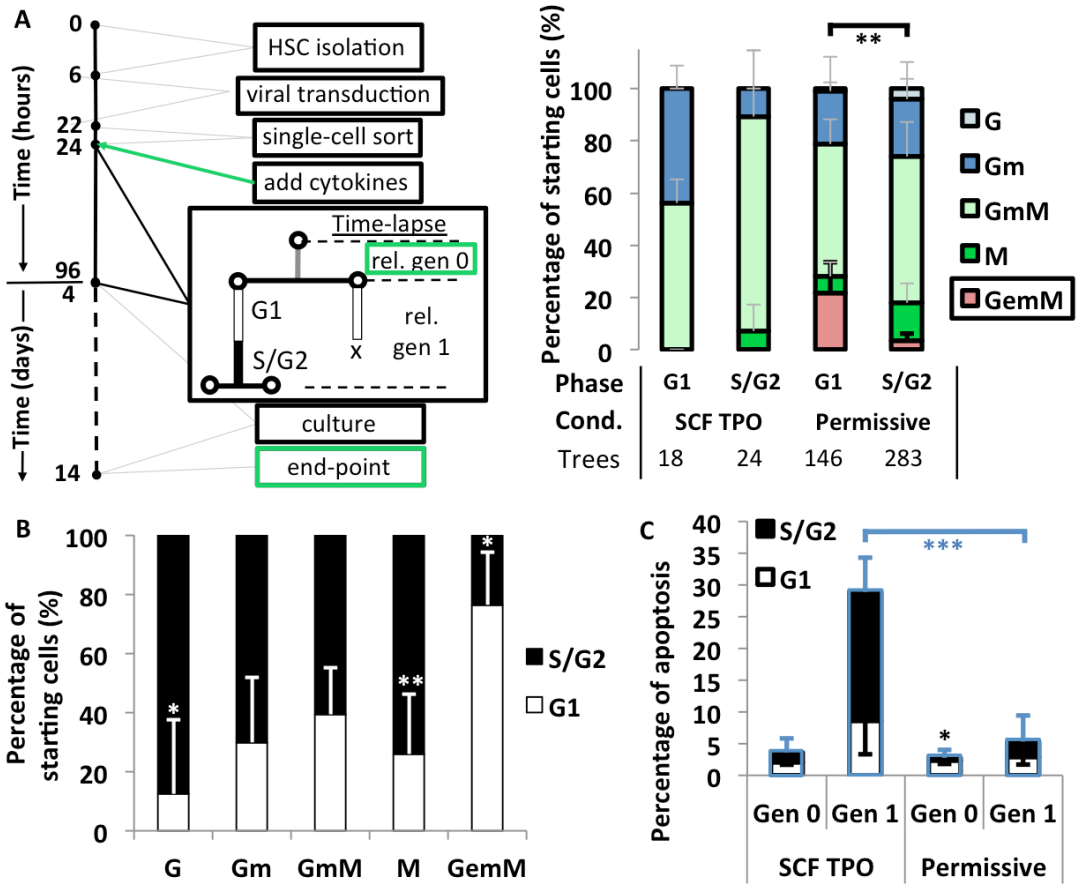

Figure 4.6-1: Clonal GemM production is enhanced in G_1-phase cells

A. Experimental set-up and clonal lineage production showing an increased production of all myeloid lineages during G_1-phase and exclusively under permissive conditions. Phases indicate initial starting phase in generation 0. AB. G=granulocytes, m=macrophages, M=megakaryocytes, e=erythrocytes. SCF TPO (n=3), Permissive (n=6). B. Correction for initial cell-cycle prevalence shows distinct lineage production that is cell-cycle dependent. ABC. * p-value<0.05, ** p-value<0.01, *** p-value<0.001). Blue bars and asterisks indicate total levels, black and white asterisks show cell-cycle specific significance. C. Permissive cytokine conditions induce survival in generation 1 cells that is independent of initial cell-cycle phase upon cytokine administration (generation 0).

To correct for the higher starting cell number being in S/G_2-phase at the time of cytokine addition (see also Figure 4.3-1C), initial cell-cycle phase prevalence was compared per lineage (Figure 4.6-1B). This correction then revealed that single-cells producing lineages restricted to one cell type, i.e. granulocytes (G) or megakaryocytes (M), were more prevalent in starting cells that were in S/G_2 phase at the moment of cytokine addition (n=6). This is in line with previous work claiming megakaryocytes are more likely to arise from early S-phase cells upon cytokine change (Colvin, Dooner et al. 2007). My results however demonstrate this occurs at a single-cell resolution rather than on a population level.

To investigate whether a negative selection might occur, i.e. cells that would have produced other lineages would not survive, apoptosis rates during pre-incubation

or within early generations were assessed and correlated with initial cell-cycle phase upon cytokine addition and start of time-lapse imaging (Figure 4.6-1C). For both control cells and cells in permissive conditions, initial apoptosis rates were low (2-5%) and can be explained by the potential toxicity of viral transduction and the stress of double-sorting within 24 hours. G_1-phase cells under permissive conditions showed more sensitivity to medium change and had an increase in apoptosis levels, albeit with very low total levels. For generation 1 cells however, controls had a significantly higher apoptosis rate than cells cultured in permissive conditions. Thus, addition of permissive cytokines and serum rescues cells that would have otherwise undergone apoptosis. However, no effect could be observed with respect to initial cell-cycle phase. The very low apoptosis rate in subsequent generations under permissive conditions therefore does not affect selectivity with respect to lineage production, i.e. the higher prevalence of GemM lineage production from G_1-phase starting cells is not caused by selective apoptosis.

4.7 Increased multilineage production from G_1 phase cells is reversible.

The observed effect of increased GemM production from G_1-phase cells poses the question whether subsequent generations are also more susceptible to produce GemM lineage when receiving permissive cytokines during G_1-phase. To test this, HSCs were pre-incubated for 44 hours, a time-point at which >95% of cells are no longer in generation 0 but, instead, in generation 1. Furthermore, at this time-point a maximum was found for G_1-phase prevalence, reaching ~50% of generation 1 cells (see Figure 4.3-1C). Following the same experimental set-up (Figure 4.6-1A), lineage production was again correlated with the cell-cycle phase upon cytokine addition and start of time-lapse imaging (Figure 4.7-1A, left). The data shows again that G_1-phase cells are producing more GemM lineage compared with S/G_2-phase cells. In addition, the amount of Gm lineage producing cells is increased for both cell-cycle phases when compared with permissive cytokine addition at 24 hours. This is consistent with the fact that control cells that receive permissive cytokine addition after 7 days produce higher numbers of clonal Gm lineage production, suggesting lineage-bias to occur early (generation 1).

Having lost the ontogeny and behavior of these cells during the prolonged incubation time, another approach was performed to ensure the observed effect can be attributed to generation 1 cells in culture. For this purpose, HSCs were again pre-incubated in SFEM 100 ng/mL SCF 100 ng/mL TPO for 24 hours and re-suspended in fresh control medium without permissive cytokines. Single-cells were cultured and imaged during the next 20 hours after which permissive cytokines were added. By doing so, the effect of generation 0 and generation 2 cells on lineage production could be fully excluded (Figure 4.1.7A, right). This data again shows a higher prevalence in G_1-phase cells to produce GemM lineage. Although not significantly different to either permissive cytokine addition at 24 or 44 hours, the lower tendency could be explained by repeated washing steps that could interrupt SCF and TPO signaling. However, equally apparent is the loss of restricted megakaryocyte production, again more pronounced in S/G_2-phase cells.

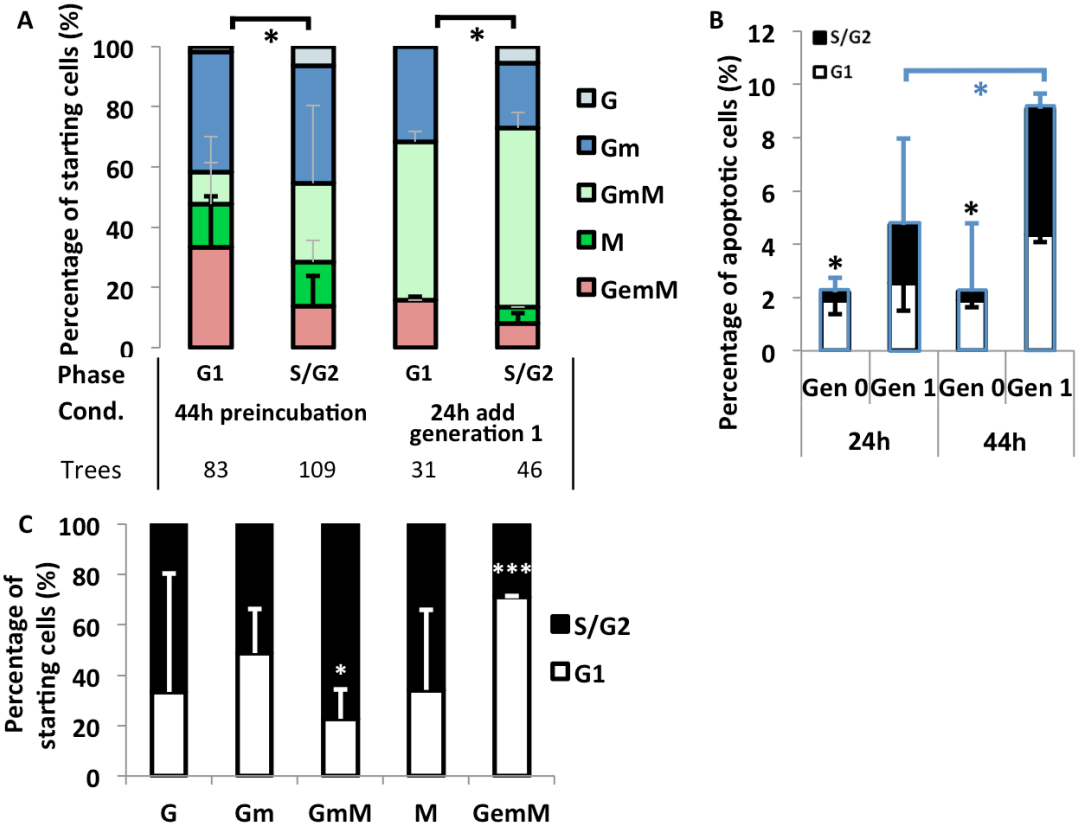

Figure 4.7-1: G_1-phase susceptibility to produce GemM is reversible in later generations
A. Enhanced clonal GemM production from G_1-phase cells re-occurs in daughter cells. At 44h preincubation (left, n=4) >95% of cells have divided. Addition to 100% generation 1 cells through imaging during preincubation (right, n=3) shows reproducibility. AC. G=granulocytes, m=macrophages, M=megakaryocytes, e=erythrocytes. B. Prolonged preincubation increases apoptosis rates in generation 1 cells but is not dependent on initial cell-cycle state. Phases indicate initial starting phase in generation 0. * p-value<0.05, ** p-value<0.01, *** p-value<0.001). Blue bars and asterisks indicate total levels, black and white asterisks show cell-cycle specific significance. C. Correction for

initial cell-cycle prevalence shows higher prevalence of GemM producing cells in G_1-phase to be consistent in daughter cells (44h preincubation).

In accordance with cytokine addition at 24 hours, G_1-phase cells are more prone for apoptosis when receiving permissive cytokines in generation 0 (Figure 4.7-1B). Total apoptosis rate, however, does not differ between incubation times. Yet, with increasing incubation time in control medium, generation 1 cells die significantly more even when receiving permissive cytokines. This increased apoptosis does not point towards a cell-cycle selective effect since when comparing starting cell-cycle states, no difference in prevalence is detectable (~50%). The observed rescue effect in generation 1 after 24 hours of pre-incubation is therefore not equally applicable for prolonged pre-incubation, although total apoptosis rates in generation 1 are still significantly less when compared with control conditions (Figure 4.6-1C).

The higher number of S/G_2-phase cells makes it difficult to compare absolute numbers of lineage producing cells for different cell-cycle phases. When correcting for this by looking at cell-cycle phase distribution per lineage, the increased production of GemM lineage from G_1-phase cells becomes highly significant (Figure 4.7-1C). In contrast, the increased susceptibility of S/G_2-phase cells to produce either granulocytes or megakaryocytes is no longer present. Although the same tendency can be observed, the loss of significance is mainly caused by the high variation. GmM lineage production however is mainly derived from S/G_2-phase cells, which could not be detected at 24 hours and is in strong contrast to GemM producing cells that in addition produce erythrocytes. These data are conflicting with previous findings that imply a continuous model for HSC susceptibility to induce lineage maturation by indicating that HSCs in culture may have a rather altered or restricted potency with increasing incubation time.

4.8 Live cell-cycle quantification reveals lineage-specific cell-cycle behavior

The strength of time-lapse microscopy lies in the fact that cell-cycle phases can not only be scored but also quantified continuously over time. With initial data suggesting differences in lineage production depending on during which initial cell-cycle phase permissive cytokines were added, the next question was whether a direct

effect on cell-cycle progression could be observed (Figure 4.8-1). For this purpose, cell-cycle phase durations of generation 1 cells were quantified and correlated with their ultimate lineage production, assessed by end-point analysis (see also 4.6-1A, left). Generation 0 cells were excluded at first, since they were not synchronized at the time of movie start. It followed that generation 1 cells ultimately producing GemM lineage had a significantly longer G_1-phase (Figure 4.8-1A, left). The lack of a significant difference between granulocyte colonies is due to the very low n-number for this population (see also Figure 4.6-1A, right). Not shown here is the fact that megakaryocyte restricted producing cells have a significantly shorter G_1-phase (p-value<0.01). Now when adding up total G_1-phase durations of mother (generation 0) and daughter (generation 1) cells, it becomes apparent that the total time-window in which cytokines can act during G_1-phase is more than 2 fold higher (Figure 4.8-1A, right) (data from three independent experiments). Since none of the control cells in SCF TPO produce GemM lineage after 14 days of culture, a direct comparison cannot be made. However, when comparing G_1-phase durations from dividing GemM producing cells with all dividing SCF TPO cells, none of the control cells reach the median G_1-phase duration of GemM producing cells, pointing to an induced effect.

Testing whether the same observation could be made using longer pre-incubation times, the same analysis was performed on dividing cells that had been pre-incubated for 44 hours (Figure 4.8-1B). For these cells, the GemM specific longer G_1-phase during generation 1 was no longer apparent, except when comparing with granulocytes and/or macrophages (Figure 4.8-1B, left). When comparing medians for all lineages, an overall shorter G_1-phase duration can be observed when compared with 24 hour pre-incubation, in line with the general observation that HSCs in *in vitro* culture gradually attain a shorter cell-cycle. For this reason, it is likely that G_1-phase durations decrease in subsequent generations and indeed, that differences in later generations are no longer detectable. In contrast, when looking at the total time-window in which cytokines act during G1-phase, i.e. when combining mother (generation 0) and daughter (generation 1) G_1-phase durations, a significant longer G_1-phase is again apparent for GemM lineage producing cells (Figure 4.8-1B, right). This indicates the higher prevalence of cells with longer G_1-phases in generation 0. Taken together, these data show that the observed longer G_1-phase durations for GemM lineage producing cells reoccurs and is reversible in subsequent generations.

When looking at S/G_2-phase durations (Figure 4.8-1C), no differences can be observed for either pre-incubation time although granulocyte restricted lineages have a much shorter S/G_2 phase (p-value<0.001). Considering S-phase to be relatively constant, this would imply G_2-phases for all lineages to be similarly long except for granulocytes, which would have a shorter G_2-phase duration. This shows G_1-phase is contributing to a general longer cell-cycle division time for GemM producing cells.

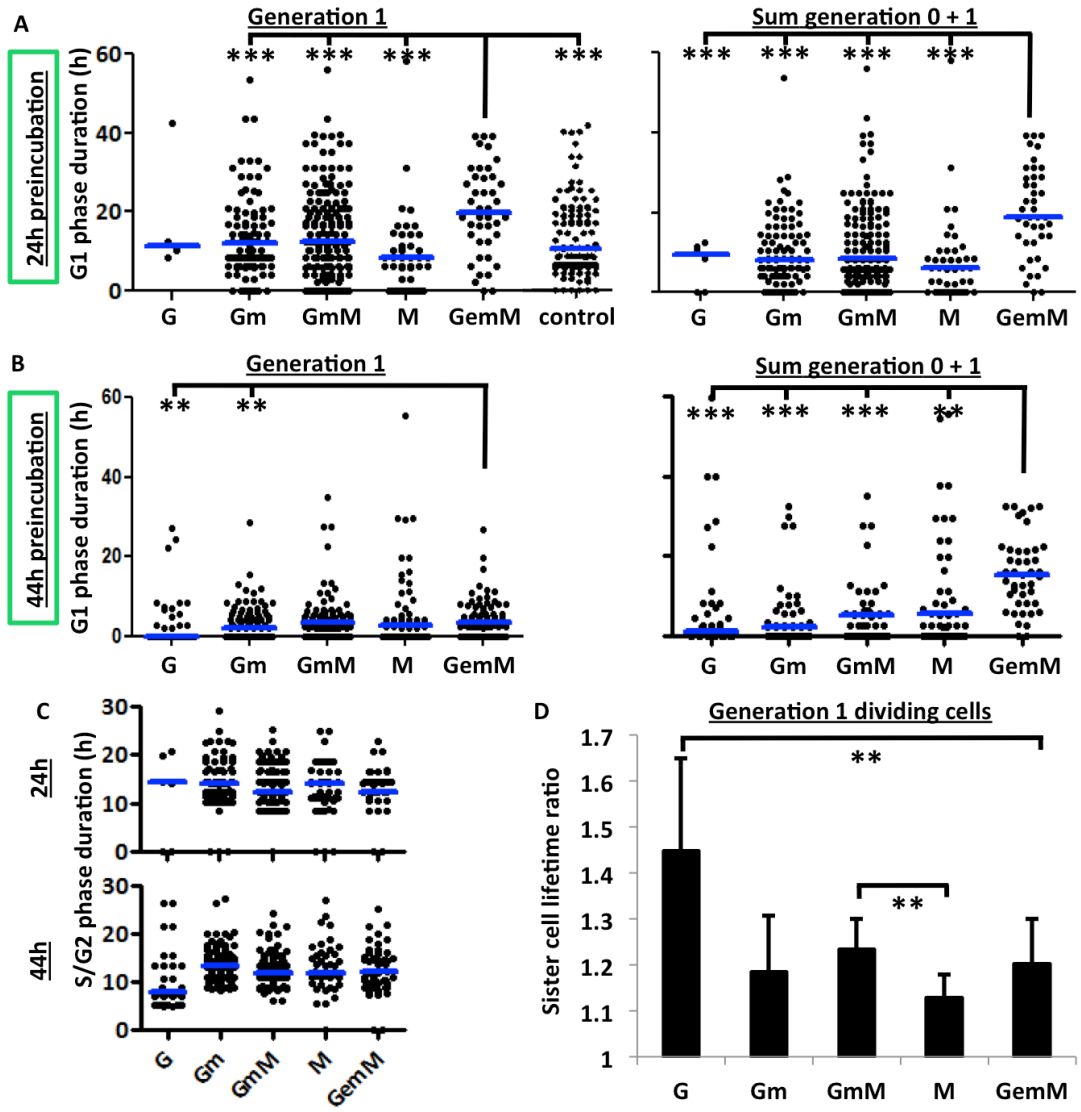

Figure 4.8-1: Clonal GemM production correlates with long G_1-phase durations

A-D. G=granulocytes, m=macrophages, M=megakaryocytes, e=erythrocytes, control (SCF TPO only). A. GemM producing cells have a longer G_1-phase duration than cells with restricted lineage production. 24 hour pre-incubation (n=3) outcome of dividing generation 1 cells (left) and cumulative dividing generations (0+1, right). B. This is reproducible in daughter cells, although to a lower extent. 44 hour pre-incubation (n=4) outcome of dividing generation 1 cells (left) and cumulative dividing generations (0+1, right). C. S/G2-phase durations for dividing generation 1 cells are not different. 24h (top) or 44h (bottom) pre-incubation. D. Kinship comparison of generation total cell lifetime shows increased synchronicity for megakaryocytes and asymmetry in granulocyte producing cells. Ratio cell lifetime daughter 1 (longer):daughter 2 (shorter) with 24 hour pre-incubation (n=6). * p-value<0.05, ** p-value<0.01, *** p-value<0.001). Blue bars indicate median value.

The use of time-lapse imaging not only allows one to track behavior and ontogeny but also allows a direct comparison of sister cells. To this purpose, cell lifetimes were directly compared between sister cells and the ratio was calculated (Figure 4.8-1D, data from 6 independent experiments). Although no clear pattern could be observed for cells producing GemM lineage, granulocyte producing cells have more asymmetry when compared with other lineages (p-value<0.01). In contrast, cells that are restricted towards the megakaryocyte lineage have an increased symmetry, i.e. dividing daughter cells have a similar cell lifetime. The reason for this is not yet clear and may require in-depth analysis of later generations, including live quantification of marker onset.

4.9 GM-CSF alters cell fate in a cell-cycle dependent manner.

Previous publications using population-based data have shown the capability of GM-CSF to induce megakaryocyte maturation within the first *in vitro* cell-cycle of HSCs (Robinson, McGrath et al. 1987; Colvin, Dooner et al. 2007). While in these studies total numbers in end-point analysis were indeed increased and correlated with pre-incubation time, it cannot be ruled out that G_1-phase cells, also present at the time of cytokine change, were equally susceptible. Furthermore, a selective effect may have occurred, inducing apoptosis or reducing proliferation of other lineages. To address this question in more detail, the same experimental set-up was chosen as above (see Figure 4.6-1A, left) allowing direct cell-cycle assessment and correlation with end-point lineage production (Figure 4.9-1). Cells were either cultured using permissive culture media or with further addition of GM-CSF. This method was thought to be least selective, since overall apoptosis rates were low under permissive conditions and all lineages could be produced.

After 24 hours of pre-incubation (data from 4 independent experiments), GM-CSF induced higher apoptosis that was specific for G_1-phase cells (Figure 4.9-1A, left). Although a similar trend could be observed for generation 1 cells, there was no significant difference between starting cell-cycle phases. After 44 hours of pre-incubation (data from 3 independent experiments), no difference between control conditions and GM-CSF addition could be detected indicating that HSCs in early

generations are most sensitive to GM-CSF induced apoptosis during G_1-phase (Figure 4.9-1A, right).

When looking at clonal lineage production, no cell-cycle specific effect of GM-CSF after 24 hours pre-incubation could be observed (Figure 4.9-1B, left), although total GemM lineage production was reduced. After 44 hours of pre-incubation however, GemM lineage production was almost exclusively observed from G_1-phase cells (Figure 4.9-1B, right). Furthermore, megakaryocyte production was significantly increased for S/G_2-phase cells ($p\text{-value}<0.05$), which follows previously published data (Colvin, Dooner et al. 2007) and is also observed after 24 hours of pre-incubation under control permissive conditions (Figure 4.6-1B). Although a direct comparison with published data cannot be drawn due to the presence of different cytokines that could bind competitively or could have either a synergistic or antagonistic effect, these data for the first time show the effect of GM-CSF on different cell-cycle phases on a single-cell resolution.

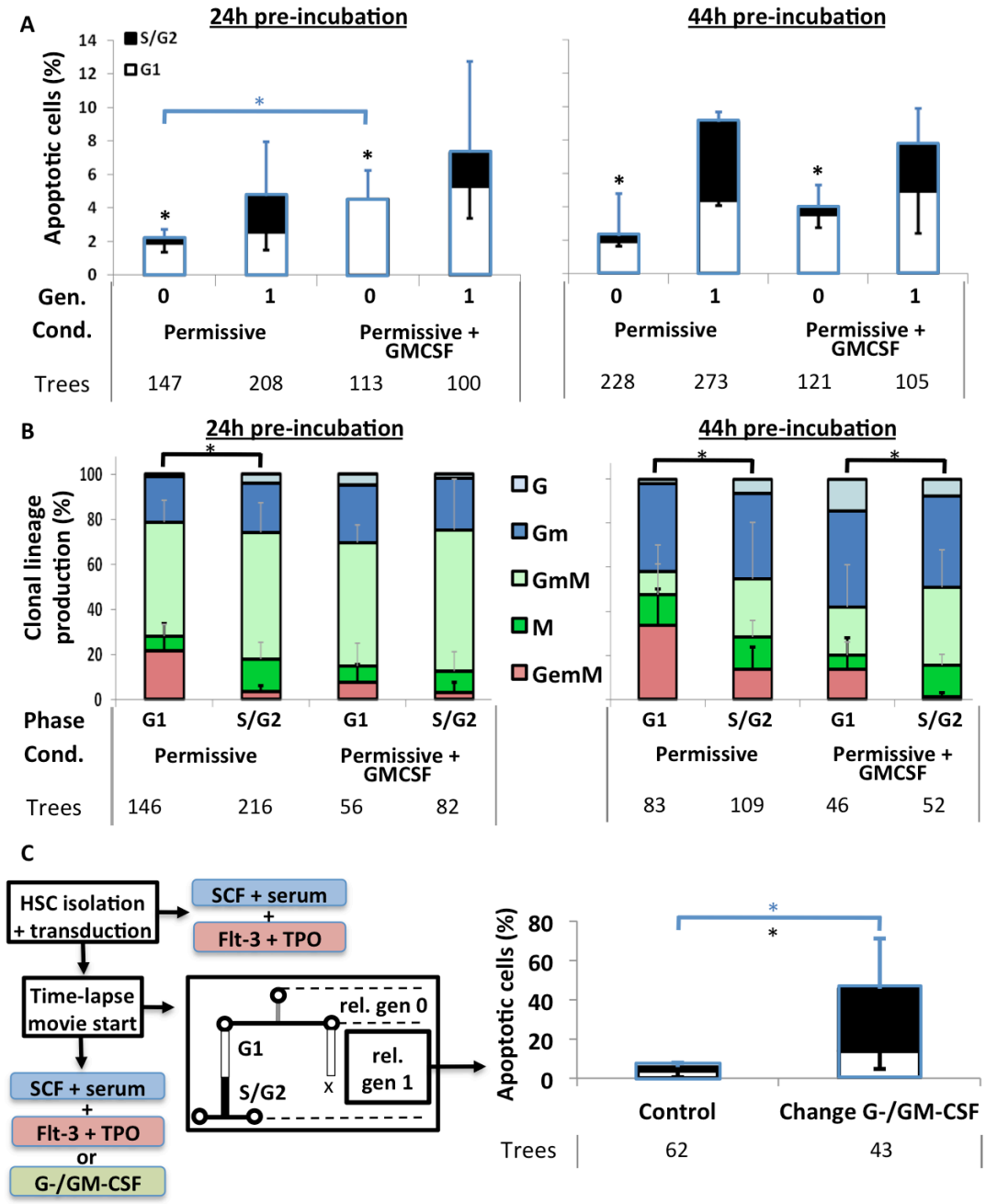

Figure 4.9-1: GM-CSF addition reduces GemM production and increases apoptosis
A. GM-CSF addition increases apoptosis in generation 0 G_1-phase cells. Cell-cycle phases indicate cell-cycle state in starting cells (generation 0) at the time of movie start and medium addition (24h n=4, 44h n=3). B. GM-CSF reduces GemM production not cell-cycle specifically. G=granulocytes, m=macrophages, M=megakaryocytes, e=erythrocytes. C. Switching to GM-CSF increases apoptosis S/G_2-phase specifically. Correlation of apoptosis in generation 1 cells with cell-cycle phase of generation 0 at time of cytokine addition. * p-value<0.05. Blue bars and asterisks indicate total levels, black asterisks show cell-cycle specific significance.

To further verify whether a selective or apoptosis-inducing effect may exist upon GM-CSF addition, published methods (Colvin, Dooner et al. 2007; Quesenberry, Dooner et al. 2010) were adopted to the current single-cell resolution

time-lapse set-up (Figure 4.9-1C, left). Following 24 hours of pre-incubation in a basal control permissive medium containing both Flt-3 and thrombopoietin, cells were washed and re-suspended in medium with G-CSF and GM-CSF or in control permissive medium. Following time-lapse imaging (data from 3 independent experiments), a 3-4 fold increase in apoptosis could be observed in generation 1 cells when changing conditions to G-/GM-CSF, the majority having been in S/G_2-phase in generation 0 at the time of medium change (Figure 4.9-1C, right). This could also imply that these cells had not yet seen these cytokines in G_1-phase and apoptosis therefore was observed within G_1-phase of the next generation. This assumption is supported by the fact that under permissive conditions, no cell-cycle specific effect on apoptosis can be detected (Figure 4.9-1A).

4.10 HSC G_1-phase enrichment can be obtained with hydroxyurea.

The increased potency of G_1-phase cells to produce GemM lineage under permissive conditions, led to the question whether this could be further enhanced by selective enrichment for G_1-phase cells. Two different methods were used to increase prevalence of G_1-phase cells (Figure 4.10-1). Using hypothermic culture at 33°C as previously established in progenitor cells (Enninga, Groenendijk et al. 1984; Mivechi and LI 1990), mCHERRYPSLD expressing MPPs (Lin^- $Ly6A/E^+$ $CD117^+$ $CD150^-$ $CD48^+$ $CD34^+$ cells) were incubated and imaged using time-lapse microscopy. Due to cooling down and potential adaptation, cell-cycle was scored after 24 hours. This time period also coincides with the 24 hour time period required for viral transduction in HSCs. At this time point, no increase in G_1-phase prevalence could be detected (Figure 4.10-1A, left) (data from 3 independent experiments). When looking at cell-cycle transitions in generation 1, an increase in G_1-phase could be detected (Figure 4.10-1A, right). However, an even stronger elongation of S/G_2-phase was observed (data from 3 independent experiments, 75 trees). The lack of G_1-phase enrichment on the one hand and the unknown effect of increased daughter cell G_1-phase and S/G_2-phase on cell fate or lineage production suggests this method is not suitable to test our hypothesis.

Chemicals that inhibit cell-cycle progression at specific stages are well established for cell-cycle enrichment. However, although most inhibitors are known

to work in cell lines, little is known about their effect and usage in primary blood cells. For this purpose, MPPs (Lin^- $Ly6A/E^+$ $CD117^+$ $CD150^-$ $CD48^+$ $CD34^+$ cells) were used and incubated with either hydroxyurea (G_1-phase arrest), l-mimosine (G_1-phase arrest) or nocodazole (G_2/M-phase arrest) as a negative control. Different incubation times and concentrations were tested. As a read-out, propidium iodide staining was used to detect cell-cycle distribution (data from 3 independent experiments, 10.000 events each) (Figure 4.10-1B, top, see also Figure 4.1-2A).

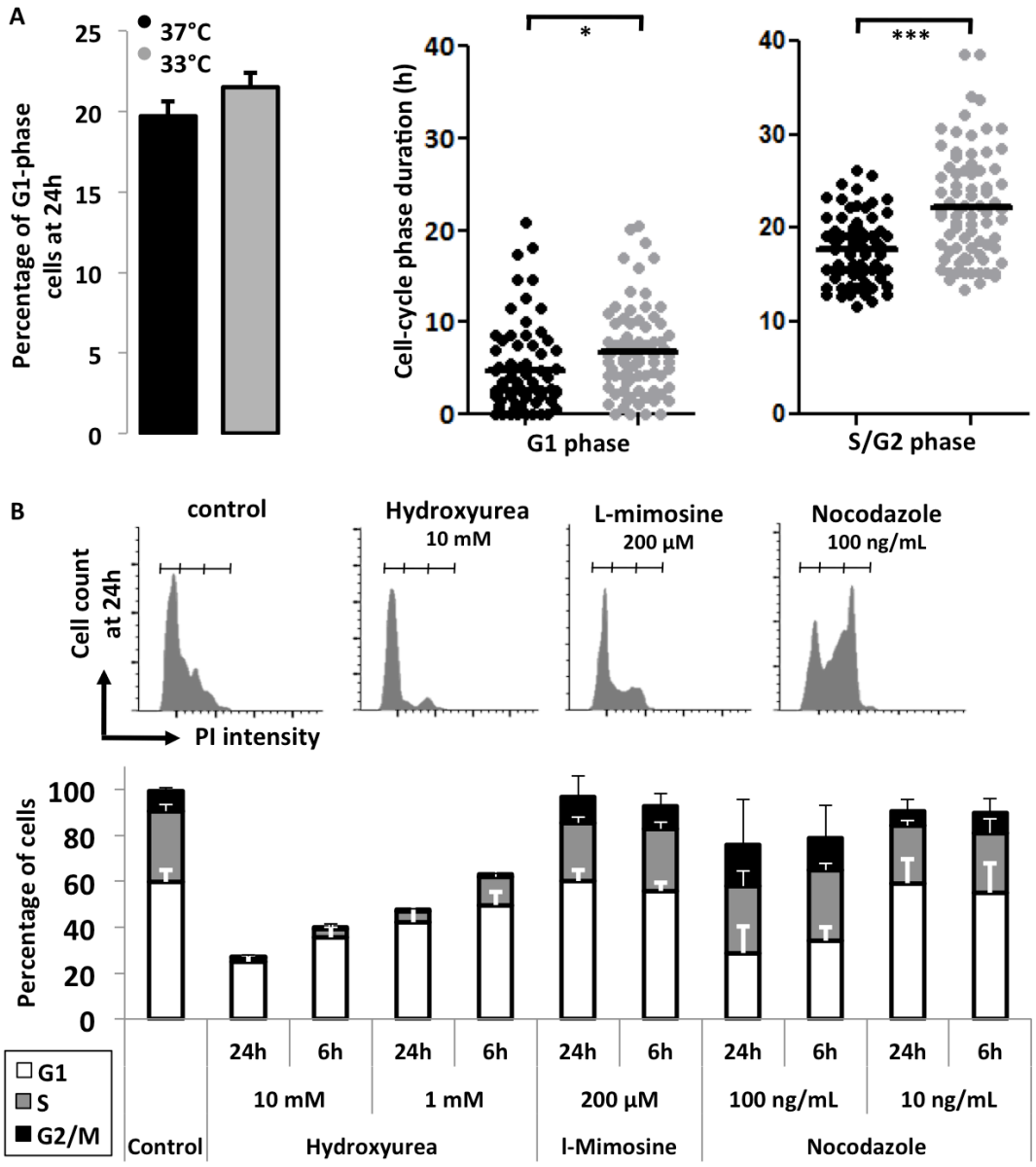

Figure 4.10-1: Hydroxyurea treatment enriches for G_1-phase cells

A. Hypothermic culture does not increase yield of G_1-phase cells and affects cell-cycle phase durations. Cell-cycle phase durations are depicted for dividing generation 1 cells (n=3). B. Incubation with hydroxyurea reduces prevalence of S/G_2-phase cells. Cell-cycle distributions according to propidium iodide staining and FACS analysis. Percentages shown are standardized to surviving cells in control condition. * p-value<0.05, *** p-value<0.001.

From this, cell-cycle state was obtained (Figure 4.10-1B, bottom). Higher doses of hydroxyurea are strongly toxic, drastically reducing the number of live cells (not shown). An optimal G_1-phase enrichment for hydroxyurea was found at 24 hours using 1 mM, retaining G_1-phase cell numbers whilst reducing the presence of S/G_2-phase cells. The method of action for G_1-phase enrichment remains unclear from this data. It may be that the case that S/G_2-phase cells either die more or reside within G_1-phase upon their next cell-cycle, or the prolonged cell-cycle retention of G_1-phase cells induces toxicity. However, initial experiments were performed in which cell-cycle inhibitor-induced apoptosis was correlated with cell-cycle phase. No correlation or cell-cycle specific effect could be found (not shown). In contrast, l-mimosine had no effect on cell-cycle phase enrichment, not even when using high, non-cytotoxic concentrations. Nocodazole treatment on the other hand showed increased G_2/M-phase cells at the expense of G_1-phase cells. For HSC G_1-phase enrichment 24 hour pre-incubation with 1 mM hydroxyurea was chosen for further experiments.

4.11 G_1-phase enrichment increases multilineage production.

To address the question whether G_1-phase enrichment leads to an increase in multilineage production, clonal lineage production was again correlated with the cell-cycle phase of generation 0 at the time of permissive cytokine addition (Figure 4.11-1, data from 3 independent experiments). Despite optimized hydroxyurea concentrations and incubation times, cytotoxicity still occurs. To verify whether cells in specific cell-cycle phases are more prone to apoptosis, viability was assessed for both generation 0 and generation 1 cells (Figure 4.11-1A). Both in generation 0 and generation 1, more cells die after being treated for 24 hours with 1mM hydroxyurea and after receiving permissive cytokine addition. Again, G_1-phase cells are more prone to apoptosis, however this is not only the case in generation 0 cells but an inherited effect is also observed in generation 1 cells. However, since the majority of the cells were in G_1-phase after hydroxyurea treatment, this may form a bias when considering a correlation with apoptosis in generation 1.

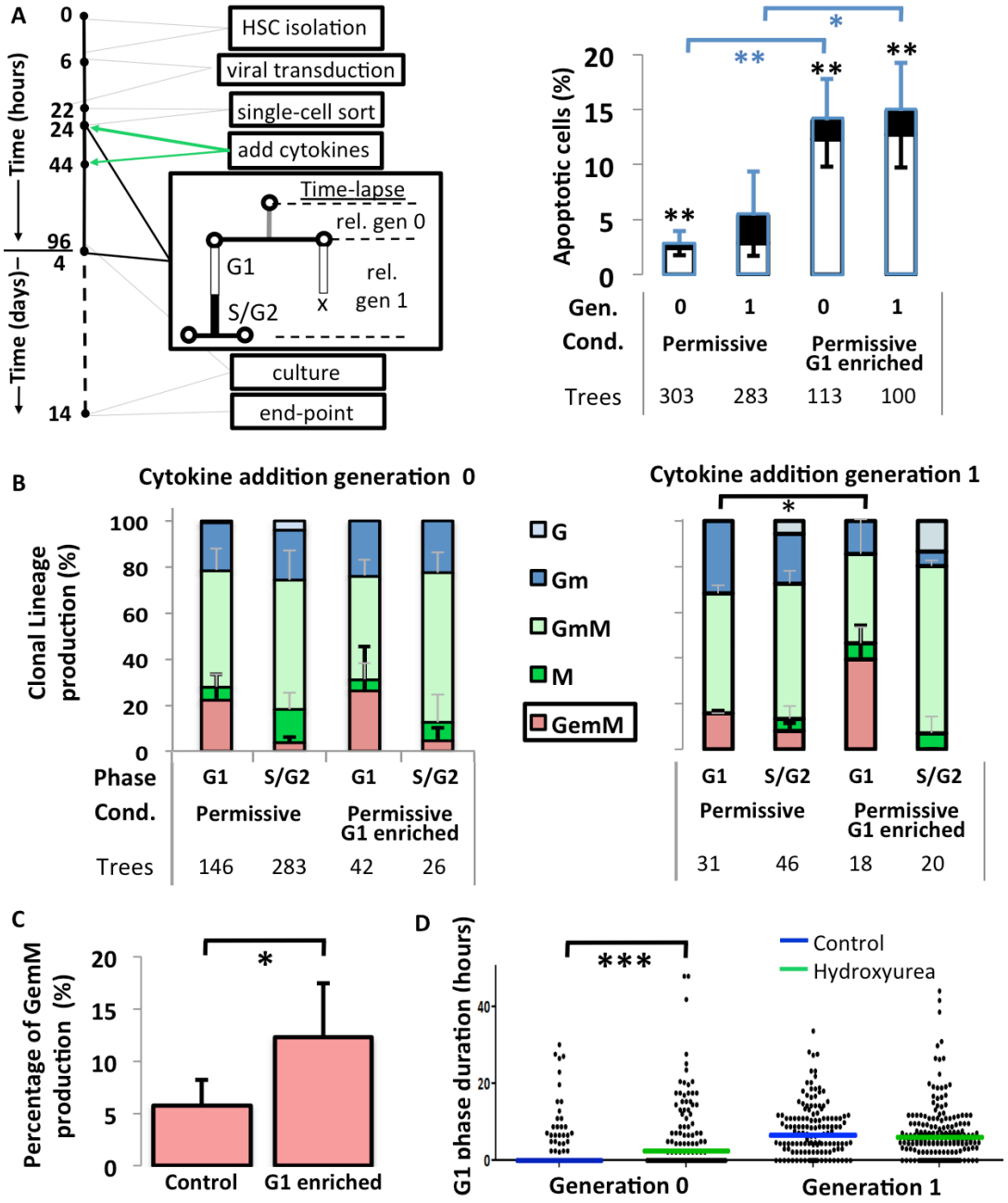

Figure 4.11-1: G_1-phase enrichment increases total GemM production

A. Hydroxyurea treatment increases apoptosis in G_1-phase cells. Cell-cycle phases indicate cell-cycle state in starting cells (generation 0) at the time of movie start and medium addition (n=3). B. G_1-phase enrichment increases total yield of GemM producing cells but does not restrict lineage production. G=granulocytes, m=macrophages, M=megakaryocytes, e=erythrocytes. Cytokine addition in generation 1 occurred at 20h after movie start, giving a total of 44h. C. Correcting for cell-cycle prevalence and apoptosis shows increased yield of GemM producing cells after hydroxyurea treatment. D. Hydroxyurea prolongs G_1-phase but does not affect daughter cells, G_1-phase durations after 24h pre-incubation. * p-value<0.05, ** p-value<0.01, *** p-value<0.001. Blue bars and asterisks indicate total levels, black asterisks show cell-cycle specific significance.

Next, end-point lineage scoring was again correlated with initial cell-cycle phase at the time of cytokine addition (Figure 4.11-1B). Although the G_1-phase enrichment (62% vs. 34% control) did not lead to an increase in the percentage of GemM lineage production, correction of the total absolute numbers (429 vs. 68, ~6.3

fold more) leads to a 2.2 fold increase of GemM producing cells from G_1-phase cells after hydroxyurea enrichment even exceeding the ~1.1 fold increase in apoptosis (Figure 4.11-1C). As a control, S/G_2-phase specific lineage production was not affected by hydroxyurea treatment. It may well be that the higher apoptosis in G_1-phase cells partly formed a lineage selection, causing total GemM lineage production to be lower. On the other hand, it has been postulated, that hydroxyurea-induced G_1-phase arrest may act too late, i.e. either late G_1-phase or early S-phase, to increase cytokine-induced differentiation.

For this reason, experiments were conducted where cells were imaged after 24 hours and cytokines were added at 44 hours, a point at which the prevalence of G_1-phase generation 1 cells is at its peak (see also Figure 4.3-1C and Figure 4.7-1A). Using this technique, the effect of cytokine addition in generation 1 could be assessed (Figure 4.11-1B, right). By doing so, an increase of GemM lineage production from G_1-phase cells could again be detected (data from 3 independent experiments). Furthermore, this was significantly higher when compared with non-enriched permissive control cells. In contrast, GemM lineage production from S/G_2-cells was completely abolished. Together this points to the effective enrichment of G_1-phase cells and the reoccurrence of GemM producing cells from G_1-phase daughter cells. The observed longer G_1-phase for GemM lineage producing cells in dividing generation 1 cells could not be detected for G_1-phase enriched cells (Figure 4.11-1D, right), but a total time frame in which cytokines can act is increased by the extension of G_1-phase in generation 0 (Figure 4.11-1D, left).

4.12 p38 signaling pathway activity is reduced during G_1-phase.

To explore the potential signaling pathways involved with G_1-phase induced lineage commitment, staining was performed for four different signaling pathways and tested for correlation with either G_1-phase or S/G_2-phase (Figure 4.12-1). Here imaging was chosen as an alternative to Western blots due to the low abundance of HSCs in bone marrow and correct localization was confirmed by confocal imaging (Figure 4.12-1A).

Correlation with cell-cycle was performed by scoring the amount of positive cells per cell-cycle phase for each signaling pathway. Scoring was performed using epifluorescence pictures, signals again being corrected for with controls consisting of only secondary antibodies. Data from three independent replicates revealed large variation and no cell-cycle specific activity (Figure 4.12-1B-C).

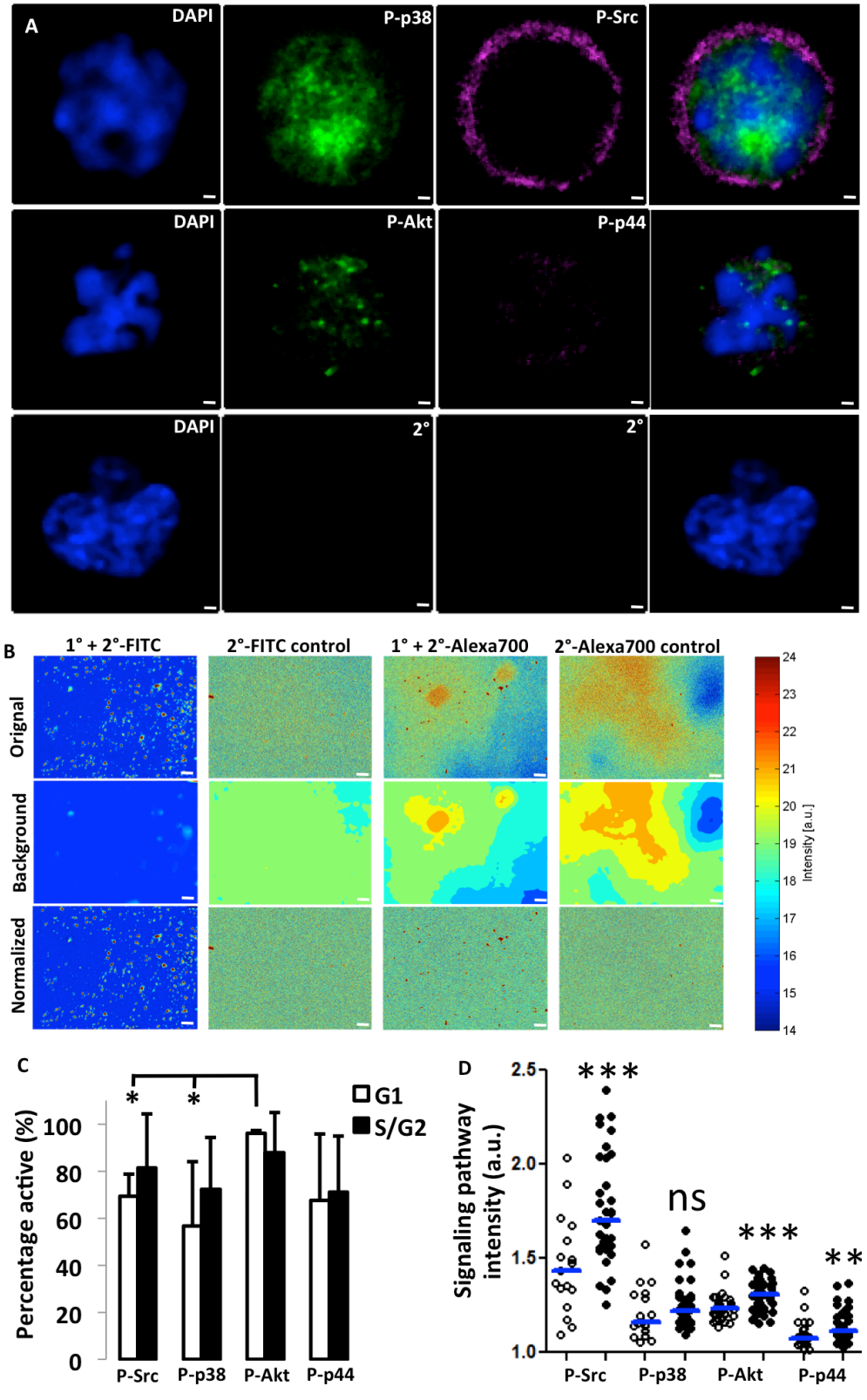

Figure 4.12-1: Src and p38 signaling pathway activity are reduced during G_1-phase
A. Activated signaling pathways show correct localization. Confocal images of p-p38 and p-Src (top), p-Akt and p-p44/p42 (middle) displayed according to secondary control (bottom). B. Background correction allowed for quantification of fluorescent staining for signaling pathway activity. C. G_1-phase cells show reduced signaling pathway activity (ON/OFF) for Src and p38 compared with Akt. PSLD cell-cycle marker was imaged after fixation. D. G_1-phase signaling intensity is weaker for P-Src P-Akt and P-p44. * p-value<0.05, ** p-value<0.01, *** p-value<0.001. Scale bar: A. 1 µm, B. 40 µm.

Akt signaling was observed in either cell-cycle phase in almost every cell. Since Akt can be activated by both SCF and TPO signaling and is thought to function downstream of phosphoinotiside 3-kinase, which is necessary for cell-cycle progression, its signaling pathway activity can also be seen as a positive control. Both p38 and Src showed significantly reduced levels during G_1-phase when compared with activated Akt signaling. For S/G_2-phase no such effect could be observed. However, signaling pathway intensities were mostly found to be lower during G_1-phase (Figure 4.12-1D).

4.13 NUP98-HOXA10hd represses progenitor marker expression.

Ever since the groundbreaking HSC expansion through NUP89-HOXA10hd (NA10hd) overexpression was first published, an outstanding question has been how this phenomenon occurs. With recent advances using time-lapse microscopy and phenotyping of *in vitro* cultured NA10hd cells first insights have been acquired yet a NA10hd signatory behavior has not yet been observed or defined (Palmqvist, Pineault et al. 2007; Even, Bennett et al. 2011; Sekulovic, Gasparetto et al. 2011; Watts, Zhang et al. 2011; Sloma, Imren et al. 2013).

To further understand the mechanism that drives multipotent HSCs to expand, NA10hd behavior was first defined on a population level (Figure 4.13-1). To ascertain correct expression of the NA10hd construct, the linked FLAG-domain at the N-terminus of NA10hd was stained and imaged using confocal microscopy. With acquisition set to unstained controls, NA10hd cells showed nuclear expression, whereas mock-infected cells only expressed the nuclear membrane-tagged VENUS signal (not shown). Simultaneously SCA-1 was highly expressed in NA10hd cells but rapidly down-regulated in mock-infected cells (not shown).

With the proposed HSC expansion model (Sekulovic, Imren et al. 2008), NA10hd positive cells will expand over ~1000 fold within 6 days of culture, meaning a minimum of 10 divisions leading to an average cell division time of ~12-14 hours. For this reason, a faster proliferation and thus higher fold expansion was assumed for NA10hd cells when compared with mock-infected cells. When looking at early time-points (day 1-7), total cell numbers are actually lower than mock-infected control cells (data from 3 independent experiments). However, in long-term culture, mock-infected cells are depleted, whereas NA10hd cells retain the potential to proliferate (Figure 4.13-1A, left). Underlying reasons for this can vary from increased short-term apoptosis to slow-cycling subpopulations, which cannot be assessed when looking on a population scale. The strong repression of the progenitor marker CD48 (Figure 4.13-1A, right) by NA10hd supports the hypothesis that NA10hd cells have not attained a fast proliferation rate, characteristic of multipotent progenitor cells that undergo lineage maturation (data from 3 independent experiments). However, a recent study has shown that NA10hd can introduce a fetal liver HSC phenotype instead, which supports the active cell-cycle while retaining multipotency.

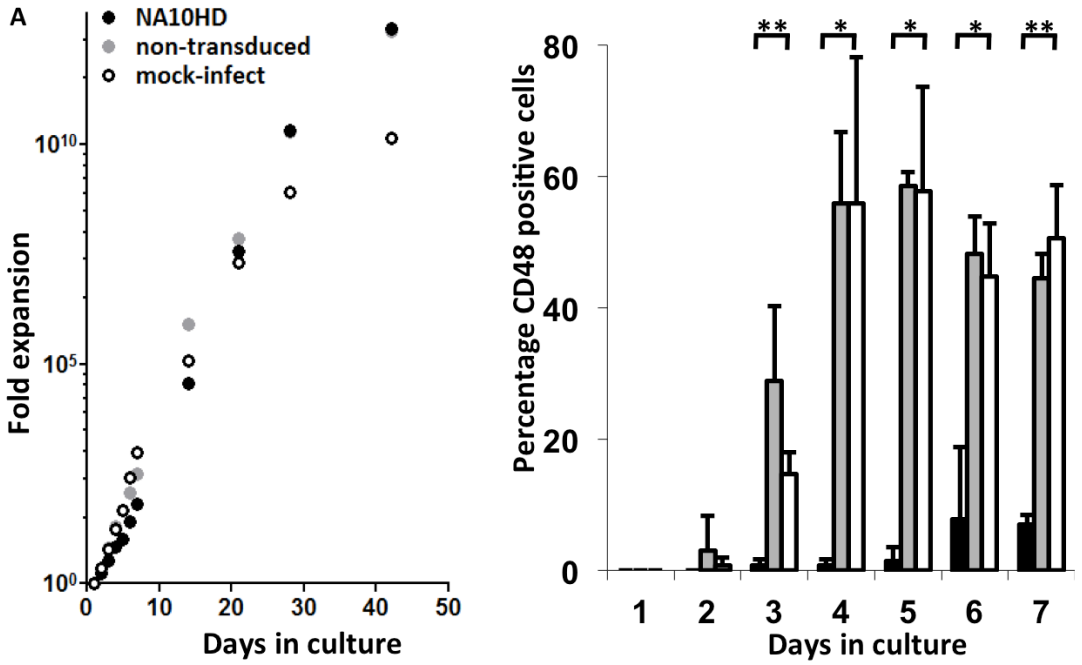

Figure 4.13-1: NUP98-HOXA10hd represses expression of progenitor surface markers
A. NA10hd cells show reduced expression of CD48 in bulk population. Average of fold expansion standardized to day 1 (100 cells) and percentage of cells expressing CD48 (n=3). * p-value<0.05, ** p-value<0.01.

4.14 NA10hd fetal liver HSC phenotype is exclusively produced by HSCs.

Next, the susceptibility of different hematopoietic stem and progenitor cells to attain a NA10hd-induced fetal liver phenotype (Lin^- $Ly6A/E^+$ $CD43^+$ $CD11b^{dim}$) was assessed by sorting HSCs (LSK $CD150^+$ $CD48^-$ $CD34^{lo}$), early MPPs (LSK $CD150^-$ $CD48^-$ $CD34^{+)}$ and late MPPs (LSK $CD150^-$ $CD48^+$ $CD34^+$), transducing them with NA10hd, followed by phenotypical analysis for surface markers 12 days later (Figure 4.14-1). At first sight, one can immediately see the strong repression of lineage marker expression, since ~70% of the NA10hd cells are not positive for these markers. This in contrast to mock-infected cells, in which the majority (>90%) lose their differentiation potential and express mature lineage markers (Figure 4.14-1A, left). This is in line with previous publications that indicate a repression of full maturation by NA10hd. It is conceivable that the addition of interleukin-3 and interleukin-6 and fetal calf serum quickly leads to loss of stemness and indeed acquisition of a mature phenotype, present in control cells. NA10hd cells, however, do not seem to be affected when it comes to lineage marker expression.

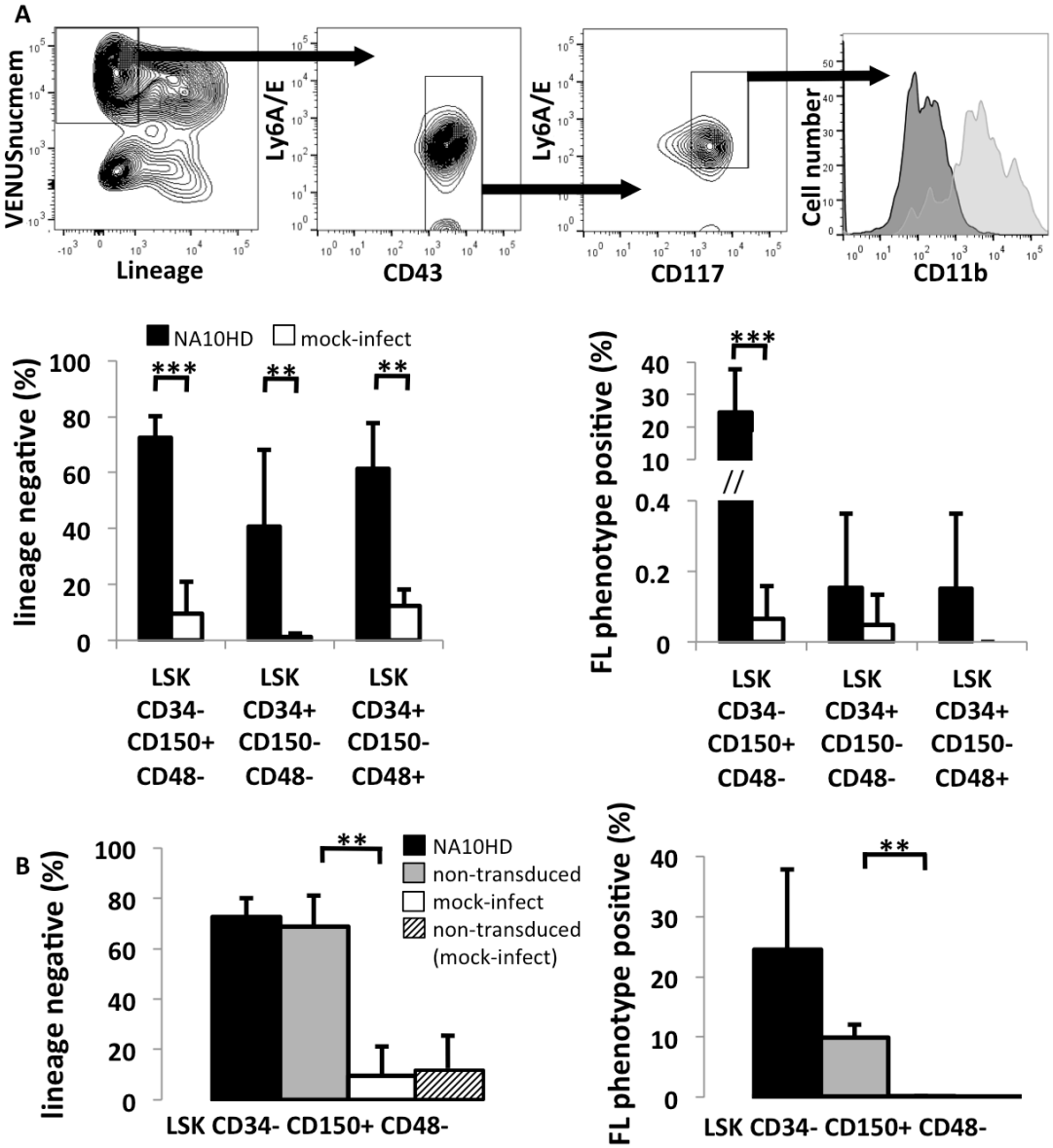

Figure 4.14-1: NA10hd induces a fetal liver HSC phenotype exclusively in HSCs
A. NA10hd represses expression of surface markers for lineage commitment in HSPCs while inducing a fetal liver HSC phenotype only in HSCs. Rectangles and arrows indicate subsequent gating schemes. Analysis performed after 12 days (n=3). Fetal liver HSC phenotype is Lin^{-} $CD43^{+}$ $Ly6A/E^{+}$ ($CD117^{+}$) $Cd11bd^{im.}$ B. Phenotype of non-transduced cells is affected by NA10hd expressing cells in co-culture (n=3). * p-value<0.05, ** p-value<0.01, *** p-value<0.001).

Their fast, apparently symmetric self-renewing proliferation posed the question whether these cells attain a fetal liver phenotype, since HSCs are quickly expanded within the fetal liver. To confirm transplantation data that indicated the presence of such a phenotype on the majority of NA10hd cells that had repopulation potential, presence of these cells was again assessed using flow cytometry (Figure 4.14-1A, right). These $NA10hd^{+}$ $Lineage^{-}$ $Ly6A/E^{+}$ $CD117^{+}$ $CD43^{+}$ $CD11b^{dim}$ cells

were indeed present after 12 days of *in vitro* culture, whereas none of the control cells showed such a phenotype (below 1% error). Furthermore, acquisition of such a NA10hd phenotype was exclusive for HSCs, since early MPPs and late MPPs did not produce this phenotype (from 3 independent experiments). Although this does not imply that these cells cannot form competitive repopulating units in *in vivo* transplantations, the lack of such a phenotype caused further experiments to be conducted with HSCs only.

After transduction, about 50% of the HSCs were successfully expressing NA10hd, observed through VENUSnucmem co-expression. Although for a more efficient workflow higher transduction rates were desirable, this allowed testing whether NA10hd cells can have an effect on non-transduced cells. Indeed, when looking at repression of lineage maturation, non-transduced showed the same effect (Figure 4.14-1B, left). Furthermore, the acquisition of a fetal liver HSC phenotype was lower than NA10hd+ cells, yet significantly distinct from control cells ($p<0.01$), in which this phenotype was barely detectable (Figure 4.14-1B, right). Together this shows that NA10hd can indeed have cell non-autonomous effect when it comes to lineage repression and marker expression. Its implications for repopulation potential still require further investigation. The observed NA10hd paracrine effect however is more likely to be accredited to secreted molecules than cell-cell contact since these cells were cultured in suspension with concentrations not exceeding 10^6 cells per mL.

4.15 NA10hd retains an inheritable slow cycling cell population.

NA10hd behavior was next compared with mock-infected cells and lifetimes for dividing cells over multiple generations were quantified (Figure 4.15-1). The gradual reduction of time needed for cell division over multiple generations indeed approaches the 12-14 hour cell-cycle, hypothesized to be required for maximal expansion (Figure 4.15-1A). However, NA10hd cells retain a population of slow cycling cells within generation 1 and 2, dividing significantly slower than mock-infected cells (p-value<0.05 and <0.001, respectively).

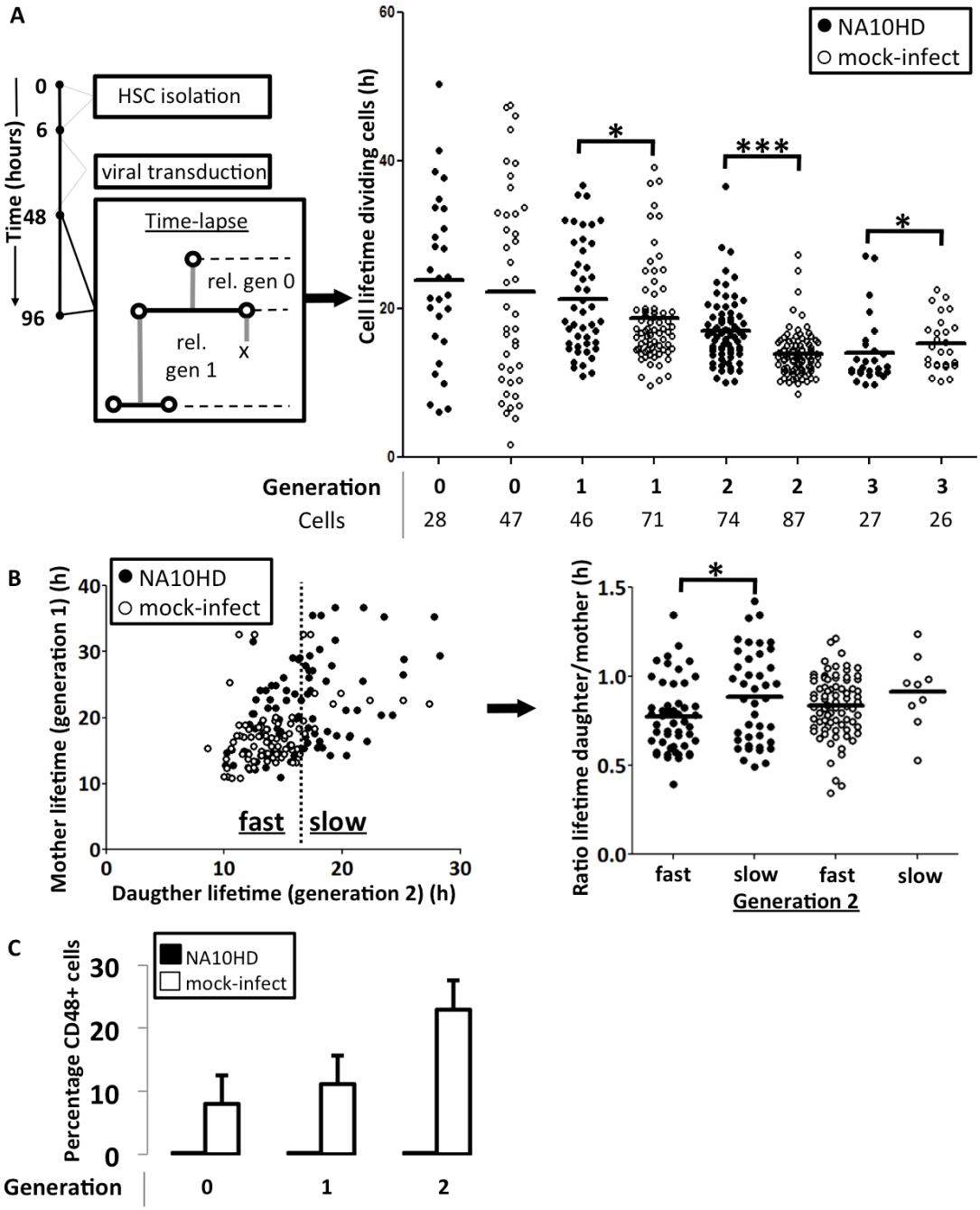

Figure 4.15-1: NA10hd cells retain a slow-cycling compartment that is inheritable
A. NA10hd population contains cells that have a slower cell-cycle in early generations (n=3). B. These slow cycling cells are derived from slow cycling ancestors. Dashed line indicates median value for NA10hd generation 2 dividing cells. Data points were gated accordingly ("fast" or "slow", lower or higher than medium, respectively). Ratios were then calculated by dividing generation 2 lifetime by generation 1 lifetime for dividing cells (n=3). AB. Thick lines indicate median value. C. Expression of CD48 is repressed in early generations also at a clonal level. CD48 expression of all cells by live antibody detection in time-lapse imaging (n=3). * p-value<0.05, ** p-value<0.01, *** p-value<0.001).

Although these cells also persist in generation 3, the majority of the NA10hd cells actually attain a faster cell-cycle when compared with mock-infected control cells (p-value<0.05) (from 3 independent experiments). To verify whether slow cycling cells produce slow cycling progeny, lifetimes of generation 2 dividing

daughter cells were compared with their generation 1 dividing mothers (Figure 4.15-1B, left). These data points were subdivided according to the NA10hd median value for generation 2, leading to a "fast" and "slow" cycling compartment. When now comparing their cell lifetime ratios with their generation 1 lifetime, one finds that slow dividing NA10hd cells indeed give rise to slow dividing progeny (p-value<0.05). The same phenomenon is true for fast dividing NA10hd cells that produce faster dividing progeny (from 3 independent experiments). This leads to an overall gradual dilution of the slow cycling compartment, therefore absent in later generations. Mock-infected control cells did not show a significant difference albeit the majority of the cells are derived from already fast dividing cells.

The absence of CD48 expression on NA10hd cells reported by others was also confirmed in time-lapse imaging (Figure 4.15-1C).

4.16 Thrombopoietin alters the NA10hd-induced phenotype

Addition of thrombopoietin (TPO) abolishes NA10hd-induced HSC expansion (Sekulovic, Gasparetto et al. 2011). To test whether this has an effect on marker expression, NA10hd HSCs were cultured with or without TPO addition and were analyzed after 12 days of culture (Figure 4.16-1, data from 3 independent experiments). Indeed, the percentage of cells with a fetal liver HSC phenotype was greatly reduced after TPO addition (p-value<0.05) (Figure 4.16-1A). However, one cannot exclude that TPO addition alters marker expression whilst retaining repopulation potential or indeed, cells with repopulation potential adopt a different phenotype when cultured with TPO addition.

To explore potential differences in NA10hd behavior, cell lifetimes were again compared over multiple generations (Figure 4.16-1B). TPO strongly increases lifetime of NA10hd dividing cells (p-value<0.001). This could imply that the previously found dividing cellular subsets with longer cell lifetime are cells that are no longer or not yet having induced self-renewal divisions. To support this hypothesis, further transplantations are required with isolated cells from time-lapse imaging.

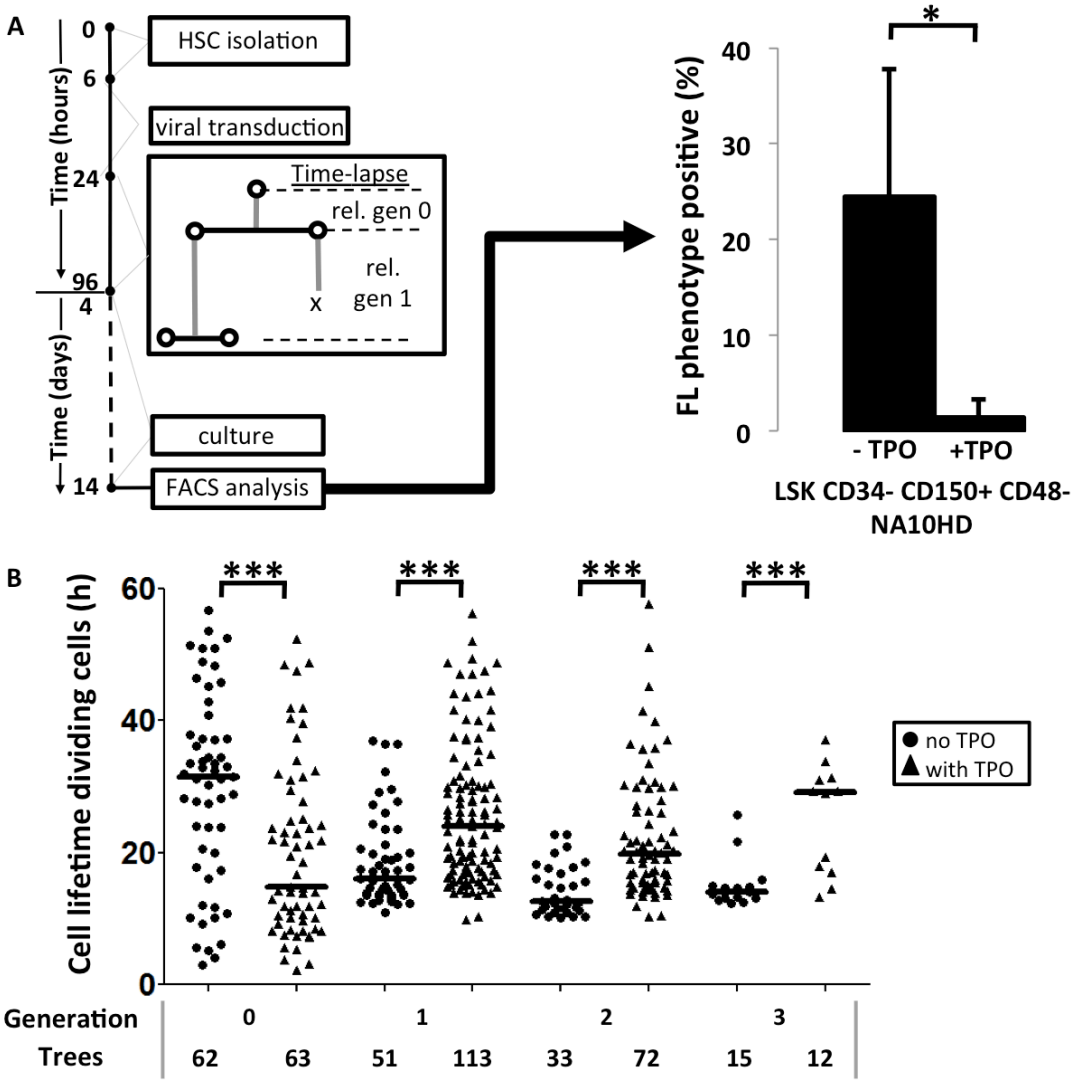

Figure 4.16-1: Thrombopoietin addition reduces fetal liver HSC phenotype in NA10hd cells

A. TPO addition reduces NA10hd fetal liver HSC phenotype. B. NA10hd cell-cycle is altered upon TPO addition. Thick lines indicate median value. Cells were imaged after 24h pre-incubation. TPO=thrombopoietin, * p-value<0.05, ** p-value<0.01, *** p-value<0.001).

4.17 Stroma interactions increase NA10hd lifetime and motility

The loss of the highly proliferative character of *in vitro* NA10hd cells upon transplantation *in vivo* as well as the *in vivo* establishment of mature lineage subsets derived from NA10hd cells is of great clinical interest, yet its method of action has not yet been unraveled. When HSCs home into their *in vivo* niche, cell-cell interactions are re-established. This interaction has been shown to be crucial for maintenance of quiescence and simultaneously controls differentiation. Here, a PA6 stromal co-culture was established to identify whether NA10hd behavior is distinct from mock-infected cells when cell-cell interactions are introduced with stroma

capable of short-term stem cell maintenance (Figure 4.17-1, data from 5 independent experiments).

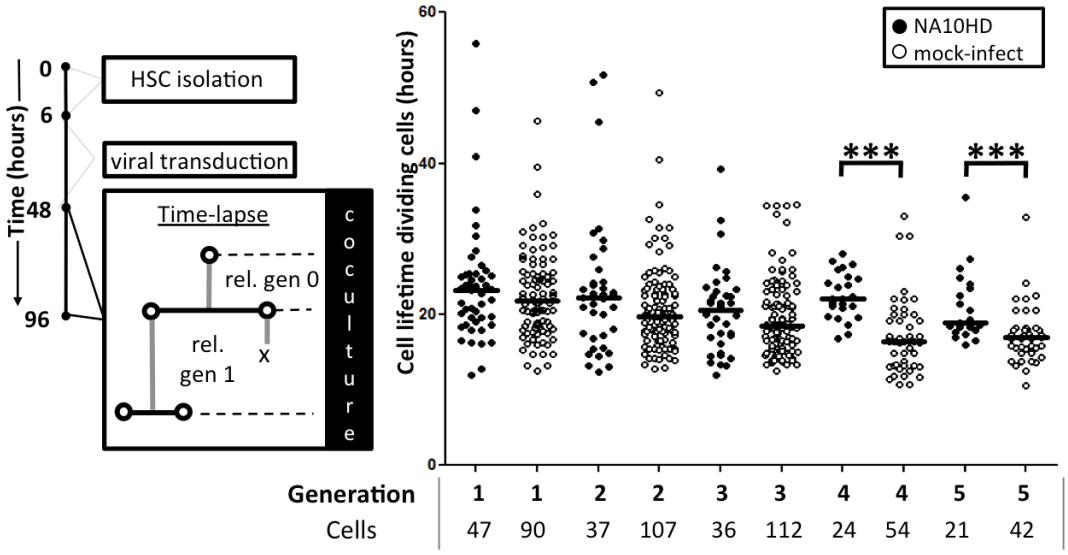

Figure 4.17-1: NA10hd cells have longer cell lifetimes in PA6 co-culture
NA10hd cell lifetimes for dividing cells are longer in late generations. n=5, * p-value<0.05, ** p-value<0.01, *** p-value<0.001. Thick horizontal lines indicate median value.

When comparing generations, initial cell lifetimes (generation 1-3) are highly heterogeneous. In later generations (i.e. 4 and 5), it becomes apparent that NA10hd have a much longer (~1.5 fold) lifetime when compared with mock-infected control cells. To check whether this correlates with cell-cell interactions, determined by adherence underneath the stroma, the percentage of adherence per cell lifetime was measured (Figure 4.17-2A, left). Large heterogeneity exists in early generations (1-3), in which cells are frequently free floating and do not fully reside underneath the stroma during their lifetime. Although NA10hd cells have subsets that have less stroma residency during generation 3 and 4, the majority of these cells are more than 90% of their lifetime underneath the stroma. Indeed, for generation 5, in which NA10hd cells have a longer cell lifetime, all cells were underneath the stroma for the complete duration of their cell-cycle.

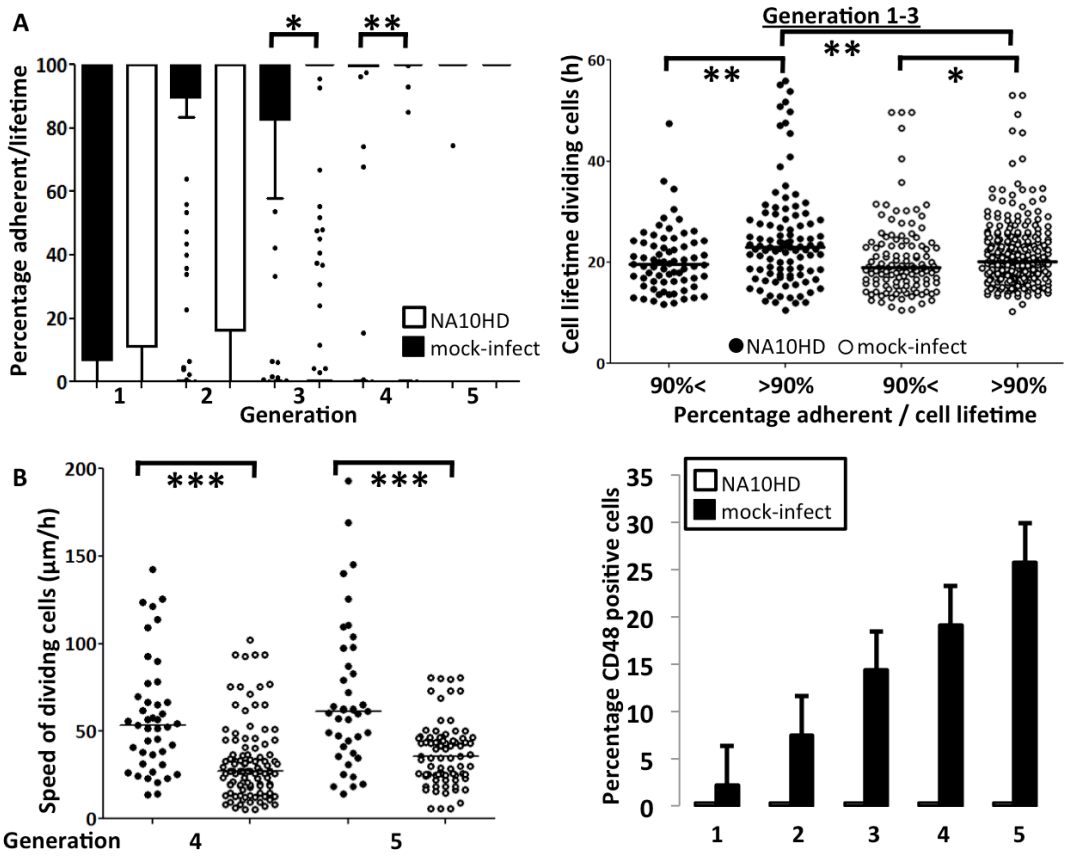

Figure 4.17-2: NA10hd specific behavior correlates with cell-cell contact

A. NA10hd adherent cells have longer cell lifetimes than non-adherent and control cells in early generations. Cell lifetimes for generation 1-3 were pooled and subsets were created depending on percentage of stroma residency. B. NA10hd cells show increased motility and repress CD48 expression in co-culture with PA6 stroma. Motility of dividing cells with 100% stroma residency was compared. n=5, * p-value<0.05, ** p-value<0.01, *** p-value<0.001. Thick horizontal lines indicate median value.

For more in-depth analysis of earlier generations, cells were subdivided according to their stroma residency. For this purpose, cells were pooled from generation 1-3 and subsets containing >90% of stroma residency were compared with subsets containing <90% of stroma residency. By doing so, NA10hd cells with higher stroma residency were found to have longer lifetimes, compared both with NA10hd cells with less stroma residency and mock-infected control cells, independent of stroma residency (Figure 4.17-2A, right). This shows, that the longer lifetime found for NA10hd cells is either cell-contact specific and not caused by soluble factors or slow dividing NA10hd cells have a better adherence. Together this shows that through all generations, NA10hd have a longer lifetime when in direct contact with PA6 cells.

Not only does PA6 co-culture allow quantification of adherent state, other attributes such as cell-size, nucleus size and migration can be measured as well.

Perhaps most interesting is the ability to quantify motility, which under liquid culture conditions difficult to measure due to high variations, gradient differences and flux of cells towards certain areas of culture plates due to tilting, motorized stage movement or non-uniform heating. To reduce heterogeneity, cell motility was quantified for cells that were underneath the stroma for the full duration of their cell-cycle (Figure 4.17-2B, left). NA10hd cells in generation 4 and 5 show an almost 2-fold increase in motility when compared to mock-infected control cells.

The NA10hd-induced repression of CD48 also occurs in stroma co-culture (Figure 4.17-2B, right). Further experiments are required to test whether the expression of CD48 on mock-infected control cells correlates with their reduced motility and cell lifetime.

5 Discussion

5.1 Optimization of a clonal read-out

Despite the tremendous amount of work in the last decades on optimization of HSCs purification schemes and defining their phenotypical identity, a uniform consensus or methodology has not yet been achieved. In this work, a sorting scheme using expression of surface markers was adapted (Kiel, Yilmaz et al. 2005; Raval, Kusler et al. 2012) and used for HSC purification. Previous work on HSCs that explored the susceptibility of different cell-cycle phases to induce lineage production upon cytokine addition has also been performed using purification methods based on dye efflux (Goodell, Brose et al. 1996; Matsuzaki, Kinjo et al. 2004). Although dye efflux has been proven useful to increase the yield of quiescent cells, the addition of CD34 to SLAM markers in order to further distinguish quiescent cells from activated cycling cells (Sato, Laver et al. 1999; Tajima, Sato et al. 2000; Ogawa, Tajima et al. 2001) also results in highly efficient retrieval of quiescent HSC populations. The HSC populations used in this work, however, may differ from other published work in terms of pre-sorting lineage bias or quiescent state and comparison of results thereof need to be interpreted with care. Although single-cell transplantations were not performed in the course of this work, preliminary experiments using limiting dilution assays in c-kit deficient mice were performed, confirming high HSC purification levels of the isolated cells (not shown). Furthermore, the purity and quiescent state of these cells was confirmed by the time necessary for the first *in vitro* cell division and comparison with multipotent progenitors, which correlates with the *in vivo* repopulation capacity as previously described (Dykstra, Ramunas et al. 2006; Nygren, D et al. 2006; Benveniste, Frelin et al. 2010).

The lack of robust and reliable live cell-cycle markers made continuous cell-cycle quantification difficult to perform. With the coming of a cell-cycle reporter mouse expressing FUCCI, S/G_2 phase can be visualized by onset of fluorescence. However, the signal was not always detectable and cumbersome post-processing was required in order to quantify cell-cycle state. The combination with another fluorescent protein knock-in to visualize G_1-phase made this process more reliable

and workable in *in vivo* setting, yet still required post-processing and the use of another fluorescent protein reduced the potential use of fluorescent antibody combinations or demanded even higher optical resolution thereby challenging temporal resolution. Furthermore, FUCCI expression was found to be non-ubiquitous and indeed time-lapse imaging of isolated *in vitro* cultivated HSCs showed too low expression to conduct any further experiments (not shown). Very recently the authors confirmed this observation and developed different mouse lines for this purpose (Sakaue-Sawano, Hoshida et al. 2013). To circumvent this problem, PSLD was virally transduced into HSCs resulting in a robust expression of a valid cell-cycle reporter. During 24 hour pre-incubation, >95% of the cells still reside within their first *in vitro* cell-cycle and although cells may have lost their HSC potential, the majority of the cells had not lost their multipotency, due to their cultivation in a previously described medium that can maintain HSCs (Ema, Takano et al. 2000). This is in line with other purification methods and the late cell-cycle entry found in population-based data (Reddy, CY et al. 1997; Colvin, Dooner et al. 2007). With this system, it was possible to quantify and show how HSCs transit through different cell-cycle phases over multiple generations in a heterogeneous fashion for the first time, while simultaneously assessing their *in vitro* lineage production. Future work, however, should profit from new robust methods allowing live continuous cell-cycle assessment directly after isolation without applying invasive techniques.

The problem with many published population-based data is the loss of cellular genealogy. To be able to identify cell-specific behavior and compare kinship not only requires continuous time-lapse imaging on a single-cell resolution, but in order to exclude a direct (e.g. cell-cell) or indirect (e.g. secreted molecules) interaction potentially influencing cell fate, such an analysis must be performed clonally, e.g. 1 well containing 1 cell. Of course, one could argue that once cells proliferate, cell density increases accordingly, especially in static cultures where cells only reside on the bottom surface area. Soluble and secreted molecules produced may then again affect the fate of other cells, however since all cells are ultimately derived from one starting cell the decision to do so consequently has been made up in the hierarchy. In addition, analysis of bulk populations leaves uncertainties about the existing of subpopulations that may mask the overall observed effect. As is the case with many *in vivo* studies, bulk culture could furthermore provide compensatory mechanisms, e.g.

the large amount of different secreted molecules by various cells may lead to variable, even false conclusions. Clonal assays abolish most of these problems. Today such clonal assays have been optimized with help of lab-on-a-chip microfluidic culture devices that allow continuous observation (Faley, Copland et al. 2009; Wlodkowic, Skommer et al. 2009; Lecault, Vaninsberghe et al. 2011) yet the number of off-the-shelve products is limited.

The problem with many scaled-down bioreactors lies in the fact that upon proliferation cell density increases. This not only prevents long-term single-cell tracking but may also influence cell fate as known for many primary cell types (Baksh, Zandstra et al. 2007; Kirouac, Madlambayan et al. 2009; Lee, Kim et al. 2013; Vaquette, Ivanovski et al. 2013). For this project a gas-perfusable clonal read-out was established that provided both high-throughput imaging on single-cell resolution and long-term cultivation without reaching confluence. However, in order to study cell-cell interactions, culture devices still require improvement. Perfusion culture by membrane separation (Lecault, Vaninsberghe et al. 2011; Ratcliffe, Glen et al. 2012) ensures continuous availability of fresh media and other than static conditions or serial dilutions reduces accumulation of cytokines and medium degradation products that may selectively affect cell fate. The rather static conditions used in this work therefore could show different results when compared with dynamic culture conditions. Such work is required to rule out cell extrinsic factors produced by other cells and simultaneously study the effect of self-produced cytokines or extracellular matrix proteins to create a local environment.

On the other hand, increasing cell density is another problem, which needs further strategic development in order to study the influence of cell-cell interactions in suspension culture. The fact that clinical studies focusing on human HSPC expansion showed a positive correlation of HSPC expansion with increasing cell density (Zandstra, Eaves et al. 1994), shows low density suspension culture and can even prove beneficial. The accompanied reduction of oxidative stress may also play a role in selective apoptosis or lineage production. Recent developments in protein stamping (Rottgermann, Alberola et al. 2014) and microwell structures by soft lithography (Chen, Li et al. 2011) could be of interest in studying cell-cell interactions, permitting or inducing migration with their effect on maturation and specialization. Combining

this with titrated perfusion and cytokine addition would encompass many requirements to study both cell intrinsic and extrinsic factors. Such a device has recently been developed and not only enables these features but also could be used to follow up development of genealogy and perform daughter separation by cell trapping (Frank and Tay 2013). Although so far no work on primary cells has been published, preliminary results obtained with cell lines show robust methodology and should be of interest to study HSC fate and function.

Different media conditions allow for different lineage production and maturation. Testing of different media conditions in this work led to different outcome in terms of apoptosis, survival and lineage production. Although not the main focus in this thesis, these results proved reproducible and could be of future interest to study potential selective effects of cytokines. However, to increase efficiency in high-throughput screening, reduction of high numbers of apoptotic events was desirable. Simultaneously, high apoptosis rates as well as exclusion of development of certain lineage subsets could indicate a selective mechanism (Enver, Heyworth et al. 1998; Josefsen, Blomhoff et al. 1999; Rieger, Hoppe et al. 2009; Mossadegh-Keller, Sarrazin et al. 2013) and the development of pre-biased cells would not be read out. To reduce this occurrence and its complexity when it comes to cell-cycle specific lineage production, medium supplements were chosen that were permissive for the development of all mature lineage subsets and had an overall low occurrence of apoptosis. Furthermore, media conditions that resulted in early detection of lineage subsets were favored because 1) this drastically reduced workload by avoiding media refreshment, which on itself could also affect lineage production and 2) an earlier observed effect on differentiation could be better correlated with initial cell-cycle phase. For these reasons, media supplements were chosen, based on previously published methods that allowed high and early prevalence of all mature myeloid lineage subsets (Takano, Ema et al. 2004). Again, comparison of results in perfusion culture to ensure optimal medium conditions will need to be performed and used concentrations require further titrations to point out efficiency and validity of cytokine function.

Culture conditions without co-culture with stromal cells were chosen to 1) relate lineage production to added rather than secreted cytokines and molecules and 2)

improve optical quality and ability to follow HSC behavior and cell-cycle durations over time. However, the lack of lymphoid maturation poses the question whether culture conditions could be further optimized to read-out lineage potential. Addition of interleukin-7 would most likely ensure that lymphoid cells could be produced. However, lymphoid cells require much longer developing and detection of these cells only occurs at later stages, similar to *in vivo* repopulation kinetics. The strong proliferation observed under these media conditions in *in vitro* culture (10^4 to 10^5 cells after 14 days), points to the necessity of multiple instances of media refreshment and usage of large incubation devices. Since the aim was to explore multilineage production in relation to cell-cycle, lymphoid reconstitution was omitted from the scope of this thesis. Nevertheless, the detection of all myeloid lineage subsets *in vitro* has been correlated with *in vivo* multilineage (including lymphoid) reconstitution potential (Takano, Ema et al. 2004), allowing a bridge to HSC functionality, although ultimately transplants would be required to prove this point.

The data presented in this thesis shows lower clonal multilineage production when compared with published data. On one hand, this could be explained by the fact that certain media supplements such as insulin or transferrin were not added since this reduced the amount of variables that could influence cell fate. On the other hand, in this work cells were pre-incubated for 24 hours and cytokines were added then rather than immediately after isolation. Although the pre-incubation medium should maintain multipotency for the majority of the cells, it could well be that this affected lineage potential after further addition of permissive cytokines. Taking into consideration however that the majority of the cells at 24 hours no longer reside within G_1-phase (>70%), cytokine addition may have different effects when compared to freshly isolated cells that all pass G_1-phase when receiving permissive cytokines. Together, this might explain the reduced potential but for the scope of this work this effect was less relevant since comparisons were made with control cells not receiving permissive cytokine addition. Furthermore, the megakaryocyte producing potential was not undermined by pre-incubation.

The time-point at which end-point lineage production was assessed is derived from LTC-IC data, both published (Kerst, Slaper-Cortenbach et al. 1992; Verfaillie 1992; Smith, Bender et al. 1993; Verfaillie 1993; Henschler, Brugger et al. 1994;

Petzer, Hogge et al. 1996) and established in this lab. Considering the *in vivo* longevity of lineage subsets (~5-6 days for neutrophils/granulocytes, 100-120 days for erythrocytes, ~60 days for macrophages and 7-10 days for megakaryocytes) this however does not mean that *in vitro* lifespan compare. Optimal detection for all lineages including erythrocytes was found between day 12 and 14 for freshly isolated HSCs. Including pre-incubation time of 24 hours, cells were therefore analyzed 13 days after permissive cytokine addition, i.e. 14 days after isolation. This work offers a comparison after 14 days of culture. It must be said that earlier lineage commitment, maturation and even apoptosis of different lineage subsets cannot be excluded, as well as lineage production after this time-point. Ideally, multiple time-points or continuous time-lapse imaging would provide such more in-depth information about proliferation kinetics and dynamics of lineage production. This would also shed light on lineage potency at different stages in genealogy, yet the exact point of lineage decision was beyond the scope of this thesis.

5.2 Cell-cycle and its role in lineage production

The quest of inducing specific lineage subsets has been an equal struggle as the quest to understand how it occurs. Indeed, with in-depth knowledge about the mechanism, lineage decision can be orchestrated with higher efficiency. For a long time it has been hypothesized and assumed that cytokines can induce different cell fates, depending on the cell-cycle phase they act on. Moreover, it has been postulated that certain cytokines might only function within certain cell-cycle phases. This thesis provides evidence that such relations indeed exist and simultaneously provides a robust method for future research that allows direct quantitation of cytokine-specific and cell-cycle phase-specific effects.

Many cells that undergo differentiation reside within G_1 phase, based upon their DNA content. Furthermore, forced cell-cycle inhibition through ectopic expression of CKI, was found to not only lead to up-regulation of differentiation markers but also induce differentiation into muscle cells (Shih, Tevosian et al. 1998), shown to enhance nerve growth (Erhardt and Pittman 1998) and was shown to be essential for erythroid differentiation (Tamir 2000). In these studies, however, cells were already

within a mature, less potent stage and thereby could not show that cytokine induced lineage production was related to cell-cycle phase earlier in genealogy and hierarchy. To be able to link lineage production to cell-cycle, clonal identity needs to be preserved and visualization of cell-cycle is required. This is challenging in many vertebrate systems, in which *in vivo* imaging resolution is limited and the number of possible serial time-points is often restricted. Recently, the successful FUCCI-based mouse model has been translated to zebrafish, which due to its optical clarity may facilitate continuous cell-cycle quantification *in vivo* (Sugiyama, Sakaue-Sawano et al. 2009).

Studies on astrocyte function, proliferation and function have revealed that niche-specific interaction and location during cell-cycle are essential for future cell fate in terms of differentiation (Pilz, Shitamukai et al. 2013). In addition, cell-cycle specific up-regulation of different genes were found to be correlating with and directing differentiation (Robel, Bardehle et al. 2011; Bardehle, Kruger et al. 2013). Yet the *in vivo* abundance of extracellular signaling pathways often form compensatory mechanisms that make it hard to relate cytokine function and cell-cycle to cell fate. For most of these cell types, controlled cultivation in an *in vitro* setting is difficult and results are often skeptically interpreted as artifacts. Since the majority of the *in vivo* hematopoietic system has a non-adherent character, *in vitro* cultivation has been very well established and media supplements such as cytokine concentrations have been optimized to ensure optimal culture conditions. Despite studies on gene profiling during proliferation in HSPCs (Passegue, Wagers et al. 2005), to date still little is known about cytokine function in various cell-cycle phases and how this relates to cell fate.

The observation described in this thesis that GemM lineage production is mainly derived from G_1-phase cells at the time of permissive cytokine addition whereas megakaryocytes are mostly produced from S/G_2-phase cells is the first direct evidence on a clonal basis that cytokines added at different cell-cycle phases can induce diverging cell fates. However, this does not occur with 100% penetrance, i.e. lineage production is not cell-cycle exclusive. One reason previous work could not show the same results on a clonal basis, might be that cell-cycle phases were based on population-based distributions and could not be assessed live on a single-cell

resolution (Colvin, Dooner et al. 2007). S/G_2-phase cells also produce granulocytes, macrophages and indeed full GemM lineage albeit to a much lower extent. Hence the question arises whether these occurrences are really cytokine and cell-cycle dependent or if they are cell-intrinsic features, e.g. cells with a longer G_1-phase have a higher probability of receiving permissive cytokine addition in G_1-phase whilst having an increased intrinsic potential to develop full GemM lineage. Quantification of G_1 phase duration during which the cells received cytokine signaling, an advantage of using time-lapse imaging, did not reveal a dependency on G_1 phase duration and excluded such an effect to be caused by probability. The fact that the same effect can be observed when adding cytokines to daughter (generation 1) cells, independent of mother (generation 0) cell-cycle durations shows that this is a reversible feature that is maintained in progeny, yet does not prove or disprove a cell-intrinsic effect. To further explore this possibility, cells were forcefully pushed or retained in G_1-phase using cell-cycle inhibitors. Although percentages of GemM production from G_1-phase cells were not increased, strikingly, the absolute number of GemM colonies was indeed found higher after G_1-phase enrichment, since the number of G_1-phase cells was increased (~2 fold more) and G_1-phase specific apoptosis was found to be only slightly higher (~10%). As a negative control, S/G_2-phase cells show no effect of G_1-phase enrichment.

The general higher occurrence of apoptosis in cells in G_1-phase in generation 0 could point to a potential selective lineage production, i.e. certain HSC subsets in G_1-phase that could be primed for specific lineages would not survive and hence the percentage of GemM lineage production could be an artifact. However, since GemM lineage production is actually increased for G_1-phase cells, the loss of G_1-phase cells could simultaneously indicate a loss of GemM lineage production. To circumvent this problem and study this theory, experiments should be performed in which apoptosis is abolished. Further directions could therefore be pointed towards use of purified HSCs from constitutively active *bcl-2*$^{+/+}$ mice as a control, in which cells are no longer undergoing apoptosis. Furthermore, the stressful isolation steps and re-sorting of HSCs after 24 hours do not allow thorough adaptation to change of environment and it may be that G_0 or G_1 phase HSCs are more sensitive to signaling disruption. This has been shown in leukemic cell lines (Jedema, Barge et al. 2003) but remains inconclusive for primary HSCs.

When cytokines were added to daughter cells (generation 1) derived from G_1-phase enriched mother cells (generation 0), GemM production was again increased for G_1-phase daughter cells. Although the observed effect is even stronger when compared with non-enriched control cells, the occurrence of apoptosis in generation 1 is also increased, which could again point to potential selectivity. This data supports the hypothesis that indeed hydroxyurea treatment may push the cells in G_1-phase, but the actual effect takes place during its next cell-cycle where it passes the G_1-phase related different retinoblastoma phosphorylation stages. Previous studies have postulated that hydroxyurea arrests cell-cycle transition at a later G_1-phase stage or indeed when early S-phase has already begun (Murciano, Zamora et al. 2002). If this is true, it could be that the G_1-phase specific restriction point had already been passed, resulting in a potential lower frequency of GemM lineage production. After division of these cells their daughter cells can receive cytokine addition in G_1-phase, which may occur at other stages that were no longer accessible due to hydroxyurea treatment. This is supported by data showing that protein-DNA interactions are lost upon S-phase specific dissociation and are re-established during G_1-phase in which transcription factors and proteins controlling epigenetic mechanisms are re-associated (Blomen and Boonstra 2011). On the other hand, clinical studies that use hydroxyurea to induce erythroid differentiation have also shown that subpopulations undergoing stress response adaptation are less prone for apoptosis while having a higher potential to develop mature erythrocytes (Pourfarzad, von Lindern et al. 2013). GemM lineage production would still be more efficient when using hydroxyurea for G_1-phase enrichment but experiments with use of a constitutively active *bcl-2*$^{+/+}$ mouse model, which would reduce the hydroxyurea induced apoptosis (Liu, Aiello et al. 2012), are required to study a potential selective effect.

G_1-phase transition is mainly controlled by the phosphorylation state of retinoblastoma in which p18 and to a lower extent p16 are normally involved in inhibition of the cyclin D / CDK4-6 activity. First experiments with a p16 double knockout model in C57Bl/6 mice yielded no ablation of GemM lineage production, in fact no effect on lineage detection could be observed (not shown). This again demonstrates that the G_1-phase stage in which cytokines are received and act upon in order to make lineage decision may not be within early G_1-phase in which cell-cycle entry takes place. In line with this is the fact that multipotent progenitor cells are also

capable of producing GemM lineage, albeit to a lower extent. Since these cells generally have a faster cell-cycle, it does not seem farfetched that the time-frame in which the cytokines can act is shorter and this causes a lower yield of GemM colonies.

An *in vitro* read-out that could predict lineage production and multipotency would facilitate both clinical therapies as well as many other scientific approaches such as daughter cell comparison, studying stem cell maintenance and expansion, asymmetric cell divisions and gene profiling. Current read-outs such as cobblestone formation or colony assays provide end-point information about potency but do not allow usage of cells before lineage commitment. To date many models exist; however, a prediction model on the HSC level has not yet been succeeded (Glauche, Cross et al. 2007; Loose, Swiers et al. 2007; Kirouac, Madlambayan et al. 2009; Marr, Strasser et al. 2012; Teles, Pina et al. 2013). Prediction of cell fate through cell-cycle phase progression has been successful in pluripotent cell lines that could show a correlation of G_1-phase elongation with development into neural stem- and progenitor cells (Roccio, Schmitter et al. 2013) or G_2-phase elongation to be essential for *in vivo* neurulation (Ogura, Sakaue-Sawano et al. 2011). In general differentiation and purification of pluripotent stem cells can be achieved by selection and manipulation of G_1-phase durations (Calder, Roth-Albin et al. 2013; Coronado, Godet et al. 2013; Pauklin and Vallier 2013). Although differentiation into specific lineages in the hematopoietic system has also been correlated with G_1-phase elongation (Furukawa, Kikuchi et al. 2000; Hsieh 2000; Tamir 2000; Munoz-Alonso, Ceballos et al. 2012), this has never been shown in multipotent cells upstream in the hierarchy. In this study not only does initial cell-cycle phase seem to correlate with end-point lineage output, continuous time-lapse imaging also revealed lineage-specific cell-cycle phase durations and cell division times. Although not providing a prediction model on itself, when combining different features, lineage-specific behavior could in the future prove to be mutually exclusive. The GemM specific longer G_1-phase in daughter cells (generation 1) together with the overall symmetric division times for kinship and the higher prevalence of G_1-phase in their ancestry (generation 0) would with the current status already exclude the development of granulocytes which ancestors have an overall shorter G_1-phase and S/G_2-phase while having a higher occurrence of asymmetric daughter cell lifetimes. Megakaryocytes on the other hand have highly

symmetric daughter cell lifetimes while having significantly shorter G_1-phase durations and are more prevalent in S/G_2 phase during generation 0. With more in-depth cell-cycle analysis of these characteristics, e.g. with another cell-cycle reporter such as PCNA that allows a more qualitative cell-cycle analysis, combined with morphological features and with higher temporal resolution, these results provide future directions that could ultimately predict lineage commitment in early *in vitro* cell divisions.

The effect of GM-CSF on megakaryocyte development has been contradictory. Here, addition of GM-CSF reduced GemM lineage production whilst increasing megakaryocyte production from S/G_2-phase cells. However, apoptosis was significantly increased for G_1-phase cells when compared to control cells without GM-CSF addition. The fact that changing of media conditions towards GM-CSF resulted in much higher apoptosis indicates the beneficial permissive conditions, albeit even under these culture conditions selective apoptosis cannot be excluded. Furthermore, GM-CSF on itself increased apoptosis in S/G_2-phase cells, in contrast to addition to permissive conditions. Together this hints towards a potential synergistic effect with other cytokines. The mixture of cytokines present in permissive conditions could provide stronger competition when considering binding affinity and could potentially have a conflicting effect in signaling pathway activation. More work is still required to unravel the complex signaling network topology involved.

Following *in vivo* studies (Asami, Pilz et al. 2011) and work on leukemic cell lines (Matsumura, Ishikawa et al. 1997) that correlated cell-cycle specific gene up-regulation to be essential for differentiation in progeny, signaling pathway activation in *in vitro* cultivated HSCs was quantified. Initial experiments showed cell-cycle phase heterogeneity in the activity of four different signaling pathways. PI3K had been previously described to be necessary to transit through cell-cycle and indeed was found to be active in >90% of the cells. With the prospect of exploring cell-cycle specific activity, mCHERRYPSLD expressing cells were fixed and imaged before staining with antibodies specific for phosphorylated signaling pathways. This experimental setup was not ideal since fixation caused a significant drop in cell-cycle reporter levels, which hampered clear detection and quantification. Imaging of cells prior to fixation led to loss of cell identity after staining of activated signaling

pathways. Although ambiguous cells and cell-cycle states were not counted, future work should further improve this method, preferably using live biosensors. Such work has already been performed in cell lines and progenitor populations but not in HSCs and is further complicated by the need of serum starvation (Haugh, Codazzi et al. 2000). Live methods would furthermore facilitate correlation with future cell fate. Overall, none of the signaling pathways showed cell-cycle phase-specific activity. When comparing absolute levels however, both p38 and Src had reduced activity in G_1-phase when compared with PI3K. p38 is known to be important for megakaryocyte development, whereas Src has been implied to be essential for macrophage development (Melemed, JW et al. 1997; Whalen, SC et al. 1997; Fichelson and Freyssinier JM 1999; Jacquel, Herrant et al. 2006; Bourgin-Hierle, Gobert-Gosse et al. 2008; Kaminska, Klimczak-Jajor et al. 2008; Severin, Ghevaert et al. 2010). Despite these first hints for correlation with potential lineage commitment, no clear pattern could be observed yet.

The capacity to induce more than a 10,000 fold increase in HSC numbers within 2 weeks of culture without a potential risk of leukemia made NA10hd revolutionary in the field of blood stem cell biology. Both the necessary proliferation rate as well as the co-localization of NA10hd with p300 led to the hypothesis that NA10hd may have an impact on cell-cycle and cell lifetime. To date, little is known about the *in vitro* NA10hd-specific behavior, and even proliferation rates on a clonal level did not shed light onto the potential mechanism of NA10hd-induced *in vitro* HSC expansion. Here, evidence is presented for the first time that different subsets within the NA10hd+ compartment exist and can be separated according to cell lifetime: cells with longer lifetimes are more abundant in NA10hd+ populations compared with mock-infected control cells. Furthermore, by comparing progeny with ancestry over multiple generations, these features were shown to be inheritable. Simultaneously however, NA10hd+ cells with a faster cell-cycle were equally derived from mother cells with a faster cell cycle, together pointing to the gradual exhaustion of slow cycling NA10hd+ cells. Indeed, after several days, these differences are no longer detectable. This shows again the strength of single-cell continuous time-lapse observation and that read-out of created pedigree-based data provides much more information when compared with bulk population-derived data.

Recently, NA10hd has been found to induce a fetal liver HSC phenotype. This lineage^{-} Ly6A/E^{+} CD117^{+} CD43^{+} CD11b^{dim} population contained the majority (25-50%) of *in vitro* expanded HSCs with *in vivo* repopulation capacity. Since original studies were performed with bulk populations containing ~1% HSCs and recent published data has shown a higher number of CRU containing wells than initially purified and clonally seeded, the potential of early multipotent progenitor cells to induce such a phenotype was assessed in this study. Surprisingly, only HSCs were susceptible to acquire such a phenotype. This however does not mean that none of the multipotent progenitors were capable of forming *in vivo* CRUs; it may well be the case that they attain a different phenotype. Indeed, not all cells possessing a fetal liver phenotype were capable of *in vivo* repopulation, neither did all HSCs express such a phenotype (Sekulovic, Gasparetto et al. 2011). Furthermore, suggested by their data, the NA10hd mechanism to induce HSC expansion may even be caused by an induced self-renewing and repressed differentiation onset in multipotent progenitors. The fact that addition of thrombopoietin drastically reduces such a phenotype whilst simultaneously abolishing repopulation potential makes it of future interest to compare these populations and quantify their dynamics of marker expression, ideally through time-lapse imaging, in order to define their behavior.

So far, only Sca-1 was observed to be strongly retained on NA10hd+ cells in comparison with mock-infected control cells. Nevertheless, expression levels through quantification did not show any correlation with NA10hd expression nor with cell lifetime of these cells (not shown).

This data is derived from liquid culture in which many cells were not effectively transduced with NA10hd. The lineage marker repression and the acquisition of a fetal liver phenotype in many of the non-transduced cells points to a paracrine effect, either through cell-cell signaling or by secretion of extracellular proteins and soluble molecules. This effect has not been previously described, possibly due to the different and highly efficient transduction protocols used by other labs that reach >95% transduction efficiency. Although this paracrine effect can be of interest on itself, one may not exclude the effect of non-transduced cells on NA10hd+ cells: HSC expansion may be effectively altered by cells producing mature lineage subsets or secreting and expressing different molecules than NA10hd+ cells. Initial colony assays after 2 weeks of *in vitro* culture however showed a high prevalence of

blast and GemM lineage producing cells, indicating their immature nature and multipotency, respectively (not shown).

To further investigate the influence of environment and cell-cell contact as well as to mimic the *in vivo* niche influence on NA10hd cells, a stromal co-culture was established with PA6 cells. These cells are known to be able to maintain stemness in a proportion of cells (Kodama, Amagai et al. 1982; Kodama, Nose et al. 1992) and due to their optical clarity and contact inhibition, offer a good platform to study NA10hd+ cells behavior. Interestingly, NA10hd cells were shown to have a much longer cell lifetime for dividing cells in both early and late generations which was dependent on their adherent state: cells that were underneath the stroma had a longer cell-cycle when compared with cells that had a shorter stromal residency. This indicates that a NA10hd+ cell-PA6 interaction rather than secreted molecules causes the extension of cell lifetime. Whereas mock-infected control cells contain a subpopulation retaining this long lifetime in early generations, these are no longer present in later generations. Since PA6 cells can maintain stemness over multiple days, it could well be that this property is lost after multiple days of culture. This is supported with the faster onset of CD48, an *in vitro* progenitor marker in mock-infected control cells when compared with NA10hd cells. In later generations, however, a proportion of NA10hd+ cells also expresses CD48.

PA6 cells express CXCL5 ligand, which functions as a chemoattractant. CXCL5 binding is known to repress megakaryocyte development. After 6-7 days of PA6 co-culture, mock-infected control cells produce megakaryocytes (Supplemental movie 3 and 4). After 7 days of culture, NA10hd cells had not developed any megakaryocytes. If their increased motility when underneath PA6 stroma is indeed caused by increased binding of the chemoattractant CXCL5, this would support this finding and is in line with improved homing of HSCs *in vivo* (Yoon, Cho et al. 2012). Preliminary marker screens performed prior to these observations indicated an increased expression of CXCR4, which belongs to the same family of proteins. Further experiments to support and test this hypothesis will need to be performed in future work as well as transplantations to correlate to HSC functionality. On the same line this could imply that these cells favor stroma residency whilst up-regulating integrin expression that allows for the higher motility found in NA10hd cells. On the

other hand, these cells may in fact seek ways to exit cell-cell contact. This, however, is unlikely since all cells gradually favor to be underneath stroma, even when cultured in lower stroma co-culture densities.

The two different environments covered by this thesis thus provide two different read-outs. Whereas longer cell lifetime for dividing cells in liquid culture could indicate a less active NA10hd-induced fetal liver HSC cycling, the longer lifetime found when cultured on PA6 stroma could indicate retention of stemness or repression of differentiation. Transplantations after clonal PA6 stromal co-culture combined with time-lapse imaging could test these hypotheses.

5.3 Scientific contribution

In this thesis, I have provided new discoveries on two different subjects that both involve definition of *in vitro* HSC behavior. Live quantification of cell-cycle phase duration in HSCs showed that even highly purified stem cells transit through cell-cycle in a highly heterogeneous fashion over multiple generations when receiving the same media supplements. Furthermore, the discovery of lineage-choice behavior with respect to cell-cycle stage on a single-cell resolution had not yet been achieved and here I showed concrete evidence that such a correlation can exist. This could have both clinical and scientific implications when HSC expansion without multilineage potential loss is required. On one hand HLA competent cells could be more specifically directed to increase specific lineages *ex vivo* or purification could be enhanced through selection in short-term culture. This could be of interest for potential clinical applications where patients are depleted with certain mature lineage subsets or require long-term contribution for all lineages, as is the case with HSC transplantations. With future work still required, this would also provide new insight in the underlying mechanisms and factors that influence cell fate decisions and could be useful for therapies that cope with disruption of these mechanisms in hematological diseases. On the other hand, scientific research could benefit from the results provided in this thesis, not only because HSC and lineage-specific behavior could be determined but also because this assists future predictive models regarding lineage potential that, when functional, could reduce workload and necessity of long-

term *in vitro* assays. In fact, the robust read-out provided, using continuous cell-cycle quantification and clonal multilineage production, can easily be translated to other long outstanding questions such as asymmetric cell division, cell type specific morphological and behavioral characteristics, HSC maintenance under co-culture or cytokine instructed differentiation, allowing a deeper in-sight towards cell-cycle dynamics of these cells and provide a stepping stone to fully understand HSC biology.

The results I've provided here from the NA10hd project show for the first time that different NA10hd+ subsets exist with respect to cell lifetime and that to a certain extent these properties are inheritable, yet only become visible when using time-lapse imaging that allows following their cellular genealogy and inferring inheritable properties and their relation to their ancestry. The improved motility of these cells as well as the influence of NA10h cell-PA6 cell interactions furthermore provide new insights in NA10hd behavior and forms first steps towards *in vivo* translation and a deeper understanding of the requirements of HSC expansion.

6 Bibliography

Abramovich, C., Pineault, N., et al. (2005). "Hox Genes: From Leukemia to Hematopoietic Stem Cell Expansion." Ann. N.Y. Acad. Sci. **1044**: 109-116.

Adolfsson, J., O. Borge, et al. (2001). "Upregulation of Flt3 Expression within the Bone Marrow Lin-Sca1+c-kit+ Stem Cell Compartment Is Accompanied by Loss of Self-Renewal Capacity." Immunity **15**: 659-669.

Akashi, K., X. He, et al. (2003). "Transcriptional accessibility for genes of multiple tissues and hematopoietic lineages is hierarchically controlled during early hematopoiesis." Blood **101**(2): 383-389.

Akashi, K., D. Traver, et al. (2000). "A clonogenic common myeloid progenitor that gives rise to all myeloid lineages." Nature **404**: 193-197.

Antonchuck, J., G. Sauvageau, et al. (2002). "HOXB4-Induced Expansion of Adult Hematopoietic Stem Cells Ex Vivo." Cell **109**: 39-45.

Antonchuk, J., G. Sauvageau, et al. (2001). "HOXB4 overexpression mediates very rapid stem cell regeneration and competitive hematopoietic repopulation." Exp Hem **29**: 1125-1134.

Arai, F., A. Hirao, et al. (2004). "Tie2/angiopoietin-1 signaling regulates hematopoietic stem cell quiescence in the bone marrow niche." Cell **118**: 149-161.

Arai, F., K. Hosokawa, et al. (2012). "Role of N-cadherin in the regulation of hematopoietic stem cells in the bone marrow niche." Annals of the New York Academy of Sciences **1266**: 72-77.

Asami, M., G. A. Pilz, et al. (2011). "The role of Pax6 in regulating the orientation and mode of cell division of progenitors in the mouse cerebral cortex." Development **138**(23): 5067-5078.

Baksh, D., P. W. Zandstra, et al. (2007). "A non-contact suspension culture approach to the culture of osteogenic cells derived from a CD49elow subpopulation of human bone marrow-derived cells." Biotechnology and bioengineering **98**(6): 1195-1208.

Bardehle, S., M. Kruger, et al. (2013). "Live imaging of astrocyte responses to acute injury reveals selective juxtavascular proliferation." Nature neuroscience **16**(5): 580-586.

Becker, A., E. McCulloch, et al. (1963). "Cytological Demonstration of the Clonal Nature of Spleen Colonies Derived from Transplanted Mouse Marrow Cells." Nature **197**: 452-454.

Becker, P. S., S. K. Nilsson, et al. (1999). "Adhesion receptor expression by hematopoietic cell lines and murine progenitors: modulation by cytokines and cell cycle status." Experimental hematology **27**(3): 533-541.

Beckmann, J. and W. P. Scheitza S, Fischer JC, Giebel B (2007). "Asymmetric cell division within the human hematopoietic stem and progenitor cell compartment: identification of asymmetrically segregating proteins." Blood **109**: 5494-5501.

Benveniste, P., C. Frelin, et al. (2010). "Intermediate-term hematopoietic stem cells with extended but time-limited reconstitution potential." Cell stem cell **6**(1): 48-58.

Benz, C., M. R. Copley, et al. (2012). "Hematopoietic stem cell subtypes expand differentially during development and display distinct lymphopoietic programs." Cell stem cell **10**(3): 273-283.

Bergh, G., Telleus, A. , Fritzon, A. , Kornfält, S. , Johnson, E. , Ollson, I. and Gullberg, U. (2001). "Forced expression of the cyclin-dependent kinase inhibitor p16INK4a in leukemic u-937 cells reveals dissociation between cell cycle and differentiation." Exp. Hematol. **29**: 1382-1391.

Bertrand, J. Y., N. C. Chi, et al. (2010). "Haematopoietic stem cells derive directly from aortic endothelium during development." Nature **464**(7285): 108-111.

Blazar, B. R., W. J. Murphy, et al. (2012). "Advances in graft-versus-host disease biology and therapy." Nature reviews. Immunology **12**(6): 443-458.

Blomen, V. A. and J. Boonstra (2007). "Cell fate determination during G1 phase progression." Cellular and molecular life sciences : CMLS **64**(23): 3084-3104.

Blomen, V. A. and J. Boonstra (2011). "Stable transmission of reversible modifications: maintenance of epigenetic information through the cell cycle." Cellular and molecular life sciences : CMLS **68**(1): 27-44.

Borrow, J., A. Shearman, et al. (1996). "The t(7;11)(p15;p15) translocation in acute myeloid leukaemia fuses the genes for nucleoporin NUP98 and class I homeoprotein HOXA9." Nature Genetics **12**: 159-167.

Bourgin-Hierle, C., S. Gobert-Gosse, et al. (2008). "Src-family kinases play an essential role in differentiation signaling downstream of macrophage colony-stimulating factor receptors mediating persistent phosphorylation of phospholipase C-gamma2 and MAP kinases ERK1 and ERK2." Leukemia **22**(1): 161-169.

Bowie, M. B., D. G. Kent, et al. (2007). "Identification of a new intrinsically timed developmental checkpoint that reprograms key hematopoietic stem cell properties." Proceedings of the National Academy of Sciences of the United States of America **104**(14): 5878-5882.

Bowie, M. B., K. D. McKnight, et al. (2006). "Hematopoietic stem cells proliferate until after birth and show a reversible phase-specific engraftment defect." The Journal of clinical investigation **116**(10): 2808-2816.

Bradley, H. and T. B. Hawley, KD (2002). "Cell intrinsic defects in cytokine responsiveness of STAT5-deficient hematopoietic stem cells." Blood **100**(12): 3983-3989.

Bradley, R. and D. Metcalf (1966). "The Growth of Mouse Bone Marrow Cells in vitro." Aust. J. exp. Biol. med. Sci **44**: 287-300.

Bravo, R., R. Frank,, et al. (1987). "Cyclin/PCNA is the auxiliary protein of DNA polymerase-delta." Nature **326**: 515-517.

Briddell, R. A., J.E. Brandt, et al. (1992). "Role of cytokines in sustaining long-term human megakaryocytopoiesis in vitro." Blood **79**: 332-337.

Buhring, H. J., C. A. Muller, et al. (1991). "Endoglin is expressed on a subpopulation of immature erythroid cells of normal human bone marrow." Leukemia **5**(10): 841-847.

Burgess, A. and Metcalf, D. (1980). "The Nature and Action of Granulocyte-Macrophage Colony Stimulating Factors." J Am Soc Hem **56**(6): 947-958.

Burney, R., A. Lee, et al. (2007). "A Transgenic Mouse Model for High Content, Cell Cycle Phenotype Screening in Live Primary Cells." Cell Cycle **6**.

Buske, C., M. Feuring-Buske, et al. (2002). "Deregulated expression of HOXB4 enhances the primitive growth activity of human hematopoietic cells." Blood **100**(3): 862-868.

Buske, C., Feuring-Buske, M., et al. (2001). "Overexpression of HOXA10 perturbs human lymphomyelopoiesis in vitro and in vivo." Blood **97**(8): 2286-2292.

Calder, A., I. Roth-Albin, et al. (2013). "Lengthened G1 phase indicates differentiation status in human embryonic stem cells." Stem cells and development **22**(2): 279-295.

Calvi, L., G. Adams, et al. (2003). "Osteoblastic cells regulate the haematopoietic stem cell niche." Nature **425**: 841-846.

Calvo, K., D. Sykes, et al. (2002). "Nup98-HoxA9 immortalizes myeloid progenitors, enforces expression of Hoxa9, Hoxa7 and Meis1, and alters cytokine-specific responses in a manner similar to that induced by retroviral co-expression of Hoxa9 and Meis1." Oncogene **21**: 4247-4256.

Challen, G. A., N. C. Boles, et al. (2010). "Distinct hematopoietic stem cell subtypes are differentially regulated by TGF-beta1." Cell stem cell **6**(3): 265-278.

Chen, H., J. Li, et al. (2011). "Microwell perfusion array for high-throughput, long-term imaging of clonal growth." Biomicrofluidics **5**(4): 44117-4411713.

Chesier, S., S. Morrison, et al. (1999). "In vivo proliferation and cell cycle kinetics of long-term self-renewing hematopoietic stem cells." PNAS **96**: 3120-3125.

Christensen, J. L. and I. L. Weissman (2001). "Flk-2 is a marker in hematopoietic stem cell differentiation: a simple method to isolate long-term stem cells." Proceedings of the National Academy of Sciences of the United States of America **98**(25): 14541-14546.

Clarke, A. R., E. R. Maandag, et al. (1992). "Requirement for a functional Rb-1 gene in murine development." Nature **359**(6393): 328-330.

Colvin, G. A., M. S. Dooner, et al. (2007). "Stem cell continuum: directed differentiation hotspots." Experimental hematology **35**(1): 96-107.

Coronado, D., M. Godet, et al. (2013). "A short G1 phase is an intrinsic determinant of naive embryonic stem cell pluripotency." Stem cell research **10**(1): 118-131.

Das, S., S. Kar Mahapatra, et al. (2007). "Oxidative stress in lymphocytes, neutrophils, and serum of oral cavity cancer patients: modulatory array of L-glutamine." Supportive care in cancer : official journal of the Multinational Association of Supportive Care in Cancer **15**(12): 1399-1405.

Deneault, E., S. Cellot, et al. (2009). "A functional screen to identify novel effectors of hematopoietic stem cell activity." Cell **137**(2): 369-379.

Deneault, E., B. T. Wilhelm, et al. (2013). "Identification of non-cell-autonomous networks from engineered feeder cells that enhance murine hematopoietic stem cell activity." Experimental hematology **41**(5): 470-478 e474.

Ding, L. and S. J. Morrison (2013). "Haematopoietic stem cells and early lymphoid progenitors occupy distinct bone marrow niches." Nature **495**(7440): 231-235.

Ding, L., T. L. Saunders, et al. (2012). "Endothelial and perivascular cells maintain haematopoietic stem cells." Nature **481**(7382): 457-462.

Domen, J., S. H. Cheshier, et al. (2000). "The role of apoptosis in the regulation of hematopoietic stem cells: Overexpression of Bcl-2 increases both their number and repopulation potential." The Journal of experimental medicine **191**(2): 253-264.

Dooner, G. J., G. A. Colvin, et al. (2008). "Gene expression fluctuations in murine hematopoietic stem cells with cell cycle progression." Journal of cellular physiology **214**(3): 786-795.

Dykstra, B., D. Kent, et al. (2007). "Long-term propagation of distinct hematopoietic differentiation programs in vivo." Cell stem cell **1**(2): 218-229.

Dykstra, B., J. Ramunas, et al. (2006). "High-resolution video monitoring of hematopoietic stem cells cultured in single-cell arrays identifies new features of self-renewal." Proceedings of the National Academy of Sciences of the United States of America **103**(21): 8185-8190.

Eilken, H. M., S. Nishikawa, et al. (2009). "Continuous single-cell imaging of blood generation from haemogenic endothelium." Nature **457**(7231): 896-900.

Eliason, J., N. Testa, et al. (1979). "Erythropoietin-stimulated erythropoiesis in long-term bone marrow culture." Nature **281**: 382-384.

Ema, H., H. Takano, et al. (2000). "In Vitro Self-Renewal Division of Hematopoietic Stem Cells." J. Exp. Med. **192**(9): 1281-1288.

Enninga, I., R. Groenendijk, et al. (1984). "Use of low temperature for growth arrest and synchronization of human diploid fibroblasts." Mutation Research **130**: 343-352.

Enver, T., C. M. Heyworth, et al. (1998). "Do stem cells play dice?" Blood **92**(2): 348-351; discussion 352.

Erhardt, J. A. and R. N. Pittman (1998). "Ectopic p21(WAF1) expression induces differentiation-specific cell cycle changes in PC12 cells characteristic of nerve growth factor treatment." The Journal of biological chemistry **273**(36): 23517-23523.

Estment, C. and F. Ruscetti (1982). "Evaluation of erythropoiesis in long-term hamster bone marrow suspension cultures: absence of a requirement for adherent monolayer cells." Blood **60**(4): 999-1006.

Even, Y., J. L. Bennett, et al. (2011). "NUP98-HOXA10hd-expanded hematopoietic stem cells efficiently reconstitute bone marrow of mismatched recipients and induce tolerance." Cell transplantation **20**(7): 1099-1108.

Faley, S. L., M. Copland, et al. (2009). "Microfluidic single cell arrays to interrogate signalling dynamics of individual, patient-derived hematopoietic stem cells." Lab on a chip **9**(18): 2659-2664.

Fang, J., M. Menon, et al. (2007). "EPO modulation of cell-cycle regulatory genes, and cell division, in primary bone marrow erythroblasts." Blood **110**(7): 2361-2370.

Ferrara, J. L., J. E. Levine, et al. (2009). "Graft-versus-host disease." Lancet **373**(9674): 1550-1561.

Fichelson, S. and P. F. Freyssinier JM, Fontenay-Roupie M, Guesnu M, Cherai M, Gisselbrecht S, Porteu F (1999). "Megakaryocyte Growth and Development Factor-Induced Proliferation and Differentiation Are Regulated by the Mitogen-Activated Protein Kinase Pathway in Primitive Cord Blood Hematopoietic Progenitors." Blood **94**(5): 1601-1613.

Fleming, H., V. Janzen, et al. (2008). "Wnt Signaling in the Niche Enforces Hematopoietic Stem Cell Quiescence and Is Necessary to Preserve Self-Renewal In Vivo." Cell Stem Cell **2**: 274-283.

Fox, N., G. Priestley, et al. (2002). "Thrombopoietin expands hematopoietic stem cells after transplantation." J. Clin. Invest. **110**(3): 389-394.

Frank, T. and S. Tay (2013). "Flow-switching allows independently programmable, extremely stable, high-throughput diffusion-based gradients." Lab on a chip **13**(7): 1273-1281.

Furukawa, Y., J. Kikuchi, et al. (2000). "Lineage-specific regulation of cell cycle control gene expression during haematopoietic cell differentiation." British journal of haematology **110**(3): 663-673.

Gekas, C. and T. Graf (2013). "CD41 expression marks myeloid-biased adult hematopoietic stem cells and increases with age." Blood **121**(22): 4463-4472.

Ghannam, G., A. Takeda, et al. (2004). "The oncogene Nup98-HOXA9 induces gene transcription in myeloid cells." The Journal of biological chemistry **279**(2): 866-875.

Giebel, B., T. Zhang, et al. (2006). "Primitive human hematopoietic cells give rise to differentially specified daughter cells upon their initial cell division." Blood **107**(5): 2146-2152.

Glauche, I., M. Cross, et al. (2007). "Lineage specification of hematopoietic stem cells: mathematical modeling and biological implications." Stem cells **25**(7): 1791-1799.

Glimm, H., I. H. Oh, et al. (2000). "Human hematopoietic stem cells stimulated to proliferate in vitro lose engraftment potential during their S/G(2)/M transit and do not reenter G(0)." Blood **96**(13): 4185-4193.

Goldman, D., A. Bailey, et al. (2009). "BMP4 regulates the hematopoietic stem cell niche." Blood **114**(20): 4393-4401.

Goodell, M., K. Brose, et al. (1996). "Isolation and Functional Properties of Murine Hematopoietic Stem Cells that are Replicating In Vivo." J. Exp. Med. **183**: 1797-1806.

Greenbaum, A., Y. M. Hsu, et al. (2013). "CXCL12 in early mesenchymal progenitors is required for haematopoietic stem-cell maintenance." Nature **495**(7440): 227-230.

Gu, J., X. Xia, et al. (2004). "Cell cycle-dependent regulation of a human DNA helicase that localizes in DNA damage foci." Molecular biology of the cell **15**(7): 3320-3332.

Haddad, R., F. Pflumio, et al. (2008). "The HOXB4 homeoprotein differentially promotes ex vivo expansion of early human lymphoid progenitors." Stem cells **26**(2): 312-322.

Hahn, A. T., Jones, J.T., et al. (2009). "Quantitative analysis of cell cycle phase durations and PC12 differentiation using fluorescent biosensors." Cell Cycle **8**(7): 1044-1052.

Harris, D. T., M. J. Schumacher, et al. (1992). "Phenotypic and functional immaturity of human umbilical cord blood T lymphocytes." Proceedings of the National Academy of Sciences of the United States of America **89**(21): 10006-10010.

Hartwell, L. H., Culotti. J, et al. (1970). "Genetic Control of the Cell-Division Cycle in Yeast, I. DetectionofMutants." Proc. Nat. Acad. Sc. **66**(2): 352-359.

Haugh, J. M., F. Codazzi, et al. (2000). "Spatial sensing in fibroblasts mediated by 3' phosphoinositides." The Journal of cell biology **151**(6): 1269-1280.

Heffner, G. C., M. R. Clutter, et al. (2011). "Novel hematopoietic progenitor populations revealed by direct assessment of GATA1 protein expression and cMPL signaling events." Stem cells **29**(11): 1774-1782.

Henschler, R., W. Brugger, et al. (1994). "Maintenance of transplantation potential in ex vivo expanded CD34(+)-selected human peripheral blood progenitor cells." Blood **84**(9): 2898-2903.

Herwig, S. and M. Strauss (1997). "The retinoblastoma protein: a master regulator of cell cycle, differentiation and apoptosis." European journal of biochemistry / FEBS **246**(3): 581-601.

Herwig, S. and Strauss, M. (1997). "The retinoblastoma protein : a master regulator of cell cycle, differentiation and apoptosis." Eur. J. Biochem. **245**: 581-601.

Hesse, M., A. Raulf, et al. (2012). "Direct visualization of cell division using high-resolution imaging of M-phase of the cell cycle." Nature communications **3**: 1076.

Hodgson, G. and T. Bradley (1979). "Properties of haematopoietic stem cells surviving 5-fluorouracil treatment: evidence for a pre-cfu-s cell?" Nature **281**: 381-382.

Hoffman, R., R. Briddell, et al. (1990). "Numerous Growth Factors Can Influence in Vitro Megakaryocytopoiesis." Yale J Biol. Med. **63**: 411-418.

Hsieh, F. F., Barnett, L. A., Green, W. F., Freedman, K., Matushansky, I., Skoultchi, A. I. and Kelley, L. L. (2000). "Cell cycle exit during terminal erythroid differentiation is associ- ated with accumulation of p27KIP1 and inactivation of cdk2 kinase." Blood **96**: 2746-2754.

Hunt, T. (1989). "Under Arrest in the Cell Cycle." Nature **342**: 483-484.

Ikuta, K. and I. Weissman (1992). "Evidence that hematopoietic stem cells express mouse c-kit but do not depend on steel factor for their generation." PNAS **89**: 1502-1506.

Jacquel, A., M. Herrant, et al. (2006). "A survey of the signaling pathways involved in megakaryocytic differentiation of the human K562 leukemia cell line by molecular and c-DNA array analysis." Oncogene **25**(5): 781-794.

Jang, Y. Y. and S. J. Sharkis (2007). "A low level of reactive oxygen species selects for primitive hematopoietic stem cells that may reside in the low-oxygenic niche." Blood **110**(8): 3056-3063.

Jedema, I., R. M. Barge, et al. (2003). "High susceptibility of human leukemic cells to Fas-induced apoptosis is restricted to G1 phase of the cell cycle and can be increased by interferon treatment." Leukemia **17**(3): 576-584.

Josefsen, D., H. K. Blomhoff, et al. (1999). "Retinoic acid induces apoptosis of human CD34+ hematopoietic progenitor cells: involvement of retinoic acid receptors and retinoid X receptors depends on lineage commitment of the hematopoietic progenitor cells." Experimental hematology **27**(4): 642-653.

Kaminska, J., E. Klimczak-Jajor, et al. (2008). "Src kinases in the process of maturation megakryocyte progenitors." Postepy biochemii **54**(4): 378-383.

Kasper, L., B. PK, et al. (1999). "CREB Binding Protein Interacts with Nucleoporin-Specific FG repeats that activate transcription and mediate NUP98-HOXA9 Oncogenicticy." Mol Cell. Biology **19**(1): 764-776.

Katayama, Y., M. Battista, et al. (2005). "Signals from the Sympathetic Nervous System Regulate Hematopoietic Stem Cell Egress from Bone Marrow." Cell **124**: 407-421.

Kaushansky, K. (1995). "Thrombopoietin: the primary regulator of megakaryocyte and platelet production." Thrombosis and haemostasis **74**(1): 521-525.

Kaushansky, K. (2008). "Historical review: megakaryopoiesis and thrombopoiesis." Blood **111**(3): 981-986.

Keller, J., M. Ortiz, et al. (1995). "Steel Factor (c-kit Ligand) Promotes the Survival of Hematopoietic Stem/Progenitor Cells in the Absence of Cell Division." Blood **86**(5): 1757-1764.

Kent, D. G., M. R. Copley, et al. (2009). "Prospective isolation and molecular characterization of hematopoietic stem cells with durable self-renewal potential." Blood **113**(25): 6342-6350.

Kerst, J. M., I. C. Slaper-Cortenbach, et al. (1992). "Combined measurement of growth and differentiation in suspension cultures of purified human CD34-positive cells enables a detailed analysis of myelopoiesis." Experimental hematology **20**(10): 1188-1193.

Khameneh, H., S. Isa, et al. (2011). "GM-CSF Signalling Boosts Dramatically IL-1 Production." PLoS ONE **6**(7): 1-8.

Kiel, M. J., O. H. Yilmaz, et al. (2005). "SLAM family receptors distinguish hematopoietic stem and progenitor cells and reveal endothelial niches for stem cells." Cell **121**(7): 1109-1121.

Kimura, S., A. Roberts, et al. (1998). "Hematopoietic stem cell deficiencies in mice lacking c-Mpl, the receptor for thrombopoietin." PNAS **95**: 1195-1200.

Kinoshita, T., T. Yokota, et al. (1995). "Suppression of apoptotic death in hematopoietic cells by signalling through the IL-3/GM-CSF receptors." EMBO **14**(2): 266-275.

Kirito, K., T. Watanabe, et al. (2002). "Thrombopoietin regulates Bcl-xL gene expression through Stat5 and phosphatidylinositol 3-kinase activation pathways." The Journal of biological chemistry **277**(10): 8329-8337.

Kirouac, D. C., G. J. Madlambayan, et al. (2009). "Cell-cell interaction networks regulate blood stem and progenitor cell fate." Molecular systems biology **5**: 293.

Knoblich, J. A. (2008). "Mechanisms of asymmetric stem cell division." Cell **132**(4): 583-597.

Kodama, H., M. Nose, et al. (1992). "In Vitro Proliferation of Primitive Hemopoietic Stem Cells Supported by Stromal Cells: Evidence for the Presence of a Mechanism(s) Other Than That Involving c-kdt Receptor and Its Ligand." J Exp Med **176**: 351-361.

Kodama, H., H. Sudo, et al. (1984). "In vitro hemopoiesis within a microenvironment created by MC3T3- G2/PA6 preadipocytes." J Cell Physiol. **118**(3): 233-240.

Kodama, H. A., Y. Amagai, et al. (1982). "A new preadipose cell line derived from newborn mouse calvaria can promote the proliferation of pluripotent hemopoietic stem cells in vitro." Journal of cellular physiology **112**(1): 89-95.

Komatsu, N., H. Nakauchi, et al. (1991). "Establishment and Characterization of a Human Leukemic Cell Line with Megakaryocytic Features: Dependency on Granulocyte-Macrophage Colony-stimulating Factor, Interleukin 3, or Erythropoietin for Growth and Survival." Cancer Res **51**: 341-348.

Kotkow, K. J. and S. H. Orkin (1996). "Complexity of the erythroid transcription factor NF-E2 as revealed by gene targeting of the mouse p18 NF-E2 locus." Proceedings of the National Academy of Sciences of the United States of America **93**(8): 3514-3518.

Kretzschmar, K. and F. M. Watt (2012). "Lineage tracing." Cell **148**(1-2): 33-45.

Kroon, E., U. Thorsteinsdottir, et al. (2001). "NUP98-HOXA9 expression in hemopoietic stem cells induces chronic and acute myeloid leukemias in mice." EMBO **20**(3): 350-361.

Ku, H., Y. Yonemura, et al. (1996). "Thrombopoietin, the ligand for the Mpl receptor, synergizes with steel factor and other early acting cytokines in supporting proliferation of primitive hematopoietic progenitors of mice." Blood **87**(11): 4544-4551.

Lambert, J. F., M. Liu, et al. (2003). "Marrow stem cells shift gene expression and engraftment phenotype with cell cycle transit." The Journal of experimental medicine **197**(11): 1563-1572.

Lappin, T., D.G. Grier, et al. (2006). "HOX GENES: Seductive Science, Mysterious Mechanisms." Ulster Med J **75**: 23-31.

Larson, D. R., R. H. Singer, et al. (2009). "A single molecule view of gene expression." Trends in cell biology **19**(11): 630-637.

Latres, E., M. Malumbres, et al. (2000). "Limited overlapping roles of P15INK4b and P18INK4c cell cycle inhibitors in proliferation and tumorigenesis." EMBO **19**(13): 3496-3506.

Lawrence, H., G. Sauvageau, et al. (1996). "The Role of HOX Homeobox Genes in Normal and Leukemic Hematopoiesis." Stem Cells **14**: 281-291.

Lecault, V., M. Vaninsberghe, et al. (2011). "High-throughput analysis of single hematopoietic stem cell proliferation in microfluidic cell culture arrays." Nature methods **8**(7): 581-586.

Lee, M. and P. Nurse (1988). "Cell cycle control genes in fission yeast and mammalian cells." TIG **4**(10): 287-290.

Lee, M. W., D. S. Kim, et al. (2013). "Human bone marrow-derived mesenchymal stem cell gene expression patterns vary with culture conditions." Blood research **48**(2): 107-114.

Leonhardt, H., Rahn, H.P., Weinzierl, P., Sporbert, A., Cremer, T., Zink, D., and Cardoso, M.C. (2000). "Dynamics of DNA replication factories in living cells." J. Cell Biol. **149**: 271-279.

Lessard, J. and G. Sauvageau (2003). "Bmi-1 determines the proliferative capacity of normal and leukaemic stem cells." Nature **423**(6937): 255-260.

Li, C. and G. Johnson (1994). "Stem cell factor enhances the survival but not the self-renewal of murine hematopoietic long-term repopulating cells." Blood **84**(2): 408-414.

Lipinski, M. M. and T. Jacks (1999). "The retinoblastoma gene family in differentiation and development." Oncogene **18**: 7873-7882.

Liu, Y., A. Aiello, et al. (2012). "Bid protects the mouse hematopoietic system following hydroxyurea-induced replicative stress." Cell death and differentiation **19**(10): 1602-1612.

Loose, M., G. Swiers, et al. (2007). "Transcriptional networks regulating hematopoietic cell fate decisions." Current opinion in hematology **14**(4): 307-314.

Lopez-Bergami, P., C. Huang, et al. (2007). "Rewired ERK-JNK signaling pathways in melanoma." Cancer cell **11**(5): 447-460.

Lu, R., N. F. Neff, et al. (2011). "Tracking single hematopoietic stem cells in vivo using high-throughput sequencing in conjunction with viral genetic barcoding." Nature biotechnology **29**(10): 928-933.

Luc, S., N. Buza-Vidas, et al. (2008). "Delineating the cellular pathways of hematopoietic lineage commitment." Seminars in immunology **20**(4): 213-220.

Marr, C., M. Strasser, et al. (2012). "Multi-scale modeling of GMP differentiation based on single-cell genealogies." The FEBS journal **279**(18): 3488-3500.

Massague, J. (2004). "G1 cell-cycle control and cancer." Nature **432**(7015): 298-306.

Matsumura, I., J. Ishikawa, et al. (1997). "Thrombopoietin-induced differentiation of a human megakaryoblastic leukemia cell line, CMK, involves transcriptional activation of p21(WAF1/Cip1) by STAT5." Molecular and cellular biology **17**(5): 2933-2943.

Matsunaga, T., T. Kato, et al. (1998). "Thrombopoietin promotes the survival of murine hematopoietic long-term reconstituting cells: comparison with the effects of FLT3/FLK-2 ligand and interleukin-6." Blood **92**(2): 452-461.

Matsuzaki, Y., K. Kinjo, et al. (2004). "Unexpectedly Efficient Homing Capacity of Purified Murine Hematopoietic Stem Cells." Immunity **20**: 87-93.

Melemed, A., R. JW, et al. (1997). "Activation of the Mitogen-Activated Protein Kinase Pathway Is Involved in and Sufficient for Megakaryocytic Differentiation of CMK Cells." Blood **90**(9): 3462-3470.

Mendez-Ferrer, S., M. Battista, et al. (2010). "Cooperation of beta(2)- and beta(3)-adrenergic receptors in hematopoietic progenitor cell mobilization." Annals of the New York Academy of Sciences **1192**: 139-144.

Mendez-Ferrer, S., T. V. Michurina, et al. (2010). "Mesenchymal and haematopoietic stem cells form a unique bone marrow niche." Nature **466**(7308): 829-834.

Miller, C. L. and C. J. Eaves (1997). "Expansion in vitro of adult murine hematopoietic stem cells with transplantable lympho-myeloid reconstituting ability." Proceedings of the National Academy of Sciences of the United States of America **94**(25): 13648-13653.

Mivechi, N. and G. Li (1990). "Heat sensitivity, thermotolerance and protein synthesis of granulocyte and macrophage progenitors from mice and from long- term bone marrow cultures." Int. J. Hyperthermia **6**(3): 529-541.

Miyajima, A., A. L. Mui, et al. (1993). "Receptors for granulocyte-macrophage colony-stimulating factor, interleukin-3, and interleukin-5." Blood **82**(7): 1960-1974.

Moore, K. A., H. Ema, et al. (1997). "In vitro maintenance of highly purified, transplantable hematopoietic stem cells." Blood **89**(12): 4337-4347.

Moore, M. A. and D. Metcalf (1970). "Ontogeny of the haemopoietic system: yolk sac origin of in vivo and in vitro colony forming cells in the developing mouse embryo." British journal of haematology **18**(3): 279-296.

Morita, Y., H. Ema, et al. (2010). "Heterogeneity and hierarchy within the most primitive hematopoietic stem cell compartment." The Journal of experimental medicine **207**(6): 1173-1182.

Morrison, S., A. Wandycz, et al. (1997). "Identification of a lineage of multipotent hematopoietic progenitors." Development **124**: 1929-1939.

Mossadegh-Keller, N., S. Sarrazin, et al. (2013). "M-CSF instructs myeloid lineage fate in single haematopoietic stem cells." Nature **497**(7448): 239-243.

Müller-Sieburg, C., R. Cho, et al. (2002). "Deterministic regulation of hematopoietic stem cell self-renewal and differentiation." Blood **100**(4): 1302-1309.

Munoz-Alonso, M. J., L. Ceballos, et al. (2012). "MYC accelerates p21CIP-induced megakaryocytic differentiation involving early mitosis arrest in leukemia cells." Journal of cellular physiology **227**(5): 2069-2078.

Murciano, A., J. Zamora, et al. (2002). "Interkinetic Nuclear Movement May Provide Spatial Clues to the Regulation of Neurogenesis." Molecular and Cellular Neuroscience **21**(2): 285-300.

Nagasawa, T., Y. Omatsu, et al. (2011). "Control of hematopoietic stem cells by the bone marrow stromal niche: the role of reticular cells." Trends in immunology **32**(7): 315-320.

Ng, S. Y., T. Yoshida, et al. (2009). "Genome-wide lineage-specific transcriptional networks underscore Ikaros-dependent lymphoid priming in hematopoietic stem cells." Immunity **30**(4): 493-507.

Nilsson, S., H. Johnston, et al. (2005). "Osteopontin, a key component of the hematopoietic stem cell niche and regulator of primitive hematopoietic progenitor cells." Blood **106**(4): 1232-1239.

Nolta, J., F. Thiemann, et al. (2002). "The AFT024 stromal cell line supports long-term ex vivo maintenance of engrafting multipotent human hematopoietic progenitors." Leukemia **16**: 352-361.

Nygren, J., D. Bryder, et al. (2006). "Prolonged Cell Cycle Transit Is a Defining and Developmentally Conserved Hemopoietic Stem Cell Property." J Immunology **177**: 201-208.

Ogawa, M., F. Tajima, et al. (2001). "CD34 Expression by Murine Hematopoietic Stem Cells: Developmental Changes and Kinetic Alterations." Ann. N.Y. Acad. Sci. **938**: 139-145.

Ogura, Y., A. Sakaue-Sawano, et al. (2011). "Coordination of mitosis and morphogenesis: role of a prolonged G2 phase during chordate neurulation." Development **138**(3): 577-587.

Ohta, H., S. Sekulovic, et al. (2007). "Near-maximal expansions of hematopoietic stem cells in culture using NUP98-HOX fusions." Experimental Hematology **35**(5): 817-830.

Okada, S., H. Nakauchi, et al. (1991). "Enrichment and characterization of murine hematopoietic stem cells that express c-kit molecule." Blood **78**(7): 1706-1712.

Okada, S., H. Nakauchi, et al. (1992). "In vivo and in vitro stem cell function of c-kit- and Sca-1-positive murine hematopoietic cells." Blood **80**(12): 3044-3050.

Omatsu, Y., T. Sugiyama, et al. (2010). "The Essential Functions of Adipo-osteogenic Progenitors as the Hematopoietic Stem and Progenitor Cell Niche." Immunity **33**: 387-399.

Oostendorp, R. A., J. Audet, et al. (2000). "High-resolution tracking of cell division suggests similar cell cycle kinetics of hematopoietic stem cells stimulated in vitro and in vivo." Blood **95**(3): 855-862.

Orschell-Traycoff, C. M., K. Hiatt, et al. (2000). "Homing and engraftment potential of Sca-1(+)lin(-) cells fractionated on the basis of adhesion molecule expression and position in cell cycle." Blood **96**(4): 1380-1387.

Osawa, M., K. Hanada, et al. (1996). "Long-Term Lymphohematopoietic Reconstitutionbya SingleCD34-Low/Negative Hematopoietic Stem Cell." Science **273**(242-245).

Owens, B. and R. Hawley (2002). "HOX and Non-HOX Homeobox Genes in Leukemic Hematopoiesis." Stem Cells **20**: 364-379.

Palmqvist, L., N. Pineault, et al. (2007). "Candidate genes for expansion and transformation of hematopoietic stem cells by NUP98-HOX fusion genes." PloS one **2**(8): e768.

Park, I. K., D. Qian, et al. (2003). "Bmi-1 is required for maintenance of adult self-renewing haematopoietic stem cells." Nature **423**(6937): 302-305.

Passegue, E., A. J. Wagers, et al. (2005). "Global analysis of proliferation and cell cycle gene expression in the regulation of hematopoietic stem and progenitor cell fates." The Journal of experimental medicine **202**(11): 1599-1611.

Pauklin, S. and L. Vallier (2013). "The cell-cycle state of stem cells determines cell fate propensity." Cell **155**(1): 135-147.

Pawliuk, R., C. Eaves, et al. (1996). "Evidence of both ontogeny and transplant dose-regulated expansion of hematopoietic stem cells in vivo." Blood **88**(8): 2852-2858.

Petzer, A. L., D. E. Hogge, et al. (1996). "Self-renewal of primitive human hematopoietic cells (long-term-culture-initiating cells) in vitro and their expansion in defined medium." Proceedings of the National Academy of Sciences of the United States of America **93**(4): 1470-1474.

Pilz, G. A., A. Shitamukai, et al. (2013). "Amplification of progenitors in the mammalian telencephalon includes a new radial glial cell type." Nature communications **4**: 2125.

Pineault, N., C. Abramovich, et al. (2005). "Transplantable cell lines generated with NUP98-Hox fusion genes undergo leukemic progression by Meis1 independent of its binding to DNA." Leukemia **19**(4): 636-643.

Pineault, N., C. Abramovich, et al. (2004). "Differential and Common Leukemogenic Potentials of Multiple NUP98-Hox Fusion Proteins Alone or with Meis1." Molecular and Cellular Biology **24**(5): 1907-1917.

Ploemacher, R., v. d. J. Sluijs, et al. (1989). "An in vitro limiting-dilution assay of long-term repopulating hematopoietic stem cells in the mouse." Blood **74**(8): 2755-2763.

Pourfarzad, F., M. von Lindern, et al. (2013). "Hydroxyurea responsiveness in beta-thalassemic patients is determined by the stress response adaptation of erythroid progenitors and their differentiation propensity." Haematologica **98**(5): 696-704.

Pronk, C. J., D. J. Rossi, et al. (2007). "Elucidation of the phenotypic, functional, and molecular topography of a myeloerythroid progenitor cell hierarchy." Cell stem cell **1**(4): 428-442.

Purton, L. E., I. D. Bernstein, et al. (2000). "All-trans retinoic acid enhances the long-term repopulating activity of cultured hematopoietic stem cells." Blood **95**(2): 470-477.

Qian, H., N. Buza-Vidas, et al. (2007). "Critical Role of Thrombopoietin in Maintaining Adult Quiescent Hematopoietic Stem Cells." Cell Stem Cell **1**: 671-684.

Quesenberry, P. J., G. J. Dooner, et al. (2010). "Expression of cell cycle-related genes with cytokine-induced cell cycle progression of primitive hematopoietic stem cells." Stem cells and development **19**(4): 453-460.

Ramsfjell, V., O. J. Borge, et al. (1996). "Thrombopoietin, but not erythropoietin, directly stimulates multilineage growth of primitive murine bone marrow progenitor cells in synergy with early acting cytokines: distinct interactions with the ligands for c-kit and FLT3." Blood **88**(12): 4481-4492.

Raslova, H., V. Baccini, et al. (2006). "Mammalian target of rapamycin (mTOR) regulates both proliferation of megakaryocyte progenitors and late stages of megakaryocyte differentiation." Blood **107**(6): 2303-2310.

Ratcliffe, E., K. E. Glen, et al. (2012). "A novel automated bioreactor for scalable process optimisation of haematopoietic stem cell culture." Journal of biotechnology **161**(3): 387-390.

Raval, A., B. Kusler, et al. (2012). "Effect of nucleophosmin1 haploinsufficiency on hematopoietic stem cells." Leukemia **26**(4): 853-855.

Rebel, V. I., C. L. Miller, et al. (1996). "The repopulation potential of fetal liver hematopoietic stem cells in mice exceeds that of their liver adult bone marrow counterparts." Blood **87**(8): 3500-3507.

Reddy, G., C. Y. Tiarks, et al. (1997). "Cell Cycle Analysis and Synchronization of Pluripotent Hematopoietic Progenitor Stem Cells." Blood **90**: 2293-2299.

Rehn, M., A. Olsson, et al. (2011). "Hypoxic induction of vascular endothelial growth factor regulates murine hematopoietic stem cell function in the low-oxygenic niche." Blood **118**(6): 1534-1543.

Reya, T., A. Duncan, et al. (2003). "A role for Wnt signalling in self-renewal of haematopoietic stem cells." Nature **423**: 409-414.

Rieger, M., P. Hoppe, et al. (2009). "Hematopoietic Cytokines Can Instruct Lineage Choice." Science **325**: 217-218.

Robel, S., S. Bardehle, et al. (2011). "Genetic deletion of cdc42 reveals a crucial role for astrocyte recruitment to the injury site in vitro and in vivo." The Journal of neuroscience : the official journal of the Society for Neuroscience **31**(35): 12471-12482.

Robinson, B., H. McGrath, et al. (1987). "Recombinant Murine Granulocyte Macrophage Colony-stimulating Factor Has Megakaryocyte Colony-stimulating Activity and Augments Megakaryocyte Colony Stimulation by Interleukin 3." J. Clin. Invest. **79**: 1648-1652.

Roccio, M., D. Schmitter, et al. (2013). "Predicting stem cell fate changes by differential cell cycle progression patterns." Development **140**(2): 459-470.

Rocha, V., J. Cornish, et al. (2001). "Comparison of outcomes of unrelated bone marrow and umbilical cord blood transplants in children with acute leukemia." Blood **97**(10): 2962-2971.

Rojnuckarin, P., J.G. Drachman, et al. (1999). "Thrombopoietin-Induced Activation of the Mitogen-Activated Protein Kinase (MAPK) Pathway in Normal Megakaryocytes: Role in Endomitosis." Blood **94**: 1273-1282.

Rottgermann, P. J., A. P. Alberola, et al. (2014). "Cellular self-organization on micro-structured surfaces." Soft matter **10**(14): 2397-2404.

Rouyez, M., C. Boucheron, et al. (1997). "Control of Thrombopoietin-Induced Megakaryocytic Differentiation by the Mitogen-Activated Protein Kinase Pathway." Mol. Cell. Biol. **17**(9): 4991-5000.

Sakaue-Sawano, A., T. Hoshida, et al. (2013). "Visualizing developmentally programmed endoreplication in mammals using ubiquitin oscillators." Development **140**(22): 4624-4632.

Sakaue-Sawano, A., H. Kurokawa, et al. (2007). "Visualizing Spatiotemporal Dynamics of Multicellular Cell-Cycle Progression." Cell **132**: 487-498.

Santamarina, M., G. Hernandez, et al. (2008). "CDK redundancy guarantees cell cycle progression in Rb-negative tumor cells independently of their p16 status." Cell cycle **7**(13): 1962-1972.

Sato, T., J. H. Laver, et al. (1999). "Reversible expression of CD34 by murine hematopoietic stem cells." Blood **94**(8): 2548-2554.

Satoh, M., H. Mioh, et al. (1997). "Characterization of the molecules involved in the hematopoietic microenvironment provided by mouse stromal cell line MC3T3-G2/PA6 using a unique reporter system that analyzes the direct cell-to-cell interaction." Acta haematologica **98**(2): 95-103.

Satoh, M., H. Mioh, et al. (1997). "Mouse bone marrow stromal cell line MC3T3-G2/PA6 with hematopoietic-supporting activity expresses high levels of stem cell antigen Sca-1." Experimental hematology **25**(9): 972-979.

Sauvageau, G., N. N. Iscove, et al. (2004). "In vitro and in vivo expansion of hematopoietic stem cells." Oncogene **23**(43): 7223-7232.

Sauvageau, G., U. Thorsteinsdottir, et al. (1995). "Overexpression of HOXB4 in hematopoietic cells causes the selective expansion of more primitive populations in vitro and in vivo." Genes & development **9**(14): 1753-1765.

Schaniel, C., D. Sirabella, et al. (2011). "Wnt-inhibitory factor 1 dysregulation of the bone marrow niche exhausts hematopoietic stem cells." Blood **118**(9): 2420-2429.

Schofield, R. (1978). "The relationship between the spleen colony-forming cell and the haemopoietic stem cell." Blood cells **4**(1-2): 7-25.

Sekulovic, S., M. Gasparetto, et al. (2011). "Ontogeny stage-independent and high-level clonal expansion in vitro of mouse hematopoietic stem cells stimulated by an engineered NUP98-HOX fusion transcription factor." Blood **118**(16): 4366-4376.

Sekulovic, S., S. Imren, et al. (2008). "High level in vitro expansion of murine hematopoietic stem cells." Current protocols in stem cell biology **Chapter 2**: Unit 2A 7.

Severin, S., C. Ghevaert, et al. (2010). "The mitogen-activated protein kinase signaling pathways: role in megakaryocyte differentiation." Journal of thrombosis and haemostasis : JTH **8**(1): 17-26.

Sharpless, N., N. Bardeesy, et al. (2001). "Loss of p16Ink4a with retention of p19Arf predisposes mice to tumorigenesis." Nature **413**: 86-91.

Shih, H. H., S. G. Tevosian, et al. (1998). "Regulation of differentiation by HBP1, a target of the retinoblastoma protein." Molecular and cellular biology **18**(8): 4732-4743.

Shimizu, N., S. Noda, et al. (2008). "Identification of genes potentially involved in supporting hematopoietic stem cell activity of stromal cell line MC3T3-G2/PA6." International journal of hematology **87**(3): 239-245.

Sieburg, H. B., R. H. Cho, et al. (2006). "The hematopoietic stem compartment consists of a limited number of discrete stem cell subsets." Blood **107**(6): 2311-2316.

Sitwala, K., M. Dandekar, et al. (2008). "HOX Proteins and Leukemia." Int J Clin Exp Pathol **1**: 461-474.

Sloma, I., S. Imren, et al. (2013). "Ex vivo expansion of normal and chronic myeloid leukemic stem cells without functional alteration using a NUP98HOXA10homeodomain fusion gene." Leukemia **27**(1): 159-169.

Smith, S. L., J. G. Bender, et al. (1993). "Expansion of neutrophil precursors and progenitors in suspension cultures of CD34+ cells enriched from human bone marrow." Experimental hematology **21**(7): 870-877.

Song, Y., A. Bahnson, et al. (2010). "Stem cell traits in long-term co-culture revealed by time-lapse imaging." Leukemia **24**(1): 153-161.

Spangrude, G., S. Heimfeld, et al. (1988). "Purification and Characterization of Mouse Hematopoietic Stem Cells." Science **241**: 58-62.

Stier, S., T. Cheng, et al. (2002). "Notch1 activation increases hematopoietic stem cell self-renewal in vivo and favors lymphoid over myeloid lineage outcome." Blood **99**(7): 2369-2378.

Stubbs, S., S. Hancock, et al. (2005). "G1/S Checkpoint Reporting." GE Healthcare.

Suda, J., S. T, et al. (1984). "Analysis of differentiation of mouse hematopoeitic stem cells in culture by sequential replating of paired progenitors." Blood **64**: 393-399.

Sudo, K., H. Ema, et al. (2000). "Age-associated Characteristics of Murine Hematopoietic Stem Cells." J. Exp. Med. **192**(9): 1273-1280.

Sudo, T., M. Ito, et al. (1989). "Interleukin 7 production and function in stromal cell-dependent B cell development." The Journal of experimental medicine **170**(1): 333-338.

Sugiyama, M., A. Sakaue-Sawano, et al. (2009). "Illuminating cell-cycle progression in the developing zebrafish embryo." Proceedings of the National Academy of Sciences of the United States of America **106**(49): 20812-20817.

Sugiyama, T., H. Kohara, et al. (2006). "Maintenance of the Hematopoietic Stem Cell Pool by CXCL12-CXCR4 Chemokine Signaling in Bone Marrow Stromal Cell Niches." Immunity **25**: 977-988.

Sutherland, H., P. Lansdorp, et al. (1990). "Functional characterization of individual human hematopoietic stem cells cultured at limiting dilutionon supportive marrow stromal layers." PNAS **87**: 3584-3588.

Szekely, L., W. Q. Jiang, et al. (1992). "Cell type and differentiation dependent heterogeneity in retinoblastoma protein expression in SCID mouse fetuses." Cell growth & differentiation : the molecular biology journal of the American Association for Cancer Research **3**(3): 149-156.

Tajima, F., T. Sato, et al. (2000). "CD34 expression by murine hematopoietic stem cells mobilized by granulocyte colony-stimulating factor." Blood **96**(5): 1989-1993.

Takano, H., H. Ema, et al. (2004). "Asymmetric division and lineage commitment at the level of hematopoietic stem cells: inference from differentiation in daughter cell and granddaughter cell pairs." The Journal of experimental medicine **199**(3): 295-302.

Tamir, A., Petrocelli, T. , Stettler, K. , Chu, W. , Howard, J. , St Croix, B., Slingerland, J. and Ben-David, Y. (2000). "Stem cell factor inhibits erythroid differentiation by modulating the activity of G1-cyclin-dependent kinase complexes: a role for p27 in erythroid differentiation coupled G1 arrest." Cell Growth Differ. **11**: 269-277.

Teles, J., C. Pina, et al. (2013). "Transcriptional regulation of lineage commitment--a stochastic model of cell fate decisions." PLoS computational biology **9**(8): e1003197.

Thorén, L., K. Liuba, et al. (2008). "Kit Regulates Maintenance of Quiescent Hematopoietic Stem Cells." J Immunol **180**: 2045-2053.

Thorsteinsdottir, U., E. Kroon, et al. (2001). "Defining roles for HOX and MEIS1 genes in induction of acute myeloid leukemia." Molecular and cellular biology **21**(1): 224-234.

Thorsteinsdottir, U., A. Mamo, et al. (2002). "Overexpression of the myeloid leukemia–associated Hoxa9 gene in bone marrow cells induces stem cell expansion." Blood **99**(1): 121-129.

Thorsteinsdottir, U., G. Sauvageau, et al. (1997). "Overexpression of HOXA10 in Murine Hematopoietic Cells Perturbs both Myeloid and Lymphoid Differentiation and Leads to Acute Myeloid Leukemia." Mol. Cell. Biol. **17**(1): 495-505.

Tolar, J., K. Le Blanc, et al. (2010). "Concise review: hitting the right spot with mesenchymal stromal cells." Stem cells **28**(8): 1446-1455.

Vaquette, C., S. Ivanovski, et al. (2013). "Effect of culture conditions and calcium phosphate coating on ectopic bone formation." Biomaterials **34**(22): 5538-5551.

Varnum-Finney, B., L. Xu, et al. (2000). "Pluripotent, cytokine-dependent, hematopoietic stem cells are immortalized by constitutive Notch1 signaling." Nature medicine **6**(11): 1278-1281.

Verfaillie, C. M. (1992). "Direct contact between human primitive hematopoietic progenitors and bone marrow stroma is not required for long-term in vitro hematopoiesis." Blood **79**(11): 2821-2826.

Verfaillie, C. M. (1993). "Soluble factor(s) produced by human bone marrow stroma increase cytokine-induced proliferation and maturation of primitive hematopoietic progenitors while preventing their terminal differentiation." Blood **82**(7): 2045-2053.

Wang, W., V. Akbarian, et al. (2013). "Biochemical measurements on single erythroid progenitor cells shed light on the combinatorial regulation of red blood cell production." Molecular bioSystems **9**(2): 234-245.

Wang, Z., G. Li, et al. (2009). "Conditional deletion of STAT5 in adult mouse hematopoietic stem cells causes loss of quiescence and permits efficient nonablative stem cell replacement." Blood **113**(20): 4856-4865.

Warr, M. R., E. M. Pietras, et al. (2011). "Mechanisms controlling hematopoietic stem cell functions during normal hematopoiesis and hematological malignancies." Wiley interdisciplinary reviews. Systems biology and medicine **3**(6): 681-701.

Watts, K. L., X. Zhang, et al. (2011). "Differential effects of HOXB4 and NUP98-HOXA10hd on hematopoietic repopulating cells in a nonhuman primate model." Human gene therapy **22**(12): 1475-1482.

Whalen, A., G. SC, et al. (1997). "Megakaryocytic Differentiation Induced by Constitutive Activation of Mitogen-Activated Protein Kinase Kinase." Mol. Cell. Biol. **17**(4): 1947-1958.

Wilson, A., E. Laurenti, et al. (2008). "Hematopoietic stem cells reversibly switch from dormancy to self-renewal during homeostasis and repair." Cell **135**(6): 1118-1129.

Wilson, A. and A. Trumpp (2006). "Bone-marrow haematopoietic-stem-cell niches." Nature reviews. Immunology **6**(2): 93-106.

Wlodkowic, D., J. Skommer, et al. (2009). "Dynamic analysis of apoptosis using cyanine SYTO probes: from classical to microfluidic cytometry." Experimental cell research **315**(10): 1706-1714.

Wu, M., H. Kwon, et al. (2007). "Imaging Hematopoietic Precursor Division in Real Time." Cell Stem Cell **1**(5): 541-554.

Xie, Y., T. Yin, et al. (2009). "Detection of functional haematopoietic stem cell niche using real-time imaging." Nature **457**: 97-101.

Yagi, M., K. A. Ritchie, et al. (1999). "Sustained ex vivo expansion of hematopoietic stem cells mediated by thrombopoietin." Proceedings of the National Academy of Sciences of the United States of America **96**(14): 8126-8131.

Yamada, T., C. S. Park, et al. (2012). "The cytosolic protein G0S2 maintains quiescence in hematopoietic stem cells." PloS one **7**(5): e38280.

Yamamoto, R., Y. Morita, et al. (2013). "Clonal analysis unveils self-renewing lineage-restricted progenitors generated directly from hematopoietic stem cells." Cell **154**(5): 1112-1126.

Yamazaki, S., A. Iwama, et al. (2009). "TGF-beta as a candidate bone marrow niche signal to induce hematopoietic stem cell hibernation." Blood **113**(6): 1250-1256.

Yoder, M. C., K. Hiatt, et al. (1997). "Characterization of definitive lymphohematopoietic stem cells in the day 9 murine yolk sac." Immunity **7**(3): 335-344.

Yoon, K. A., H. S. Cho, et al. (2012). "Differential regulation of CXCL5 by FGF2 in osteoblastic and endothelial niche cells supports hematopoietic stem cell migration." Stem cells and development **21**(18): 3391-3402.

Yoshihara, H., F. Arai, et al. (2007). "Thrombopoietin/MPL signaling regulates hematopoietic stem cell quiescence and interaction with the osteoblastic niche." Cell stem cell **1**(6): 685-697.

Yu, H., Y. Yuan, et al. (2006). "Hematopoietic stem cell exhaustion impacted by p18 INK4C and p21 Cip1/Waf1 in opposite manners." Blood **107**(3): 1200-1206.

Yuan, Y., H. Shen, et al. (2004). "In vivo self-renewing divisions of haematopoietic stem cells are increased in the absence of the early G1-phase inhibitor, p18INK4C." Nature cell biology **6**(5): 436-442.

Zandstra, P. W., C. J. Eaves, et al. (1994). "Expansion of hematopoietic progenitor cell populations in stirred suspension bioreactors of normal human bone marrow cells." Bio/technology **12**(9): 909-914.

Zhang, C. C. and H. F. Lodish (2008). "Cytokines regulating hematopoietic stem cell function." Current opinion in hematology **15**(4): 307-311.

Zhang, J., C. Niu, et al. (2003). "Identification of the haematopoietic stem cell niche and control of the niche size." Nature **425**: 836-841.

Zhang, J., M. Socolovsky, et al. (2003). "Role of Ras signaling in erythroid differentiation of mouse fetal liver cells: functional analysis by a flow cytometry-based novel culture system." Blood **102**(12): 3938-3946.

Zhang, P. (1999). "The cell cycle and development: redundant roles of cell cycle regulators." Curr. Opin. Cell Biol. **11**: 655-662.

7 Supplemental movie legends

Supplemental movie 1. *Live cell-cycle time-lapse imaging in transduced NIH3T3 cells after 48 hour pre-incubation. 10x Fluar objective and 0.63x Tv adapter.*

Supplemental movie 2. *Live cell-cycle time-lapse imaging in transduced primary HSCs after 24 hour pre-incubation. 10x Fluar objective and 0.63x Tv adapter.*

Supplemental movie 3. *Live cell-cycle time-lapse imaging in transduced primary HSCs after 24 hour pre-incubation in PA6 stroma co-culture. Zoomed in to single-cell resolution in slow-motion and using fast-forward to indicate colony formation during 1 week of in vitro culture. Wavelength 1 (middle) shows VENUSnucmem signal and Wavelength 2 (right) shows onset and detection of CD48 by antibody staining. 10x Fluar objective and 0.63x Tv adapter.*

Supplemental movie 4. *Live cell-cycle time-lapse imaging in transduced primary HSCs after 24 hour pre-incubation in PA6 stroma co-culture. Zoomed in to single-cell resolution showing megakaryopoiesis during 1 week of in vitro culture. Wavelength 1 (middle) shows VENUSnucmem signal and Wavelength 2 (right) shows onset and detection of CD48 by antibody staining (negative). 10x Fluar objective and 0.63x Tv adapter.*

Eidesstattliche Versicherung

Hiermit versichere ich an Eides statt, dass ich die vorliegende Dissertation selbstständig und ohne unerlaubte Hilfe angefertigt habe. Ferner habe ich weder versucht eine Dissertation einzureichen oder eine Doktorprüfung durchzuführen, noch wurde die Dissertation oder Teile derselben einer anderen Prüfungskommission vorgelegt.

München, den 15.4.2014 Adrianus van den Berg